Aus dem Institut für Pathologie
(Prof. Dr. med. P. Ströbel)
der Medizinischen Fakultät der Universität Göttingen

One-carbon metabolism in lung cancer

INAUGURAL-DISSERTATION

zur Erlangung des Doktorgrades
der Medizinischen Fakultät der
Georg-August-Universität zu Göttingen

vorgelegt von

Sha Yao

aus

Changsha, China

Göttingen 2020

Dekan:	Prof. Dr. med. W. Brück

Betreuungsausschuss

Betreuer/in:	Prof. Dr. med. P. Ströbel
Ko-Betreuer/in:	Prof. Dr. med. V. Ellenrieder

Prüfungskommission

Referent/in:	Prof. Dr. med. P. Ströbel
Ko-Referent/in:	
Drittreferent/in:	.....

Datum der mündlichen Prüfung: .....

Table of Contents

List of figures

List of tables

Abbreviations

AC	Adenocarcinoma
Akt	Protein kinase B
ALL	Acute lymphoblastic leukemia
ALK	Anaplastic lymphoma kinase
ATCC	American type culture collection
CRC	Colorectal cancer
c-MYC	Cellular myelocytomatosis oncogene
ddH_2O	Double distilled water
DHFR	Dihydrofolate reductase
DNA	Deoxyribonucleic acid
dTMP	Deoxythymidine monophosphate
dUMP	Deoxyuridine monophosphate
EGFR	Epidermal growth factor receptor
ERK	Extracellular signal regulated kinase
EWS	Ewing's sarcoma
EDTA	Ethylenediaminetetraacetic acid
FBS	Fetal bovine serum
FDA	Food and drug administration
GARFT	Glycinamide ribonucleotide formyltransferase
IC50	Half maximal inhibitory concentration
IHC	Immunohistochemistry
MTHFD2	Methylenetetrahydrofolate dehydrogenase 2
NADPH	Nicotinamide adenine dinucleotide phosphate hydrogen
NCCN	National comprehensive cancer network
NSCLC	Non-small-cell lung cancer
PBS	Phosphate buffered saline
PGDH3	3-phosphoglycerate dehydrogenase
PI(3)K	Phosphatidylinositol-4,5-biphosphate 3-kinase
PRPP	Phosphoribosyl pyrophosphate
PSAT1	Phosphoserine aminotransferase 1

PSPH	Phosphoserine phosphatase
PVDF	Polyvinylidene difluoride
RAS	Rat sarcoma
RNA	Ribonucleic acid
RNR	Ribonucleotide reductase
RT	Room temperature
RTK	Receptor tyrosine kinase
SCLC	Small cell lung cancer
SEM	Standard error of mean
SHMT2	Serine hydroxymethyltransferase 2
SQCLC	Squamous cell lung carcinoma
TBST	Tris buffered saline with Tween 20
THF	Tetrahydrofolate
Tris	Tris (hydroymethyl) aminomethane
TYMS	Thymidylate synthase
WHO	World health organization
3-PG	3-phosphoglucerate
5-FU	5-fluorouracil

1 Introduction

1.1 Lung cancer

1.1.1 Epidemiology of lung cancer

According to the cancer report 2019, there are 606,880 Americans would die from cancer, which means that nearly 1,700 deaths per day. The greatest number of deaths arises from cancers among men and women is lung cancer (Siegel et al. 2019). Lung cancer is still the most common cancer and the leading cause of cancer direct or indirect related mortality worldwide (Brambilla and Travis 2014; Bray et al. 2018). The International agency for research reported more than 2 million new lung cases (11.6 % of the total new cancer cases) and more than 1.8 million deaths (18.4 % of the total cancer deaths) worldwide in 2018 (Figure 1) (Bray et al. 2018; Ferlay et al. 2019). The combined five-year survival rate for all stages is only 18.0 % (Siegel et al. 2018).

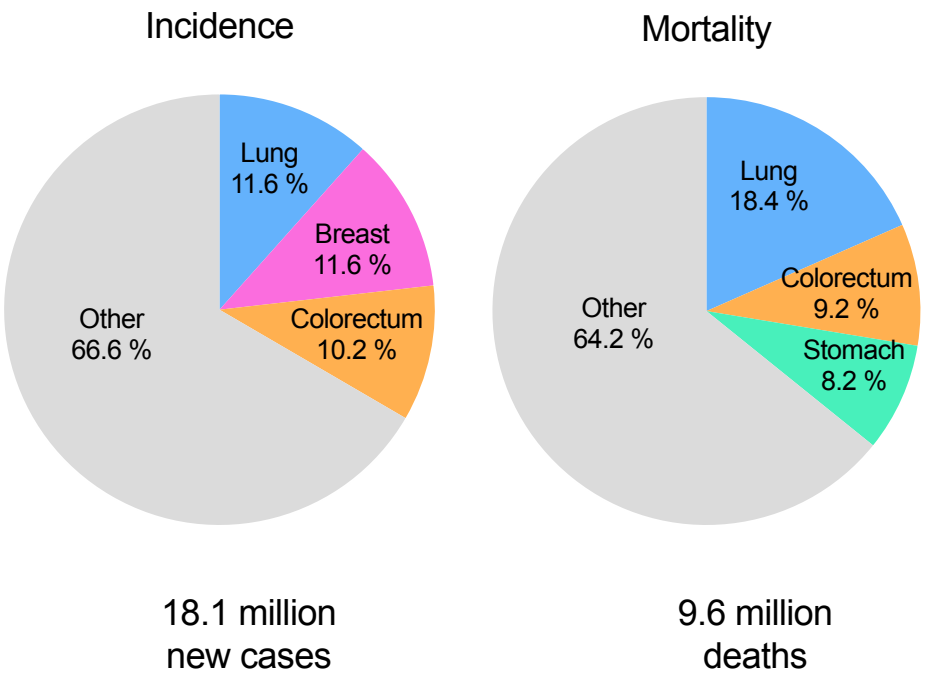

Figure 1: Distribution of cases and deaths for the three most common cancers in 2018 for both sexes.

1.1.2 Classification of lung cancer

Lung cancer is confirmed and diagnosed by a histological or cytological approach (Nizzoli et al. 2011; Rekhtman et al. 2011), and can be defined into two major types: non-small-cell lung cancer (NSCLC, 85 % of all cases) and small cell lung cancer (SCLC, 15 % of all cases) according to the World Health Organization (WHO) classification (Duruisseaux and Esteller 2018; Marx et al. 2015; Travis et al. 2015). This classification reflects the clinical differences among different types of lung cancer, including clinical manifestations, the rate of metastasis and the effectiveness of treatment. Moreover, NSCLCs are further subdivided into lung adenocarcinoma (AC) (~45.0 %) and squamous cell lung carcinoma (SQCLC) (~25.0 %) (Figure 2 (Politi and Herbst 2015; Skoulidis and Heymach 2019; Travis et al. 2015)).

The new classification of lung cancer reflects the better understanding of the molecular characteristics of lung cancer and individual therapy or multi-therapy (Skoulidis and Heymach 2019). For example, mutations of epidermal growth factor receptor (EGFR) or anaplastic lymphoma kinase (ALK) have been shown to be sensitive to targeted therapies such as tyrosine kinase inhibitors (Nakaoku et al. 2014; Shim et al. 2015; Takeuchi et al. 2012). Approximately 75.0 % of all lung adenocarcinoma harbor genetic alterations that lead to promote a series of aberrant signaling pathway such as receptor tyrosine kinase (RTK)/RAS/RAF axis (Cancer Genome Atlas Research 2014) (76.0 % of cases), p53 pathway alteration (63.0 %), and alteration of cell cycle regulators (64.0 %). These targetable genetic alterations hold the promise to be used as therapeutic targets. In SQCLC, although researches show abnormal pathway including phosphatidylinositol-4,5-biphosphate 3-kinase (PI(3)K), rat sarcoma (RAS) and RTK signaling in cancers, related targeted drugs have not been arrived clinical yet so far (Cancer Genome Atlas Research 2014). SCLC is the worst prognosis subtype. Studies have identified *SOX2* and fusion *RLF-MYCL1* as potential targets, however molecular-targeted agents has not yet been developed (Cancer Genome Atlas Research 2014; George et al. 2015).

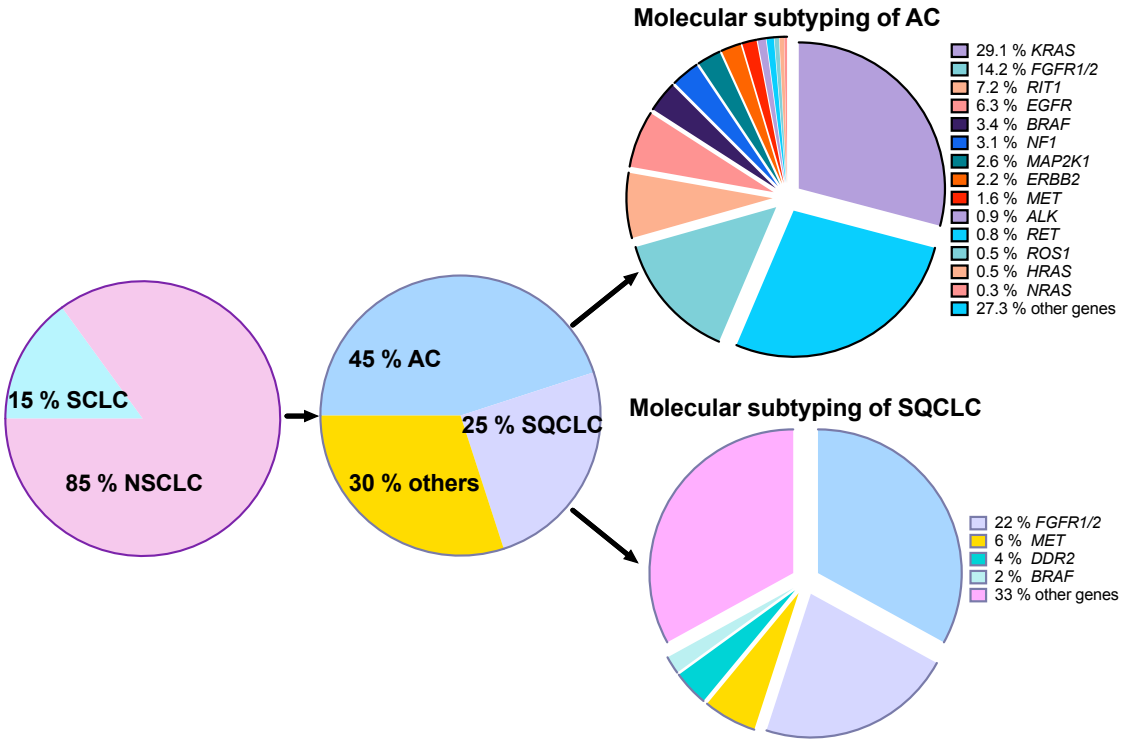

Figure 2: Histological and molecular subtypes of NSCLC. NSCLC: non-small cell lung carcinoma; AC: adenocarcinoma; SQCLC: squamous cell carcinoma.

1.1.3 Treatment of lung cancer

Over the last decades, many important discoveries and efforts have been made to improve curative therapies and decrease the mortality of lung cancer. In general, surgery is still considered standard therapy for early-stage NSCLC (Vansteenkiste et al. 2014). However, patients with NSCLC usually present in advanced stages and are unresectable and require systemic treatment. Recent developments have highlighted molecular distinct and therapeutic vulnerabilities in lung cancer subtypes. These findings have led to the development of targeted therapies and immune checkpoint inhibitors.

Molecular targeted therapy and immunotherapy are the most advanced therapeutic methods in recent years (Borghaei et al. 2015; Mok et al. 2009). Although these methods provide more choices and have substantially increased length and quality of life for some patients with lung cancer (Herbst et al. 2016; Kris et al. 2014), the limitations of these therapeutics are obvious. The molecular

targeted therapy is expensive (Djalalov et al. 2014) and only effective in patients with specific gene mutation (Paez et al. 2004). In the same manner, only some patients with NSCLC benefit from immunotherapy and the effect varies from person to person (Garon et al. 2015; Reck et al. 2016). For patients with SCLC, the chemotherapy or combination with radiotherapy is the primary therapeutic modality on account of few advances in therapeutic options (Okamoto et al. 2007; Takada et al. 2002).

Regardless of histological subtypes and stage of lung cancer, the systemic chemotherapy remains an essential treatment for patients with lung cancer. For early-stage lung cancer, it has been proved that adjuvant cisplatin based chemotherapy could increase improve survival time (Arriagada et al. 2010; Morgensztern et al. 2016; Salazar et al. 2017), and 1-year survival increases in patients with advanced lung cancers using chemotherapy (Paz-Ares et al. 2013; Sandler et al. 2006). According to the American society of clinical oncology and national comprehensive cancer network (NCCN) guidelines, chemotherapy regimens for NSCLC combine two cytotoxic agents in first-line e.g. Pemetrexed and cisplatin is a standard treatment combination for NSCLC (Scagliotti et al. 2008; Schiller et al. 2002).

Pemetrexed is a novel multi-target agent that inhibits hymidylate synthase (TYMS), dihydrofolate reductase (DHFR) and glycinamide ribonucleotide formyltransferase (GARFT) (Adjei 2000; Shih et al. 1997). Cisplatin is a widely used and well-known anticancer drug, which causes deoxyribonucleic acid (DNA) damage, block cell division and induce apoptosis in cancer cells (Dasari and Tchounwou 2014). Although pemetrexed plus cisplatin shows similar efficacy compared to other standard treatment options, the combination of pemetrexed/cisplatin in patients with adenocarcinoma demonstrated a significantly better survival than cisplatin/gemcitabine, as well as better tolerability and good performance (Gadgeel et al. 2011; Paz-Ares et al. 2012; Paz-Ares et al. 2013; Scagliotti et al. 2014; Scagliotti et al. 2008). However, chemotherapy resistance is a major issue in the clinic. Some lung tumors initially response to chemotherapy but then rapidly develop acquired resistance.

1.2 One-carbon metabolism

One-carbon metabolism is a universal metabolic cycle in health and disease and is composed of folate compounds chemical reactions. Furthermore, this pathway is important in nucleic acid synthesis, mitochondrial protein synthesis in, amino acid metabolism, vitamin metabolism (Ducker and Rabinowitz 2017; Shane and Stokstad 1985; Stipanuk 2004; Stover 2004; Tibbetts and Appling 2010).

1.2.1 One-carbon metabolism in cancer

One-carbon metabolism includes both the de novo serine synthesis pathway and folate cycles (Ducker and Rabinowitz 2017). First, 3-phosphoglucerate (3-PG) is a metabolite originated from glucose in glycolysis and can be converted into serine by 3-phosphoglycerate dehydrogenase (PGDH3). In addition, PGDH3 can regulate the release of the tetrahydrofolate (THF) into mitochondria (Fell and Snell 1988; Snell 1984). Subsequently, within the mitochondrial first step of folate cycles, the THF is converted to intermediate metabolites, 5, 10-methenylene-THF or 10-formyl-THF, by their enzymes (Hebbring et al. 2012; Snell et al. 1987), the serine methyltrasferases 2 (SHMT2), methylenetetrahydrofolate dehydrogenase 2 (MTHFD2), separately. Then, the 10-formyl-THF from the mitochondria can be regenerated and converted into the 5, 10-methenylene-THF by an enzyme in the cytosol, MTHFD1 (Tibbetts and Appling 2010; Yang and Vousden 2016). Finally, some of the 5, 10-methenylene-THF is directly converted THF, the rest is involved in the thymidylate synthesis catalyzed by an enzyme, thymidylate synthase (Ducker and Rabinowitz 2017). Furthermore, these enzymes play the key role at maintaining a complete oxidative/reductive cycle also in cancer cells including lung cancer (Figure 3 (Ducker and Rabinowitz 2017)).

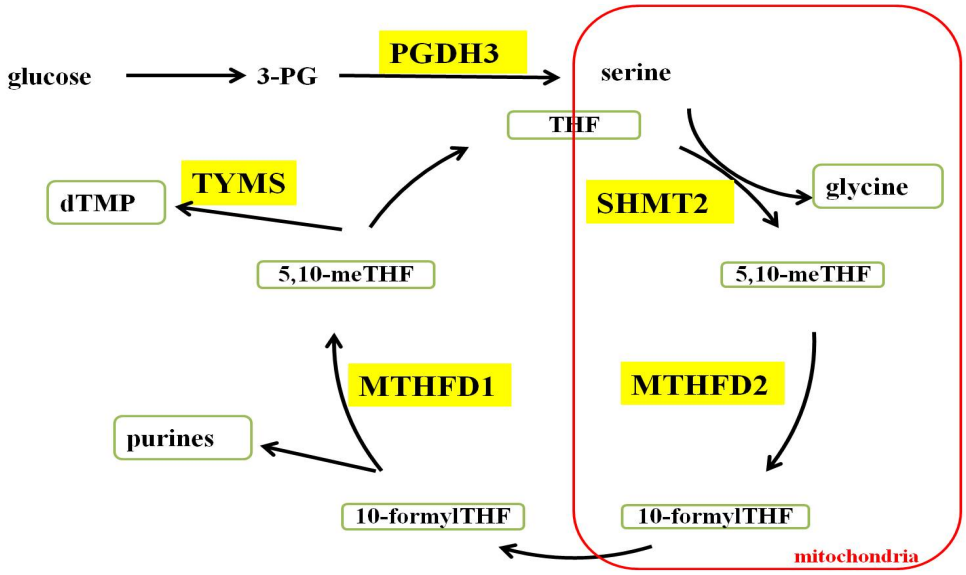

Figure 3: One-carbon metabolism in cancer cells.

Recent studies have identified the de-novo serine synthesis pathway, where the mitochondrial folate metabolism and one-carbon metabolic enzymes are upregulated in cancer cells (Ducker and Rabinowitz 2017; Mehrmohamadi et al. 2014; Newman and Maddocks 2017). These metabolic enzymes play an important role in tumorigenesis and tumor development.

PGDH3 is required for tumorigenesis and proliferation in melanoma and breast cancer cell lines (Locasale et al. 2011; Mullarky et al. 2011; Possemato et al. 2011). Furthermore, studies showed that PGDH3 contributes to cell maintenance, migration and invasion in different cancer including renal cell carcinoma, breast cancer and pancreatic cancer (Samanta et al. 2016; Song et al. 2018; Yoshino et al. 2017).

SHMT2 catalyzes mitochondrial one-carbon metabolism (Ducker and Rabinowitz 2017; Stover and Schirch 1990), is important for tumor growth in various types of cancer such as melanoma, breast cancer, and ovarian carcinoma (Lee et al. 2014) and maintains a compartmentalized one-carbon pathway in mitochondria (Minton et al. 2018).

Nilsson et al. (2014) reported that *MTHFD2* amplification and MTHFD2 protein are significantly increased in cancers such as lung cancer, breast cancer and

colon cancer and MTHFD2 over-expression was shown in proliferating tumors which enhancement growth of cancer cells related with production of excessive one-carbon units for purine synthesis (Christensen and Mackenzie 2008). A study reported that expression of MTHFD2 indicated an increased invasiveness and poor prognosis in cancers including breast cancer, renal cell cancer, and hepatocellular carcinoma (Lehtinen et al. 2013; Liu et al. 2014; Liu et al. 2016; Minton et al. 2018). Knockdown of *MTHFD2* impaired cell proliferation and induced differentiation in acute myeloid leukemia (Pikman et al. 2016).

Together, these findings have provided evidence that the one-carbon metabolism pathway is important for oncogenesis in several cancer entities.

1.2.2 One-carbon metabolism in cancer therapy

Recently, one-carbon metabolism has been developed a promising molecular target in cancer therapy (Dominguez-Salas et al. 2012; Koseki et al. 2018; Nilsson et al. 2014; Williams 2012). Various traditional cytotoxic chemotherapeutic agents, such as antifolates (e.g. Methotrexate, Pemetrexed, Aminopterin), have been developed to target the one-carbon metabolic pathway. PGDH3 has a role of serine synthesis and is associated with tumor cell proliferation. Inhibition of the serine synthesis pathway by specific inhibitors or relative RNAi highly reduces tumor cell growth (Mullarky et al. 2016; Pacold et al. 2016). For example, targeting PGDH3 reduces breast cancer cell proliferation and inhibits xenograft growth specifically in cell lines with overexpression of PGDH3 (Pacold et al. 2016). However, PGDH3 suppression inhibited proliferation in human breast cancer cells even supplementation with additional serine in media was not able to rescue a capacity of cell growth (Chen et al. 2013; Possemato et al. 2011). This suggests that it may bypass the PGDH3 to provide serine to cancer cells by other mechanisms or pathways. Naturally, residual one-carbon metabolism enzymes including SHMT2, MTHFD2, MTHFD1 and TYMS are novel potential targets for cancer treatment given their important role in cancer (Christensen and MacKenzie 2006; Tedeschi et al. 2015). Studies reported the activity of enzymes of the serine synthesis pathway is increased and expression of SHMTs is also uprelated in cancer cells (Snell and Weber 1986). 5-fluorouracil (5-FU) targets TYMS which blocks availability of thymidylate,

inhibits DNA replication and induces apoptosis (Longley et al. 2003). Raltitrexed which targets TYMS is used for the treatment of advanced colorectal cancer (Cunningham et al. 1996; Minton et al. 2018). Pemetrexed inhibits multiple folate-requiring enzymes that are involved in the synthesis of nucleotides, including TYMS, SHMTs, GARFT, and DHFR (Daidone et al. 2011; Smith et al. 2000). Moreover, deleterious side effects of chemotherapy drugs in healthy proliferating cells and chemoresistance in cancer cells are an important problem in clinical practice. The selective inhibition of individual one-carbon metabolism enzymes in cancer cells might reduce adverse side effects.

MTHFD2 is a member of MTHFD enzyme family and necessary for nucleotide synthesis. MTHFD2 is widely found in embryonic, non-differentiated tissues and is almost exclusively expressed in cancer cells (Bolusani et al. 2011; Nilsson et al. 2014). One of mitochondrial folate metabolic enzymes, MTHFD2 has paid much attention as a potential therapeutic target (Miyo et al. 2017; Nilsson et al. 2014; Pikman et al. 2016). For example, adding excess formate to cell cultures failed to rescue MTHFD2 silence cancer cells (Nilsson et al. 2014; Pikman et al. 2016), indicating that MTHFD2 expression may be required for cell growth. However, with following a shift to the cytosolic one-carbon pathway, lack of MTHFD2 did not affect cell survival (Ducker et al. 2016). SHMT2 enzyme knockdown did not observe the blockage of mitochondrial pathway and induce cell death, whereas glycine is deleted from culture medium, SHMT2-knockdown was found to impair cell growth (Jain et al. 2012; Kim et al. 2015).

Locasale et al. (2011) showed that decreasing expression of PGDH3 impaired proliferation in PGDH3 amplified cell lines by generating an inducible shRNA targeting PGDH3 which led to be blunt effects on the growth of breast cancer cells. Small molecule inhibitors of PGDH3 have been identified and were selectively toxic to cancer cell lines and successfully reduced cancer cell proliferation (Mullarky et al. 2016; Pacold et al. 2016). Studies demonstrated that high expression of SHMT2 and MTHFD2 in cancers was associated with lower recurrence-free survival and overall survival time (Koseki et al. 2018; Miyo et al. 2017).

1.3 Aims of the study

Lung cancer is a major cause of cancer related deaths worldwide. With the development of molecular targeted therapy and immunotherapy, the landscape of lung cancer treatment has changed to combination therapy. However, systemic chemotherapy is still an indispensable treatment in lung cancer. Recent studies have demonstrated that one-carbon metabolism enzymes are upregulated in cancer cells. The aim of this study is to specify the role of one-carbon metabolism in lung cancer.

The first part of the project was to characterize the expression and prognostic impact of the one-carbon metabolism enzymes PGDH3, SHMT2, MTHFD2, MTHFD1 and TYMS by immunohistochemistry in human lung cancer samples. The second to evaluate one-carbon metabolism enzymes expression in human lung cancer cell lines.

It has been demonstrated in many tumors that one-carbon metabolism enzymes promote cancer cell proliferation. Hence, RNAi-mediated silencing of one-carbon metabolism enzymes was analyzed in lung cancer cells.

Finally, the changes in the cytotoxicity of cisplatin or pemetrexed agent in lung cancer cells after silencing of one-carbon metabolism enzymes were evaluated.

2 Material

2.1 Chemicals

Table 1: List of chemicals

Chemicals	Manufacturer
Clearify Clearing Agent	American MasterTech, Lodi, California
EnVision Flex Target Retrieval Solution, Ph Low (50X)	Dako, Hamburg, Germany
EnVision Flex Target Retrieval Solution, pH High (50X)	Dako, Hamburg, Germany
Wash Buffer	Dako, Hamburg, Germany
EnVision Flex Peroxidase-Blocking Reagent	Agilent, Santa Clara, California
EnVision Flex Substrate Buffer	Agilent, Santa Clara, California
EnVision Flex+ Mouse Linker SM804	Agilent, Santa Clara, California
EnVision Flex+ Rabbit Linker SM805	Agilent, Santa Clara, California
EnVision Flex/HRP	Agilent, Santa Clara, California
EnVision Flex Substrate Working Solution DAB+ Chromogen	Agilent, Santa Clara, California
Shandon Eosin Y	Thermo Scientific, Waltham, Massachusettes
Hematoxylin 7211	Thermo Scientific, Waltham, Massachusettes
Ethanol 99 %	Chemsolute, Th. Geyer GmbH & Co. KG, Renningen, Germany
Xylol	Chemsolute, Th. Geyer GmbH & Co. KG, Renningen, Germany
Ethanol 96 %	Chemsolute, Th. Geyer GmbH & Co. KG, Renningen, Germany
RPMI-1640 medium	Gibco, Waltham, USA

Chemicals	Manufacturer
Fetal bovine serum (FBS)	Gibco, Waltham, USA
L-Glutamine	Gibco, Waltham, USA
Penicillin-Streptomycin	Gibco, Waltham, USA
0.05 %Trypsin-EDTA (1X)	Gibco, Waltham, USA
Muse™ Count & Viability Kit	Luminex, Austin, USA
4x Laemmli Samper Buffer	Bio-Rad Laboratories, Munich, Germany
10x Tris/Glycine/SDS	Bio-Rad Laboratories, Munich, Germany
Western Lightning Plus-ECL	PerkinElmer, Waltham,USA
CellTiter 96 Aqueous One Solution Reagent	Promega, Madison, Wisconsin, USA
Cisplatin	Hexal AG, Holzkirchen,Germany
HiPerFect Transfection Reagent	Qiagen, Hilden, Germany
Ponceau-S	Sigma-Aldrich, Munich, Germany
Protein marker	Thermo Scientific, Waltham, Massachusettes

2.2 Primary antibodies

Table 2: List of primary antibodies

		Western Blotting	Immunohistochemistry	
Antibodies	**Company**	**concentration**	**concentration**	**pH**
PGDH3	Sigma	1:1000	1:500	6 (low)
SHMT2	Cell signaling	1:1000	1:200	6 (low)
MTHFD2	Abnova	1:1000	1:100	6 (low)

		Western Blotting	Immunohistochemistry	
Antibodies	**Company**	**concentration**	**concentration**	**pH**
MTHFD1	ATLAS	1:1000	1:500	6 (low)
TYMS	Abcam	1:1000	1:50	9 (high)
PARK7	Abcam	1:1000		

2.3 Small interfering RNA (siRNAs)

Table 3: List of siRNAs

Targets	Company
All-star control siRNA	Qiagen, Hilden, Germany
PGDH3 (SI00090405)	Qiagen, Hilden, Germany
SHMT2 (SI04176501)	Qiagen, Hilden, Germany
MTHFD2 (SI02664928)	Qiagen, Hilden, Germany
MTHFD1 (SI02653084)	Qiagen, Hilden, Germany
TYMS (SI02780757)	Qiagen, Hilden, Germany

2.4 Equipment

Table 4: List of equipment

Equipment	Manufacturer
10 % SDS-PAGE Gel	Bio-Rad Laboratories GmbH, Munich, Germany
PVDF membrane	Bio-Rad Laboratories GmbH, Munich, Germany

Equipment	Manufacturer
Heraeus flow hood	Thermo, Fisher Scientific GmbH, Schwerte, Germany
Standard-Incubator	BINDER GmbH, Tuttlingen, Germany
4° Refrigerator	SIMENS Aktiengesellschaft, Munich, Germany
-20° Refrigerator	SIMENS Aktiengesellschaft, Munich, Germany
Systec VX-100, Autoclave	Thermo, Fisher Scientific GmbH, Schwerte, Germany
Systec VE-40, Autoclave	Thermo, Fisher Scientific GmbH, Schwerte, Germany
GFL 1004 Water Bath	GFL Gesellschaft für Labortechnik GmbH, Burgwedel, Germany
Heraeus Microbiological Incubator B12	Thermo, Fisher Scientific GmbH, Schwerte, Germany
IKA Vibrax-VXR Orbital Shaker	KA-Werke GmbH & Co. KG, Staufen, Germany
IKA Vibrax-RCT basic	KA-Werke GmbH & Co. KG, Staufen, Germany
Sanyo MDF-592 Laboratory Freezer	SANYO Electric Co., Ltd., Osaka, Japan
Nalgene® Cryo 1°C Freezing Container	Thermo, Fisher Scientific GmbH, Schwerte, Germany
Eppendorf Centrifuge 5424	Eppendorf Vertrieb Deutschland GmbH, Wesseling-Berzdorf, Germany
Eppendorf Centrifuge 5430R	Eppendorf Vertrieb Deutschland GmbH, Wesseling-Berzdorf, Germany

Equipment	Manufacturer
Eppendorf Pipettes	Eppendorf Vertrieb Deutschland GmbH, Wesseling-Berzdorf, Germany
Eppendorf Centrifuge 5804	Eppendorf Vertrieb Deutschland GmbH, Wesseling-Berzdorf, Germany
Eppendorf ThermoMixer comfort	Eppendorf Vertrieb Deutschland GmbH, Wesseling-Berzdorf, Germany
Trans-Blot® Turbo™ Transfer System	Bio-Rad Laboratories GmbH, Feldkirchen
Polymax 1040 Shakers & Mixers	Heidolph Instruments GmbH & Co.KG, Schwabach, Germany
Analytical Balance Sartorius Research R200D	Sartorius AG, Göttingen, Germany
Zeiss Axiovert 25 mycrosocpy	Carl Zeiss AG, Oberkochen, Germany
Merck's Muse Cell Analyzer	Merck KGaA, Darmstadt, Germany
Scotsman AF 80	SCOTSMAN, Milan, Italy
Olympus BX41	Olympus Europa SE & Co. KG, Hamburg, Germany
Fusion Fx Vilber Lourmat	Vilber Lourmat Deutschland GmbH, Eberhardzell, Germany
Pipette Tips	
PCR tubes	
Multi-tubes	
Reaction tubes	SARSTEDT AG & Co. KG, Nümbrecht, Germany
Cryopure tubes	
TC Flask T25/T75/T175	
Pipette 5ml/10ml/25ml	

2.5 Human tissues

Approval for using patient materials and all information in this study was obtained from the Ethics Committee of the University Medical Center Goettingen (#1-2-08). All procedures were in accordance with the standards declaration of Helsinki and institutional, state, and federal guidelines. Specimens of tumor tissues were obtained from surgical resections at the Department of Thoracic Surgery of the University Medical Center Goettingen.

2.6 Cell lines

There were 16 human lung cancer cell lines in this study, which were purchased from American Type Culture Collection (ATCC):
(1) AC cell lines: H1993, H2228, H3122, HCC44, HCC78, HCC827.
(2) SQCLC cell line: HCC15, H2170, H520, EBC-1, EBC-1KRAS $^{G12D/WT}$.
(3) SCLC cell lines: DMS114, H1339, H69, H82, HCC33

2.7 Software

Table 5: List of software

Software	Company
Microsoft office	Microsoft Corporation, Redmond, USA
ImageJ	National Institute of Health, Bethesda, USA
GraphPad Prism 7	GraphPad Software, San Diego, USA
Magellan™	Tecan Group Ltd., Männedorf, Switzerland
i-control™ Microplate Reader Software	Tecan Group Ltd., Männedorf, Switzerland
ZEN 2012 (blue edition), version 1.1.2.0	Carl Zeiss AG, Oberkochen, Germany

2.8 Laboratory made solutions

Table 6: List of buffer and solution

Buffer and solution	
Stock lysis buffer	150 mM NaCl 50 mM Tris/HCL pH 7.6 5 mM NaF 1 % NP40
Working lysis buffer	10 µl Sodium orthovanadate 40 µl Complete-EDTA 100 µl 2 % Lauryl 850 µl Stock lysis buffer
10x Tris-buffered saline (TBS)	4.2 g Tris 26 g Tris-HCL 292.4 g NaCl pH 7.4 with HCl ddH_2O to 1 L
1x Tris-buffered saline with Tween 20 (TBST)	10 ml Tween 20 1 L 10x Tris-buffered saline 9 L ddH_2O
Ponceau solution	0.2 g Ponceau-Rot 3 ml Acetic acid ddH_2O to 100 ml

3 Methods

3.1 Immunohistochemistry (IHC)

The formalin-fixed and paraffin-embedded lung cancer tissues from 323 patients were combined into tissue microarrays (TMAs). Immunohistochemistry stainings were performed on a Dako Omnis advanced staining system and on the Dako Autostainer link 48 with the following steps: 2-µm tissue sections were immersed in clearing agent for one cycle of one minute and subsequently incubated in EnVision Flex Target Retrieval Solution, pH low or high (see Material 2.2) for 30 min. Next, slides were incubated with the primary antibodies at room temperature (RT) for 30 min and blocked in EnV FLEX Peroxidase-Blocking reagent for 3 min. Then, slides were incubated with the secondary antibody EnVision FLEX/HRP for 20 min and DAB for 5 min. Finally, samples were incubated in Hematoxylin for 3 min for counterstaining.

3.2 IHC evaluation

The TMAs stainings were analyzed by light microscopy at 100x and 400x. Staining intensity of PGDH3, SHMT2, MTHFD2, MTHFD1 and TYMS in the cytoplasm of cancer cells was classified as follows: 0 means negative expression; 1 means weak expression; 2 means strong expression.

3.3 Cell culture

Human lung cancer cells preserved in liquid nitrogen -196°C were thawed in a water bath at 37°C for 2-3 min and then transferred to sterile centrifuge tubes with 9 ml complete culture medium, next, centrifuged at 1,200 rounds per minute (RPM) at RT for 5 min. The supernatant was discarded. Subsequently, cells were transferred in 5 ml culture medium to culture flasks. Cell lines were cultured in RPMI-1640 medium supplemented with 10 % fetal bovine serum (FBS), 1 % Penicillin/Streptomycin and 1 % L-Glutamine in a humidified atmosphere of 5 % CO_2 at 37°C. Generally, the medium was refreshed every 48-72 h. When the cells

were approximately 80 % confluent, they were split at a 1:2 or 1:5 split ratio. All sub-cultures of cells were under 30 passages. Cultures were monitored using an inverted microscope to evaluate cell density and to confirm that there were no bacterial, fungal and mycoplasma. Adherent cell lines were harvested when cell confluency was close to 80 %. Old media was removed, cells were washed with 1x PBS twice then added about 2-3 ml 0.05 % Trypsin-EDTA (1X) for 5 min to trypsinize cells. Cells were re-suspended and transferred into a sterile centrifuge tube with 10 ml culture media. Then, after centrifuging at 1,200 RPM and RT for 5 min, the supernatant was removed and the pellet was re-suspended by adding freezing medium. The vials were aliquoted to 1 ml per vial, then placed in a freezing container and frozen overnight at -80°C. Vials were transferred to liquid nitrogen for indefinite storage.

3.4 Cell counting

Cells were harvested and re-suspended in cell culture medium as described in the cell culture to create single-cell suspensions, and then mixed cells with Muse™ Count/Viability Reagent in a sample tube: 20 µl of cell suspension into 380 µl of Count/Viability Reagent. Samples were subjected to load and run assay by Muse™ Cell Analyzer with Count/Viability program.

3.5 Protein isolation and western blot analysis

1-5 × 10^6 cells were washed twice with cold 1x PBS and collected in Eppendorf tubes. Afterwards, cells were lysed with lysis buffer on ice for 30 min, then centrifuged at 14,000 RPM, 4°C for 20 min. The supernatant was transferred to a new Eppendorf tube. The DC™ protein assay kit was used to determine the concentration of protein. Solution S was diluted 1:50 in solution A. 20 µl of this mixture were added to a 96-well plate. 2 µl protein lysate was added and 200 µl solution B was added, then incubated for 10 min at RT. The absorbance was measured by Magellan™ software and the concentration was calculated according to an internal standard curve. The protein lysates were dissolved in 4x Laemmli Samper buffer (dilute sample 3:1 with sample buffer) then denatured at

95°C for 5 min. Then equivalent protein sample (20 µg) was separated by 4-12 % SDS-PAGE gel and electro-transferred onto polyvinylidene difluoride (PVDF) membrane by trans-blot turbo transfer system. The membrane was qualified with Ponceau-S and then blocked in 5 % fat-free milk for 1 h at RT. Subsequently, the membrane was incubated overnight in primary antibody (Table 2) on the shaker at 4°C. On the second day, the membrane was rinsed 3 times for 10-15 min at RT with 1x TBST and incubated with secondary antibody for 1 h on the shaker at RT. Next, the membrane was rinsed 3 times for 10-15 min at RT with 1x TBST. Capturing signal was performed on a fusion imaging system. PARK7 was used as internal loading control (Wisniewski and Mann 2016). A summary of primary antibodies used is shown in materials (2.2).

3.6 Cell viability assay

2.500 cells were plated in 96-well plates in 100 µl/well culture medium. After 24 h of incubation the cells were treated with various concentration of cisplatin (0 µM, 1 µM, 5 µM, 10 µM, 50 µM, 100 µM.) for 72 h or pemetrexed (0 µM, 0.005 µM, 0.025 µM, 0.05 µM, 0.25 µM, 0.5 µM, 2.5 µM, 5 µM, 25 µM, 50 µM) for 96 h. For measurements, the cells were incubated with 20 µl of CellTiter 96 aqueous one solution reagent at 37°C, 5 % CO_2 for 2 h. The 96-well plates were measured by i-control™ microplate reader software with the absorbance at 490 nm and the background absorbance at 650 nm subtracted. All experiments were repeated at least three times and each sample was plated in triplicate. The half maximal inhibitory concentration (IC50) was calculated using GraphPad Prim 7.0.

3.7 siRNAs transfection

Unless stated otherwise, cells were transfected with 20 nM siRNA using HiPerFect transfection reagent (Qiagen) according to the manufacturer's protocol. A summary of siRNAs used is shown in materials (2.3).

For cell viability assays: 1-5 × 10^4 cells/well were seeded into the 96-well plate with 175 µl culture medium. siRNAs or control siRNA were incubated in HiPerFect transfection reagent and culture medium without serum for 5-10 min at RT to allow formation of transfection complexes. 25 µl siRNA-HiPerFect reagent transfection complexes were added into a single well. After incubation for 24 h, 48 h, 72 h, 96 h, 120 h, 144 h, the 96-well plates were measured using CellTiter 96 aqueous one solution reagent.

For western blot analysis 100 µl transfection medium containing 12 µl HiPerFect, 9.6 µl siRNA/negative control (20 nM) and 78.4 µl RPMI without serum was incubated at RT for 20 min and added to 1.5-6 × 10^5 cells in 6-well plate with 2.300 µl culture medium just after seeding. Cells were collected for protein isolation and western blot analysis was performed after incubating for 72 h or 96 h.

3.8 Statistical analyses

Statistical analysis was performed using GraphPad Prim 7 and ImageJ. Overall survival was analyzed using Kaplan-Meier analyses, differences in survival were calculated by log-rank test. All cell experiments were repeated at least three times and data were expressed as mean ± standard error of mean (SEM). Statistical differences were tested by paired, two-tailed Student's *t*-test. The correlation between one-carbon metabolism enzymes and IC50 was assessed by Pearson's correlation test. Statistical differences were considered significant at $P < 0.05$.

4 Results

4.1 Expression of one-carbon metabolism enzymes in human lung cancer samples.

In order to detect the expression and role of one-carbon metabolism enzymes (highlighted in Figure 4) in human lung cancer, formalin-fixed and paraffin-embedded lung cancer tissues from 323 patients were assembled into tissue microarrays. The collection included AC (n = 103), SQCLC (n = 183) and SCLC (n = 37). The number of male patients (AC: n = 59 (57.3 %), SQCLC: n = 154 (84.2 %), SCLC: n = 27 (73.0 %)) was higher than female patients (AC: n = 44 (42.7 %), SQCLC: n = 29 (15.8 %), SCLC: n = 10 (27.0 %)). The median age (AC group: 67 years (range 34-85), SQCLC group: 66 years (range 42-83), SCLC group: 67 years (range 50-81)) was similar among these three groups. More than half of patients with AC (65.1 %) and SQCLC (76.5 %) showed a moderately differentiated disease, while all SCLC were poorly differentiated by definition (100.0 %). The frequency of T1 stage in AC patients was 50.0 %, 24.9 % in SQCLC patients, and 75.7 % in SCLC patients. The frequency of patients in with no lymph node metastasis (AC: 63.3 %, SQCLC: 55.6 %, SCLC: 75.0 %) was higher than the frequency of N1, N2 and N3 together. The median follow-up time was 23, 30 and 58 months for AC, SQCLC and SCLC, respectively and 201 deaths were reported. The clinical characteristics are shown in Table 7.

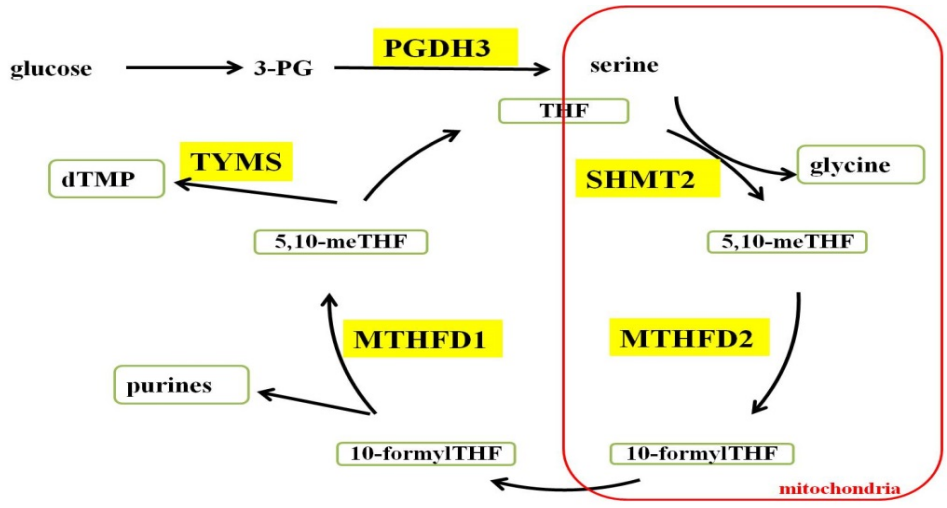

Figure 4: The one-carbon metabolism enzymes (highlighted) in cancer cells.

Table 7: Clinical data summary

Characteristic	AC (n = 103)	SQCLC (n = 183)	SCLC (n = 37)
Gender:			
Male (%)	59 (57.3)	154 (84.2)	27 (73.0)
Female (%)	44 (42.7)	29 (15.8)	10 (27.0)
Age median (range, years)	67 (34-85)	66 (42-83)	65 (50-77)
Tumor grade:			
G 1 (%)	9 (8.7)	0 (0.0)	0 (0.0)
G 2 (%)	67 (65.1)	140 (76.5)	0 (0.0)
G 3 (%)	27 (26.2)	43 (23.5)	37 (100.0)
Tumor stage:			
T stage:	n = 102	n = 181	n = 37
T 1 (%)	51 (50.0)	45 (24.9)	28 (75.7)
T 2-4 (%)	51 (50.0)	136 (75.1)	9 (24.3)
N stage:	n = 98	n = 178	n = 28
N 0 (%)	62 (63.3)	99 (55.6)	21 (75.0)
N 1-3 (%)	36 (36.7)	79 (44.4)	7 (25.0)
Median follow-up time (range, months)	23 (1-128)	26 (1-196)	34 (1-125)
Reported deaths (%)	48 (46.7)	131 (71.6)	22 (59.5)

4.1.1 Expression of PGDH3 in human lung cancer samples.

The described tissue samples of human lung cancers were immunohistochemically stained for PGDH3 and revealed a positive signal in the cytoplasma of the cancer cells. Signals were classified as either negative (Figure 5 A), weak (Figure 5 B) or strong staining (Figure 5 C) based on signal intensity. As shown in figure 5 D, the expression of PGDH3 varied considerably with a weak

or strong expression in 64.7 % of AC, 91.1 % in SQCLC and 100.0 % in SCLC. Patients with pulmonary adenocarcinomas showed significant differences (*P* = 0.036) in overall survival between negative (median survival 44 months), weak (median survival 35 months) and strong staining (median survival 32 months), while there was no significant difference in both SQCLC (*P* = 0.292) and SCLC (*P* = 0.417) (Figure 5 E).

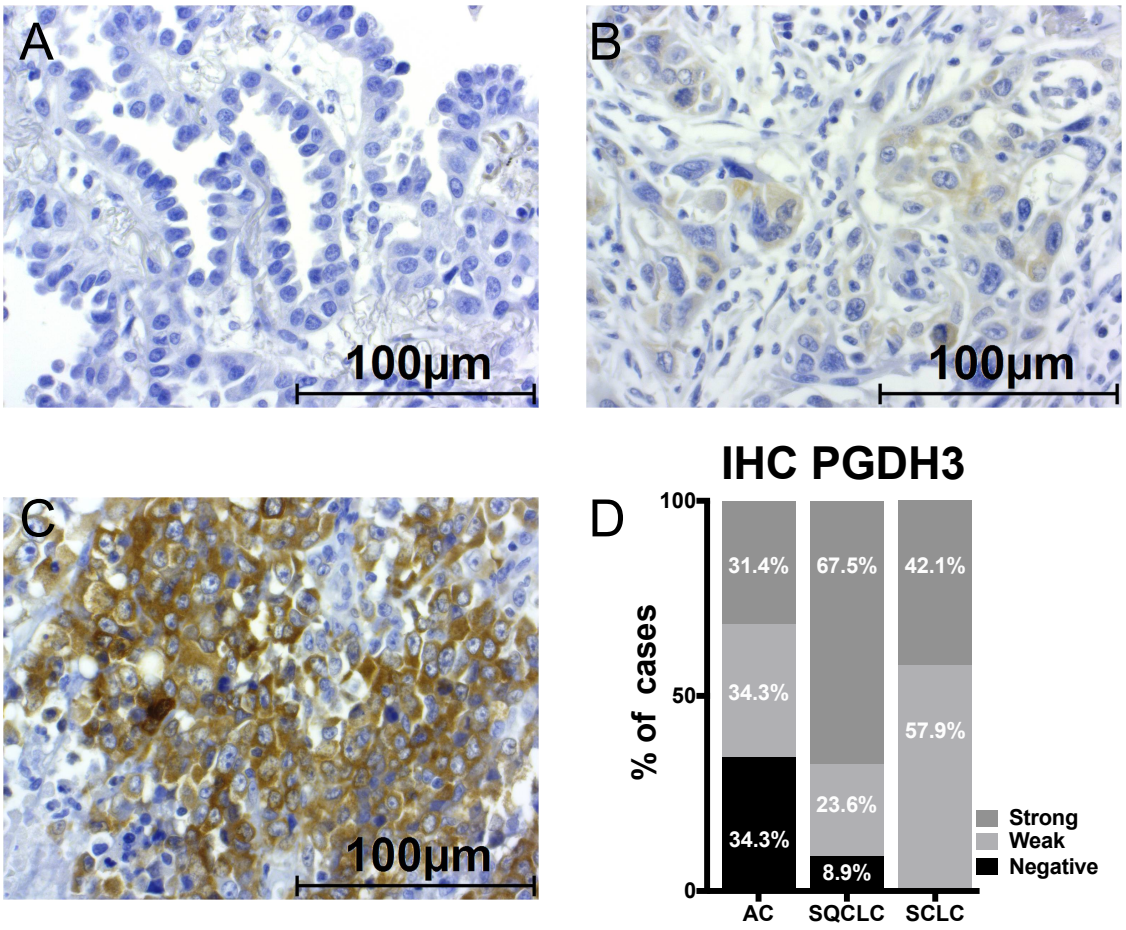

E

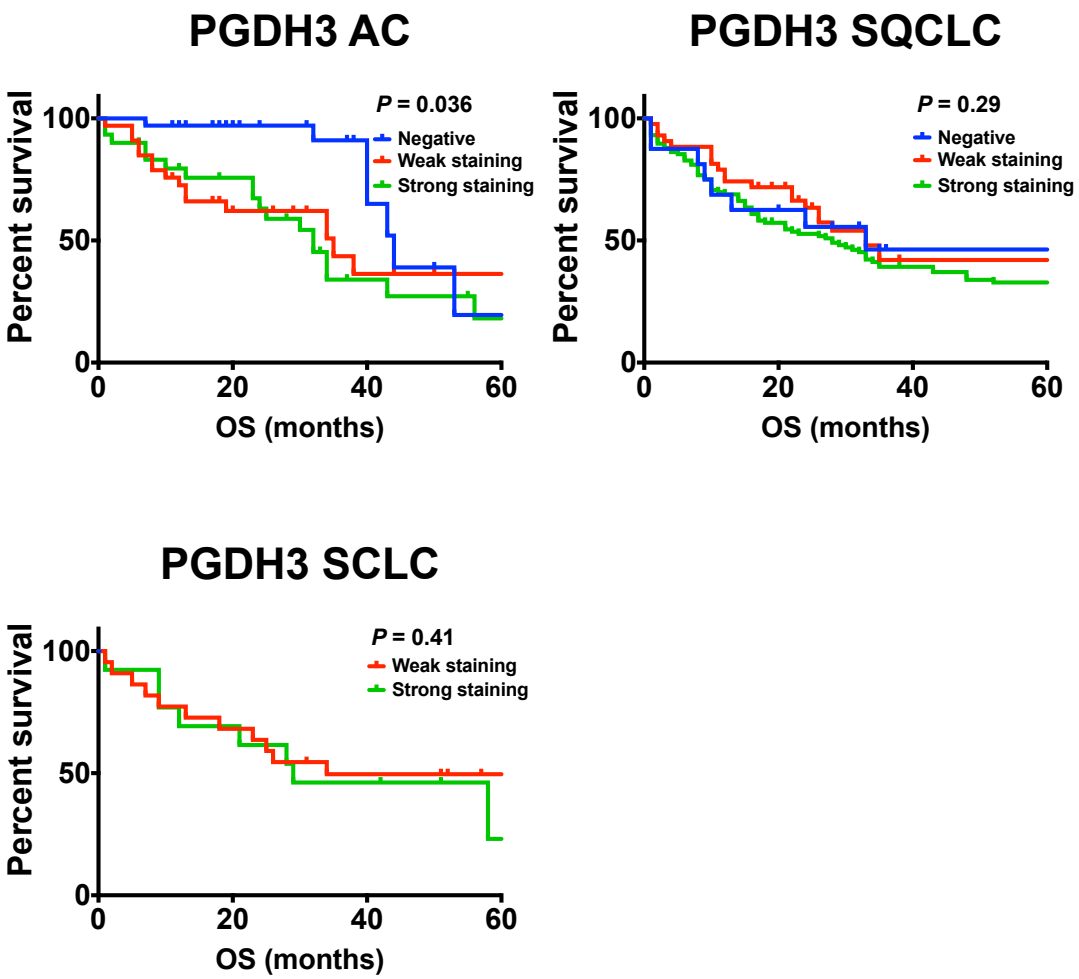

Figure 5: Prognostic significant of expression PGDH3 protein in lung cancer. A-D. Human lung cancer tissues were immunohistochemically stained to show the expression of PGDH3 protein: Negative expression of PGDH3 (A). Positive PGDH3 protein signal in the cytoplasm of cancer cells including weak staining (B) and strong staining (C) on the basis of signal intensity. (D) The fraction of PGDH3 expression in human lung cancer tissues. (E) Survival analysis using Kaplan-Meier estimate and log-rank test grouped by IHC score (IHC: immunohistochemistry, AC: adenocarcinoma, SQCLC: Squamous cell lung carcinoma, SCLC: Small cell lung cancer).

4.1.2 Expression of SHMT2 in human lung cancer samples.

As previously described for PGDH3, the expression of SHMT2 was immunohistochemically examined and classified as negative (Figure 6 A), weak (Figure 6 B) or strong staining (Figure 6 C). The expression of SHMT2 in patients with AC (63.3 %), SQCLC (85.9 %), SCLC (92.1 %) is shown in figure 3-3 D.

Kaplan-Meier analysis showed no significant differences in overall survival in patients with AC (*P* = 0.067), SQCLC (*P* = 0.42), SCLC (*P* = 0.73) (Figure 6 E).

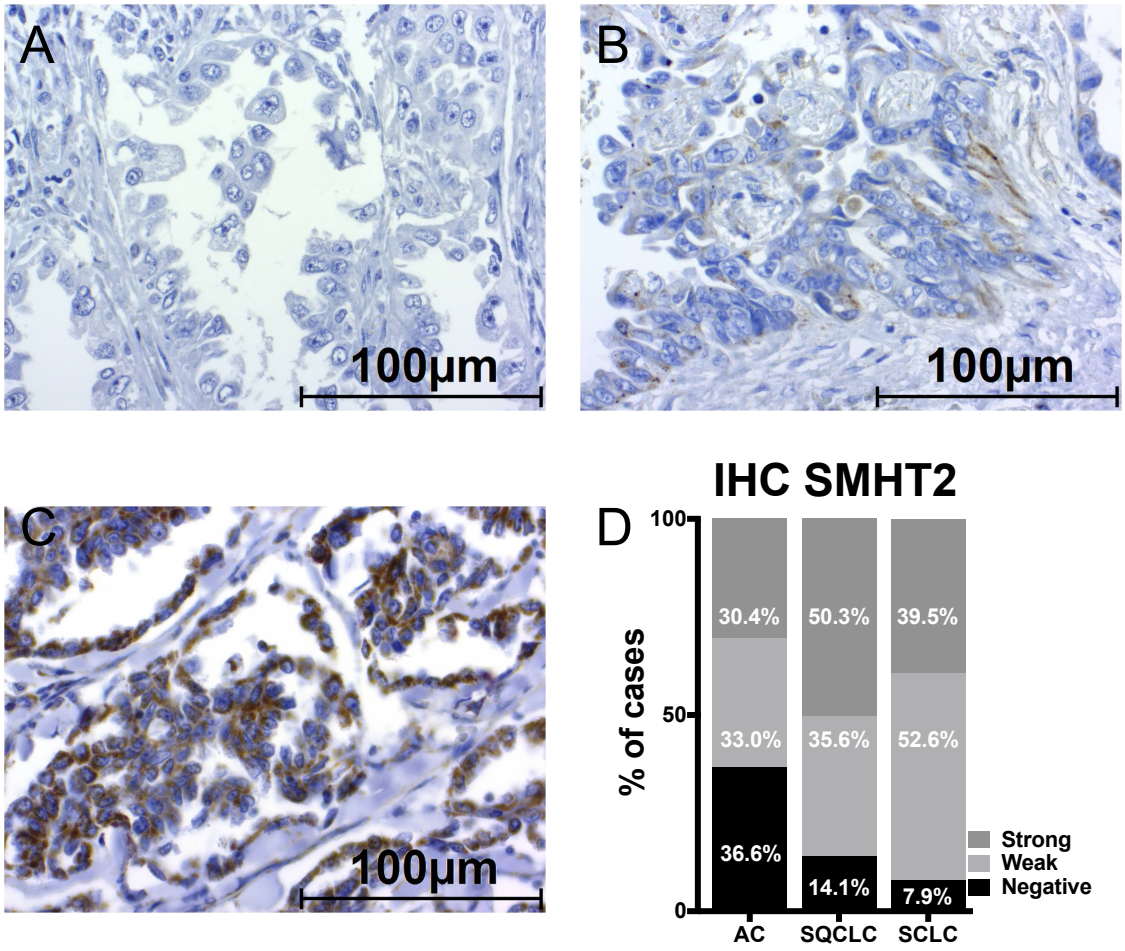

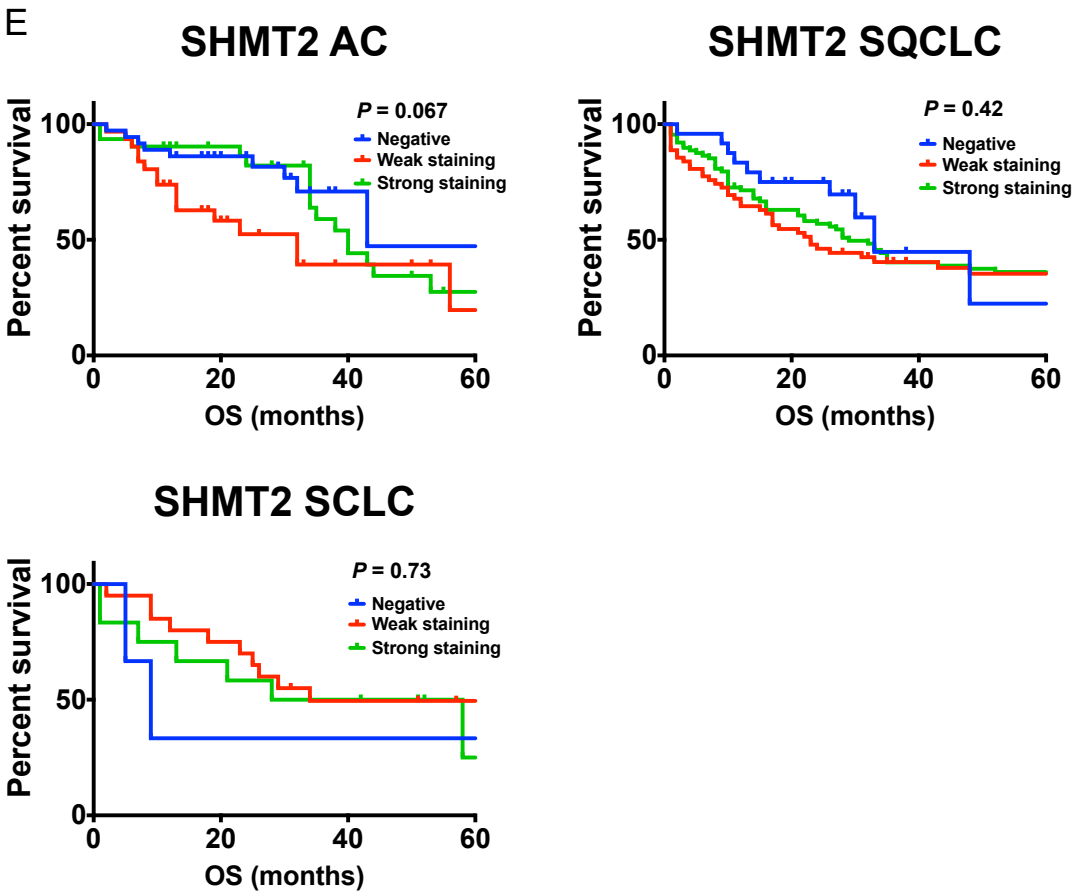

Figure 6: Expression of SHMT2 protein in lung cancer. A-D. Human lung cancer tissues were immunostained to show the expression of SHMT2 protein: Negative expression of SHMT2 (A). Positive SHMT2 protein signal in the cytoplasm of cancer cells including weak staining (B) and strong staining (C) on basis of signal intensity. (D) The fraction of SHMT2 expression in human lung cancer tissues. (E) Survival analysis using Kaplan-Meier estimate and log-rank test grouped by IHC score.

4.1.3 Expression of MTHFD2 in human lung cancer samples.

The expression of MTHFD2 was examined as described before and staining was again classified as either negative (Figure 7 A), weak (Figure 7 B) or strong staining (Figure 7 C). MTHFD2 protein was strongly expressed in SQCLC (81.2 %), SCLC (81.6 %), and AC (50.0 %) (Figure 7 D). Kaplan-Meier estimation of overall survival of patients among negative (median survival 43 months), weak staining (median survival 34 months) and strong staining (median survival 23 months) revealed a significant difference in AC (P = 0.044), but not in SQCLC and SCLC (Figure 7 E).

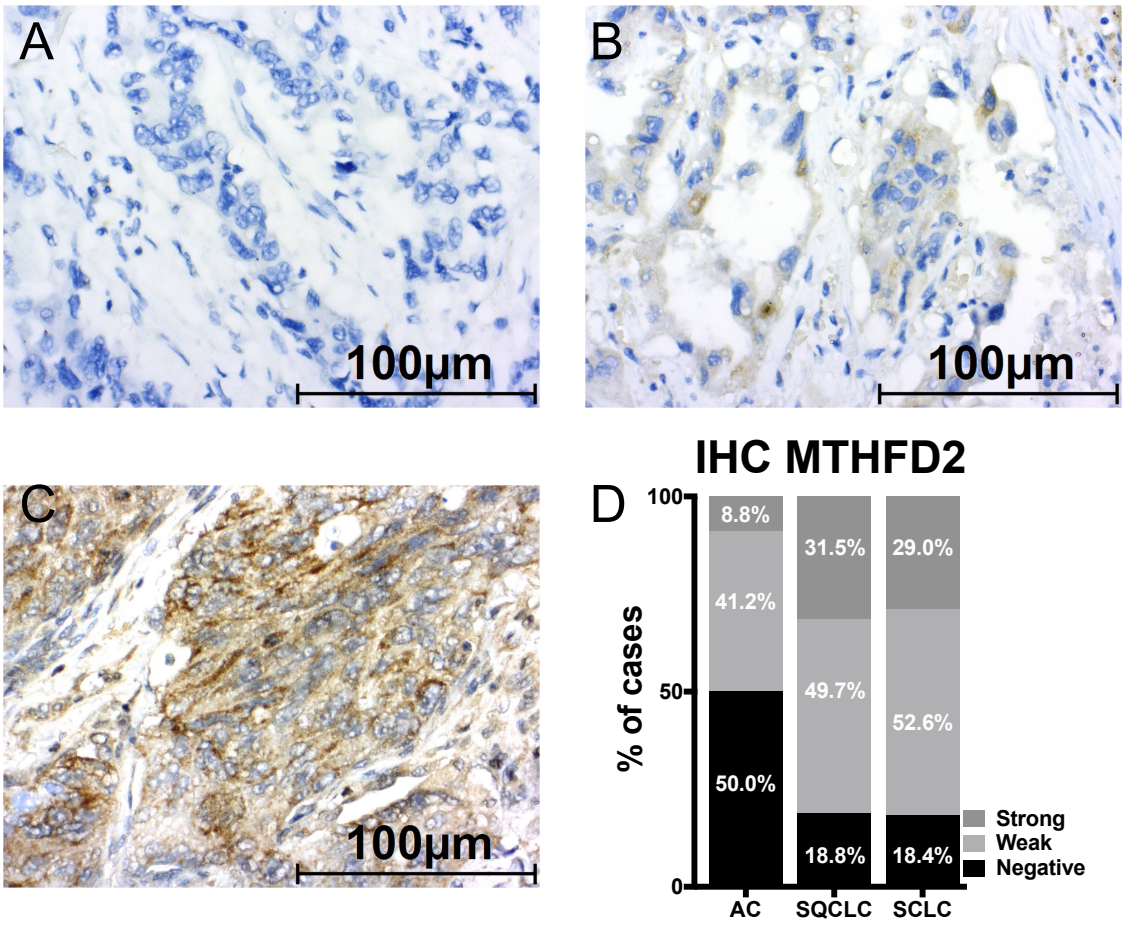

E

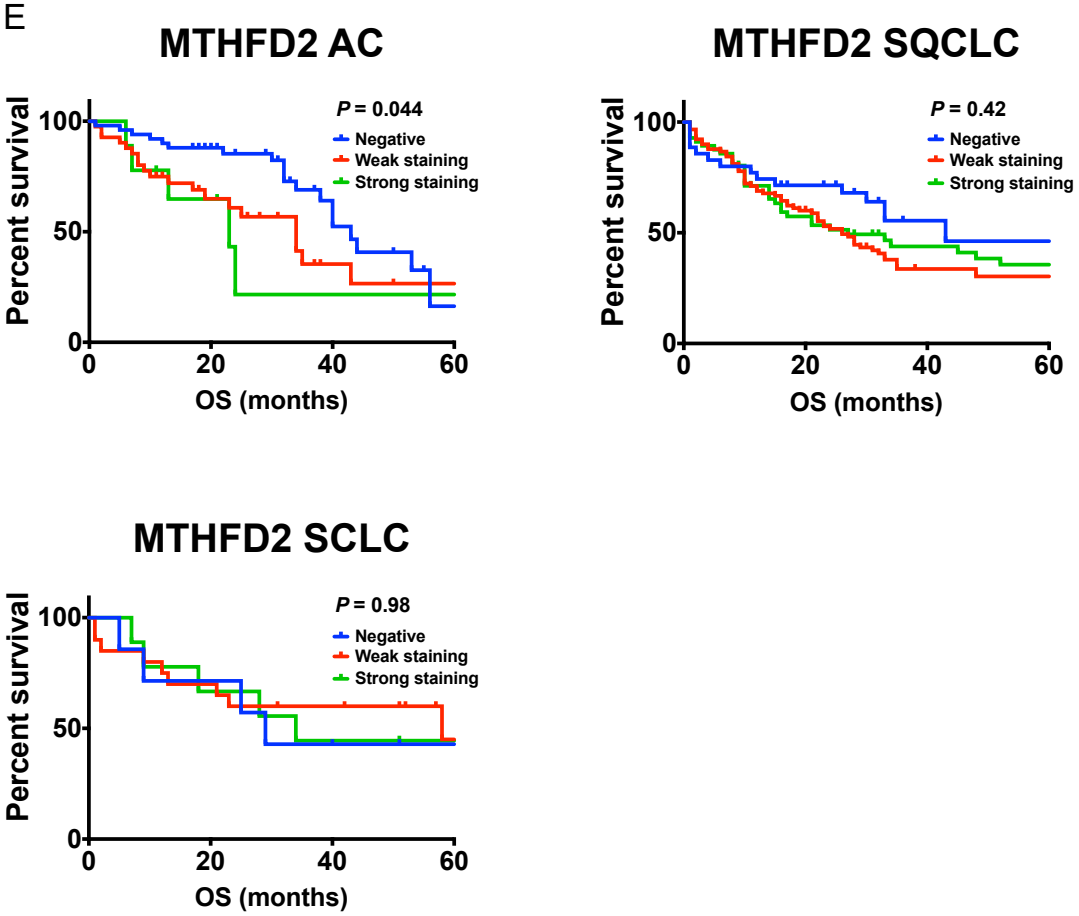

Figure 7: Prognostic significant of expression MTHFD2 protein in lung cancer. A-D. Human lung cancer tissues were immunostained to show the expression of MTHFD2 protein: Negative expression of MTHFD2 (A). Positive MTHFD2 protein signal is brown particles-like distribution in the cytoplasm of cancer cells including weak staining (B) and strong staining (C) on basis of signal intensity. (D) The fraction of MTHFD2 expression in human lung cancer tissues. (E) Survival analysis using Kaplan-Meier estimate and log-rank test grouped by IHC score.

4.1.4 Expression of MTHFD1 in human lung cancer samples.

The same immunohistochemical analysis was performed for MTHFD1 (negative (Figure 8 A), weak (Figure 8 B) and strong staining (Figure 8 C)). IHC results showed expression of MTHFD1 in patients among AC (94.0 %), SQCLC (84.8 %) and SCLC (82.4 %) (Figure 8 D). Kaplan-Meier analysis showed no significantly difference in overall survival of patients with AC (P = 0.278), SQCLC (P = 0.984), or SCLC (P = 0.991) (Figure 8 E).

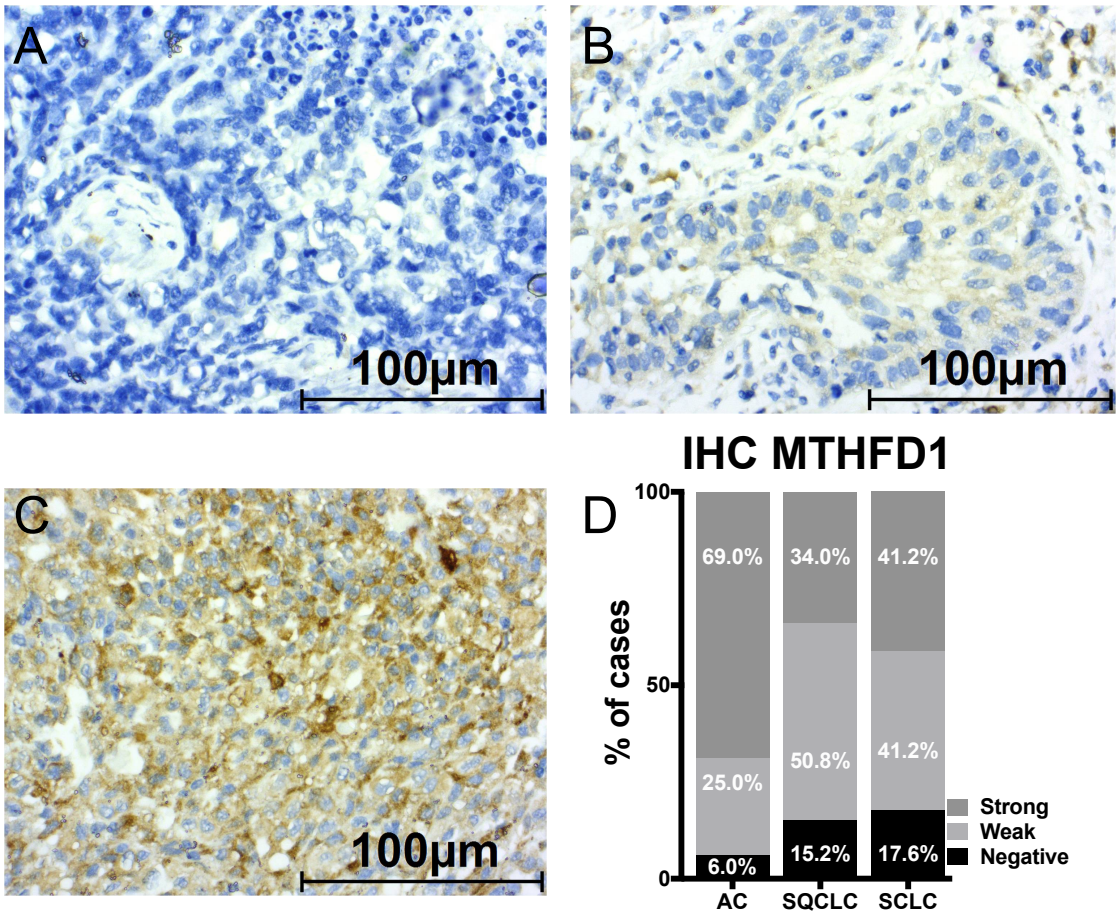
A
100μm
B
100μm
C
100μm
D
IHC MTHFD1
% of cases
100
50
0
69.0%
25.0%
6.0%
34.0%
50.8%
15.2%
41.2%
41.2%
17.6%
AC
SQCLC
SCLC
Strong
Weak
Negative

E

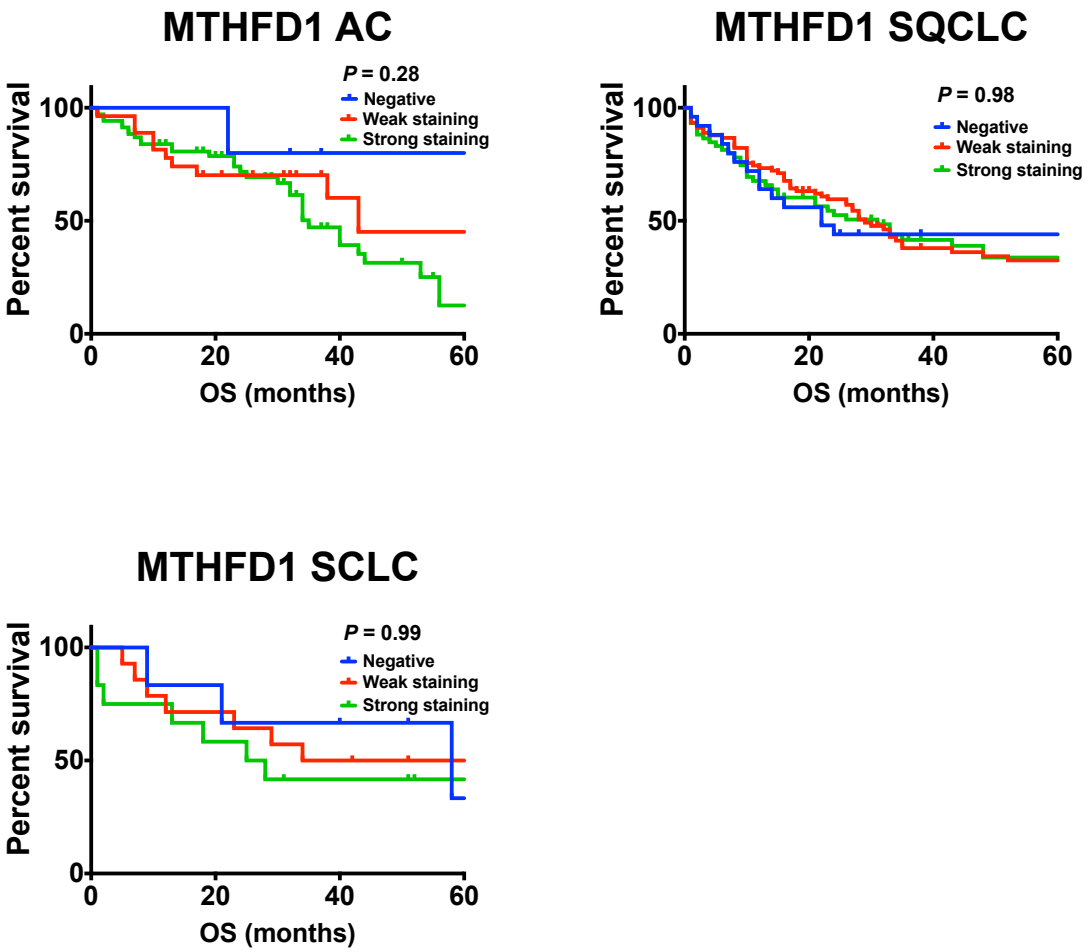

Figure 8: Expression of MTHFD1 protein in lung cancer. A-D. Human lung cancer tissues were immunostained to show the expression of MTHFD1 protein: Negative expression of MTHFD1 (A). Positive MTHFD1 protein in the cytoplasm of cancer cells including weak staining (B) and strong staining (C) on basis of signal intensity. (D). The fraction of MTHFD1 expression in human lung cancer tissues. (E). Survival analysis using Kaplan-Meier estimate and log-rank test grouped by IHC score.

4.1.5 Expression of TYMS in human lung cancer samples.

On the basis of mentioned IHC criteria, TYMS was classified as either negative (Figure 9 A), weak (Figure 9 B) or strong staining (Figure 9 C). Expression of TYMS was seen in 86.2 % of patients with AC, 80.0 % in SQCLC, and 89.2 % in SCLC (Figure 9 D). No significant differences in overall survival of patients with AC (*P* = 0.262), SQCLC (*P* = 0.349), and SCLC (*P* = 0.609) were obtained by Kaplan-Meier analysis (Figure 9 E).

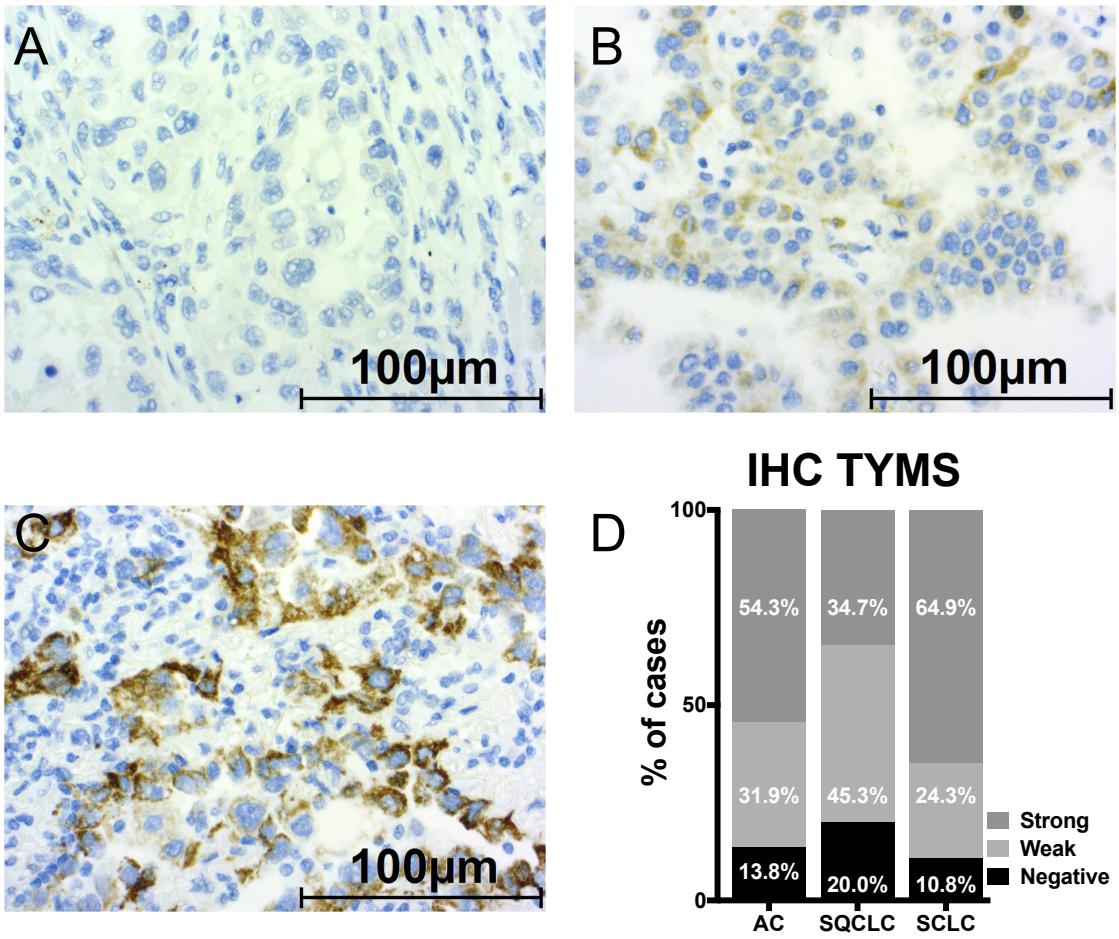

E

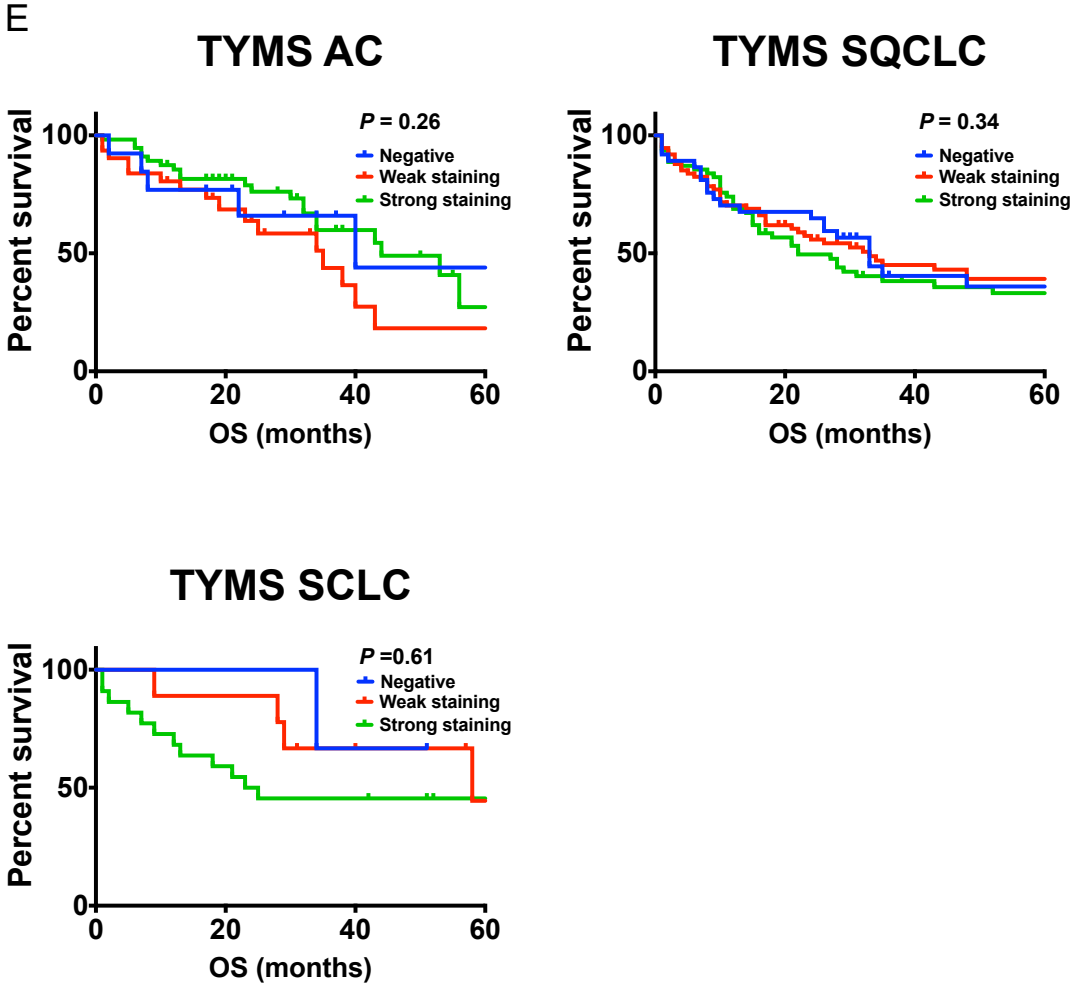

Figure 9: Expression of TYMS protein in lung cancer. A-D. Human lung cancer tissues were immunostained to show the expression of TYMS protein: Negative expression of TYMS (A). Positive TYMS protein signal in the cytoplasm of cancer cells including weak staining (B) and strong staining (C) on basis of signal intensity. (D) The fraction of TYMS expression in human lung cancer tissues. (E) Survival analysis using Kaplan-Meier estimate and log-rank test grouped by IHC score.

4.2 Expression of one-carbon metabolism enzymes in lung cancer cell lines.

In order to investigate the function of one-carbon metabolism enzymes in human lung cancer, western blot analysis and cell viability assay were performed *in vitro*. Western blot analysis was used to examine the expression of one-carbon metabolism proteins in human lung cancer cell lines grouped by AC (n = 6), SQCLC (n = 5) and SCLC (n = 5) and to validate knockdown. To explore whether the one-carbon metabolism enzymes are associated with tumor cell proliferation, a cell viability assay was used to determine the cell viability by knockdown of one-carbon metabolism enzymes through siRNAs.

4.2.1 PGDH3 enzyme in human lung cancer cell lines.

As shown in figure 10 A, western blots analysis showed a differential expression of PGDH3 in human lung cancer cell lines. Intensity of western blot bands were qualified using ImageJ and results presented in figure 10 B. The cell line with the highest expression quantity of PGDH3 was eighteen times higher than the lowest one in AC cell lines, four times higher than the lowest one in SQCLC cell lines, seven times than the lowest one in SCLC cell lines. Then, cells were transfected with siRNAs targeting *PGDH3* or control siRNA for 72 h and cell lysates were analyzed again by western immunoblotting to verify the decreased expression of PGDH3 compared to control siRNA (Figure 10 C).

Subsequently cell proliferation was assessed by cell viability assay and revealed that cell proliferation of all AC cell lines was significantly reduced by 70.0 % compared to controls at day 6 (Figure 11 A). However, cell growth did not change when PGDH3 was knocked down with siRNA in SQCLC cell lines (Figure 11 B) and SCLC cell lines (Figure 11 C). Silencing *PGDH3* did thus not affect cell proliferation of SQCLC and SCLC cell lines.

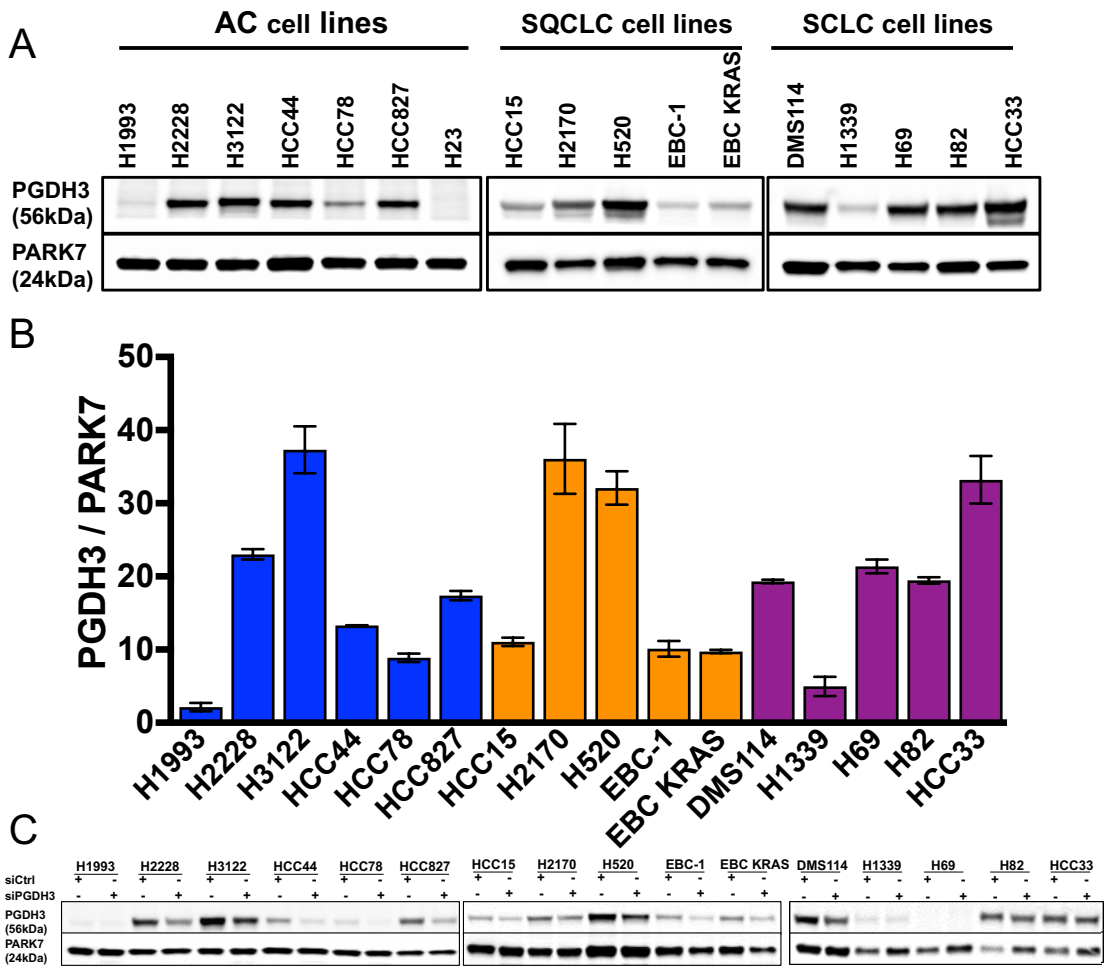

Figure 10: Expression of PGDH3 in human lung cancer cell lines. (A). Western blot analysis showing the expression of PGDH3 protein in AC, SQCLC and SCLC cell lines. PARK7 used as a loading control. Relative molecular mass in kDa shown on the left. The pictures are representative for three independent experiments. (B). Signal intensities of PGDH3 from AC, SQCLC and SCLC cell lines were normalized to PARK7 using ImageJ (the data are represented as mean ± *SEM* of three independent experiments). (C). Western blot analysis showing the effect of control siRNA and PGDH3 siRNA on expression of PGDH3 at protein lever in AC, SQCLC and SCLC cell lines after transfecting for 72 h.

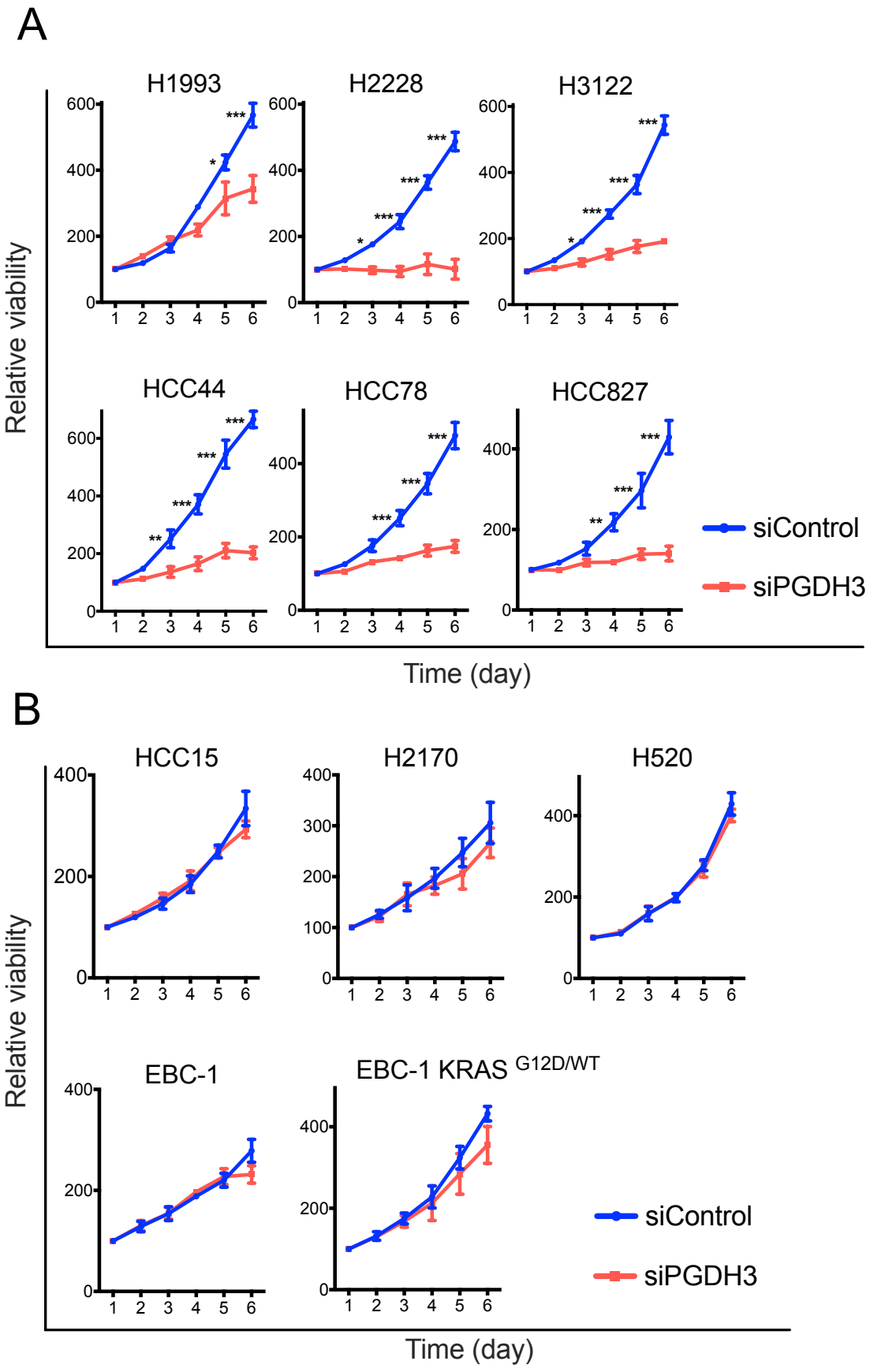
A
H1993
H2228
H3122
HCC44
HCC78
HCC827
Relative viability
Time (day)
siControl
siPGDH3
B
HCC15
H2170
H520
EBC-1
EBC-1 KRAS G12D/WT
Relative viability
Time (day)
siControl
siPGDH3

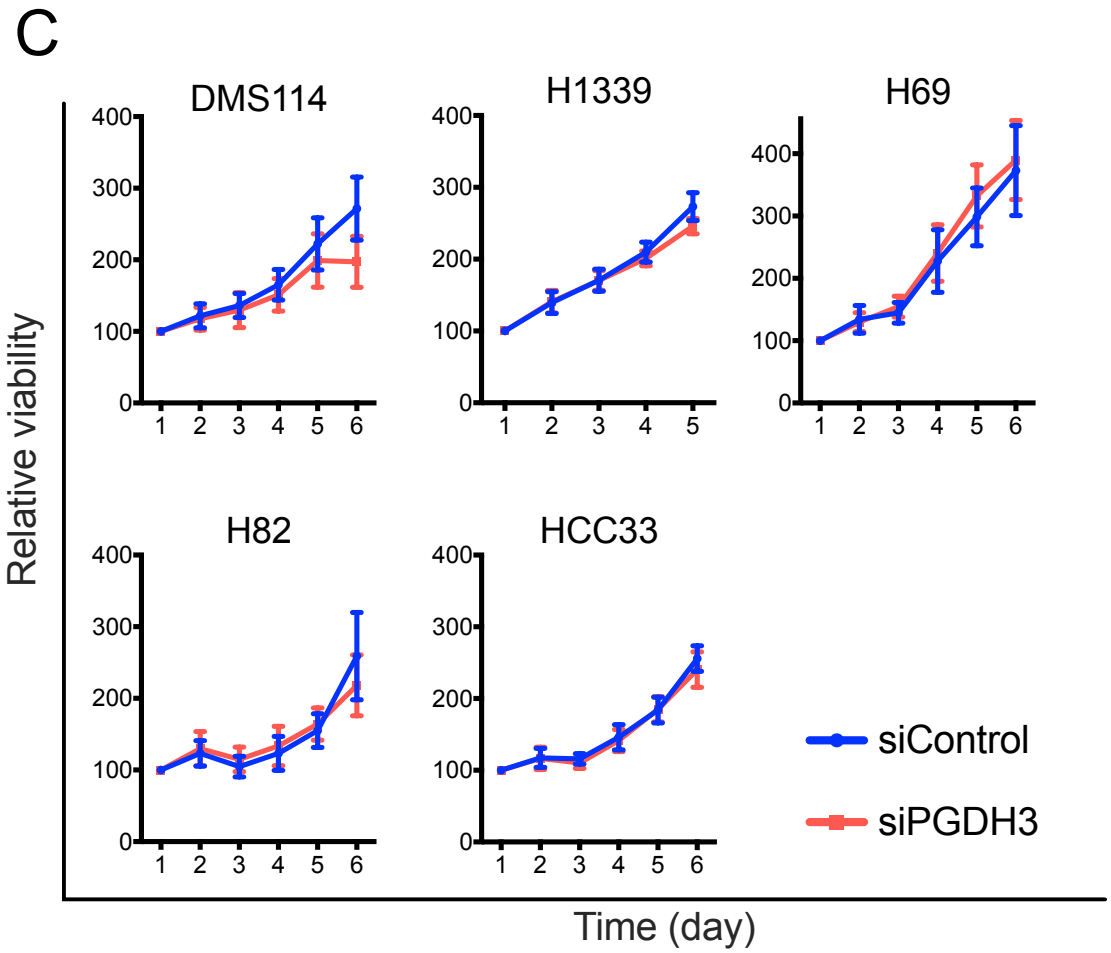

Figure 11: Knockdown of PGDH3 significant reduced cell proliferation of lung AC cell lines. Cell viability assays showing the cell proliferation of the AC (A), SQCLC (B), and SCLC cell lines (C) after transfecting of siRNA against PGDH3 or control siRNA (the data are represented as mean ± *SEM* of at least three independent experiments with three technical replicates each, two-tailed Student's t-test: * $P < 0.05$,** $P < 0.01$,*** $P < 0.001$).

4.2.2 SHMT2 enzyme in human lung cancer cell lines.

The expression of SHMT2 protein was examined by western blot analysis (Figure 12 A). Intensity of western blot bands was normalized to internal loading control PARK7 using ImageJ software. As shown in figure 12 B, all of the examined cell lines expressed SHMT2 but to a various degree. Expression of SHMT2 in AC and SCLC cell lines was similar. The highest expression of SHMT2 was found in the SQCLC cell line H2170.

Next, the described cell lines were transfected with siRNAs targeting SHMT2. Cells were incubated with SHMT2-siRNA or control siRNA for 72 h and then collected for cell lysis for western blot analysis. Results showed that SHMT2 protein levels were significantly inhibited by SHMT2 siRNA compared to control siRNA (Figure 12 C).

Further, cell proliferation was determined by cell viability assays. Cell proliferation was significantly reduced after transfecting SHMT2 siRNA for 4 days compared to control siRNA in AC cell lines (Figure 13 A). Although cell proliferation of HCC15, one of SQCLC cell lines, was decreased after transfection with SHMT2 siRNA, the rest of SQCLC cell lines did not show consistent results (Figure 13 B). Moreover, there was no impact of SHMT2 siRNA on cell proliferation of SCLC cell lines even after 6 days (Figure 13 C).

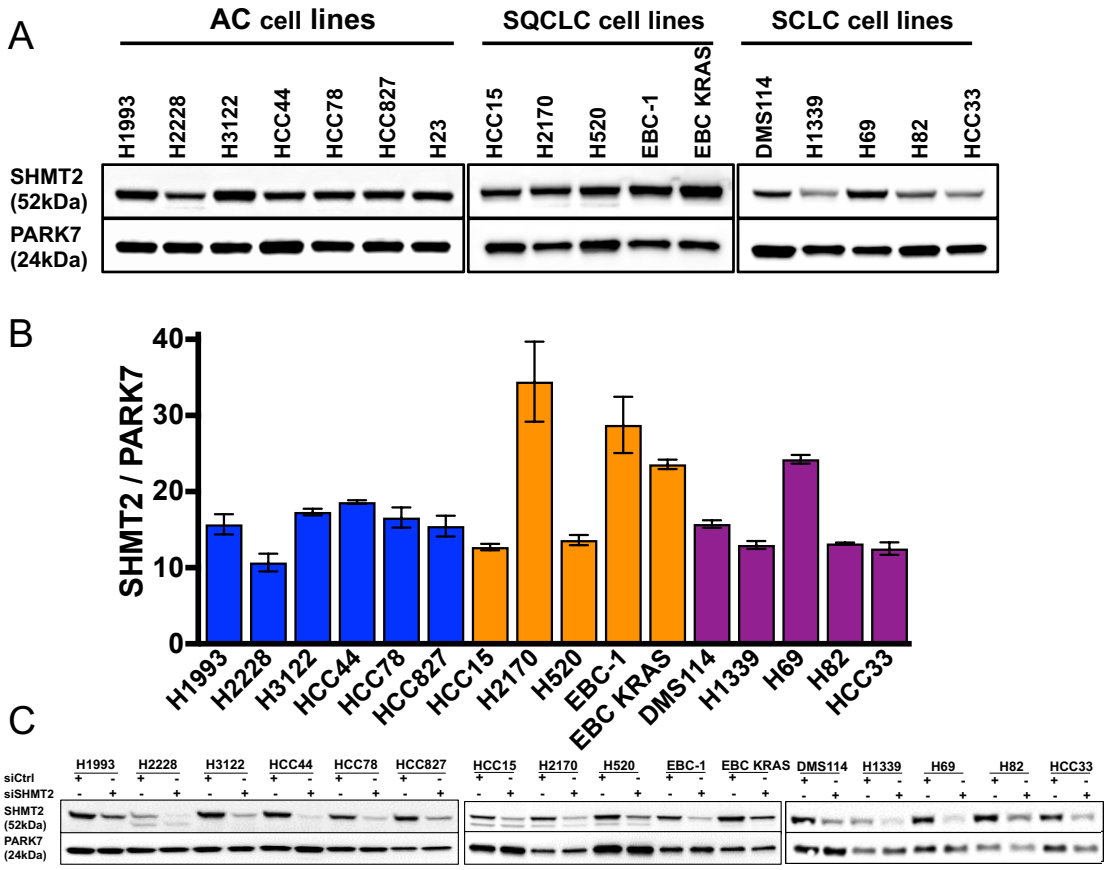

Figure 12: Expression of SHMT2 in human lung cancer cell lines. (A). Western blot analysis showing the expression of SHMT2 protein in AC, SQCLC and SCLC cell lines. PARK7 was used as loading control. Relative molecular mass in kDA is shown on the left. The pictures are representative of three independent experiments. (B). Signal intensities of SHMT2 from AC, SQCLC and SCLC cell lines were normalized to PARK7 using ImageJ (the data are represented as mean ± *SEM* of three independent experiments). (C). Western blot analysis showing the effect of control siRNA and SHMT2 siRNA on SHMT2 protein level in AC, SQCLC and SCLC cell lines after 72 h.

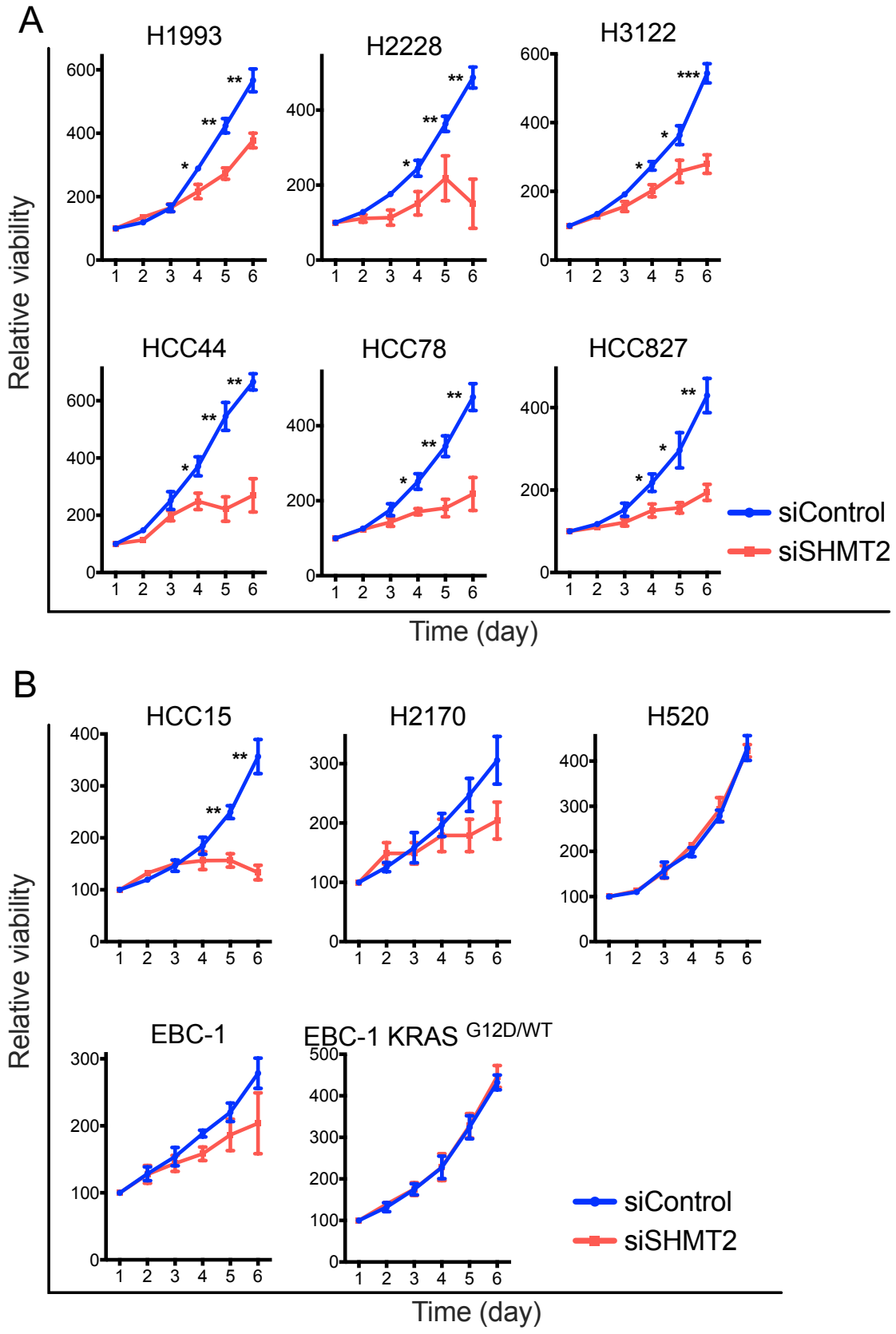
A
H1993
H2228
H3122
HCC44
HCC78
HCC827
Relative viability
Time (day)
siControl
siSHMT2
B
HCC15
H2170
H520
EBC-1
EBC-1 KRAS G12D/WT
Relative viability
Time (day)
siControl
siSHMT2

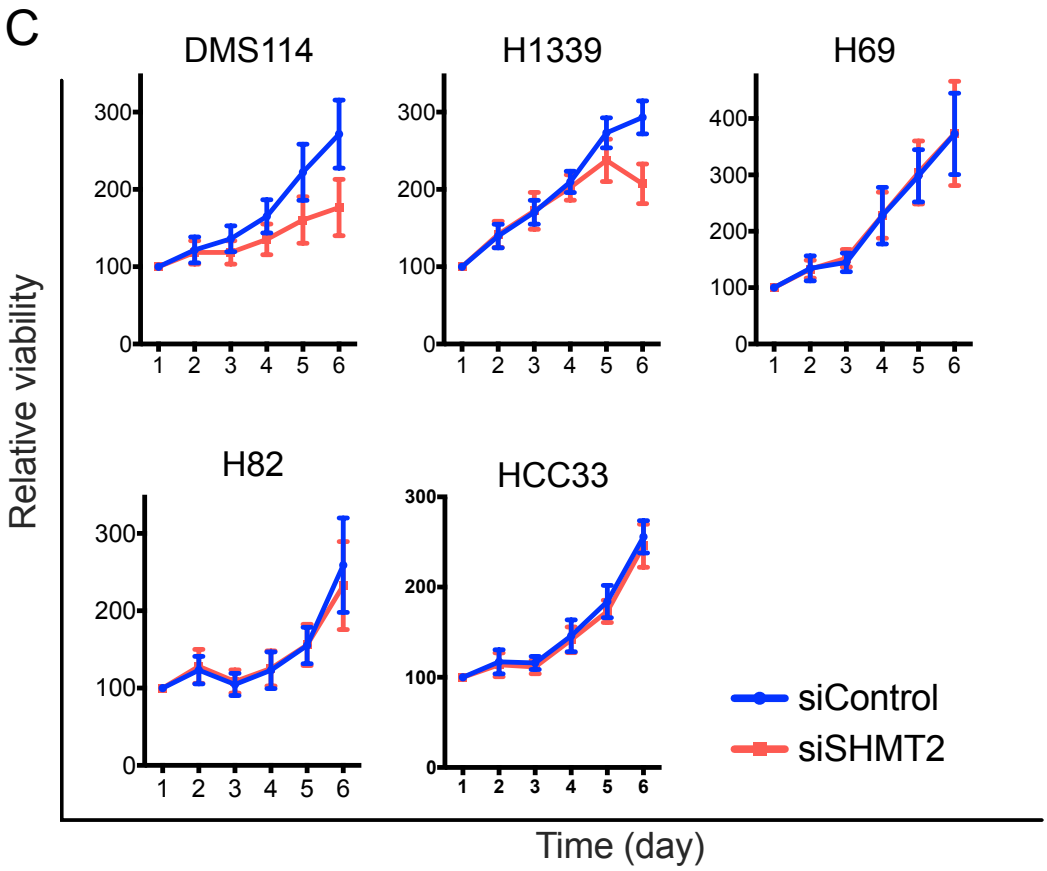

Figure 13: Knockdown of SHMT2 significant reduced cell proliferation of lung AC cell lines. Cell viability assays showing the cell proliferation of the AC (A), SQCLC (B) ,SCLC cell lines (C) after transfecting of siRNA against SHMT2 or control siRNA (the data are represented as mean ± *SEM* of at least three independent experiments with three technical replicates each, two-tailed Student's t-test: * $P < 0.05$,** $P < 0.01$,*** $P < 0.001$).

4.2.3 MTHFD2 enzyme in human lung cancer cell lines.

We detected MTHFD2 expression by western blot analysis (Figure 14 A), which showed strong expression in AC, SQCLC and SCLC cell lines. To determine the expression quantity of MTHFD2 protein, western blot bands of MTHFD2 protein were normalized to internal loading control PARK7 and results were shown in figure 14 B. All described cell lines expressed MTHFD2 protein. The AC cell line with the highest MTHFD2 protein level was HCC44. The SQCLC cell line with the highest MTHFD2 level was H2170. The lowest MTHFD2 protein level was found in the SCLC cell line H1339. Expression of MTHFD2

protein in the remaining cell lines was in a similar range. Next, cells were transfected with siRNAs targeting *MTHFD2* for 96 h. Western blot analysis showed that MTHFD2 protein was significantly reduced compared to controls (Figure 14 C).

Subsequently, cell viability assay revealed that cell proliferation was significantly inhibited upon *MTHFD2* knockdown starting from day 3 or day 4 and decreased by 50.0 % after 6 days in all AC (Figure 15 A) and SQCLC cell lines (Figure 15 B). However, cell proliferation was inhibited in only 3 of 5 SCLC cell lines by 50.0 % after 6 days (Figure 15 C).

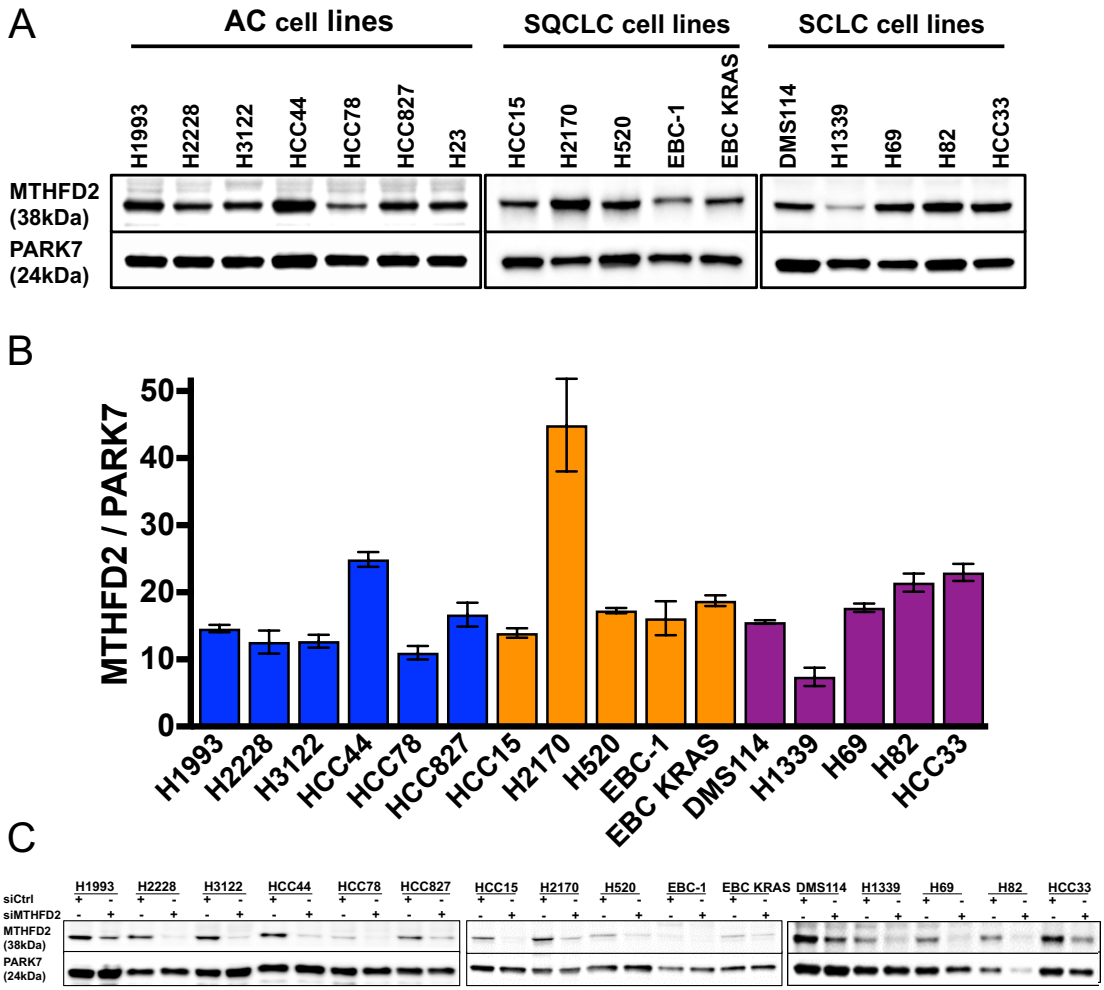

Figure 14: Expression of MTHFD2 in human lung cancer cell lines. (A). Western blot analysis showing the expression of MTHFD2 protein in AC, SQCLC and SCLC cell lines. PARK7 was used as loading control. Relative molecular mass in kDa is shown on the left. The pictures are representative for three independent experiments. (B). Signal intensities of MTHFD2 from AC, SQCLC and SCLC cell lines were normalized to PARK7 using ImageJ (the data are represented as mean ± *SEM* of three independent experiments). (C). Western blot analysis showing the effect of control siRNA and MTHFD2 siRNA on expression of MTHFD2 at protein lever in AC, SQCLC and SCLC cell lines after transfecting for 96 h.

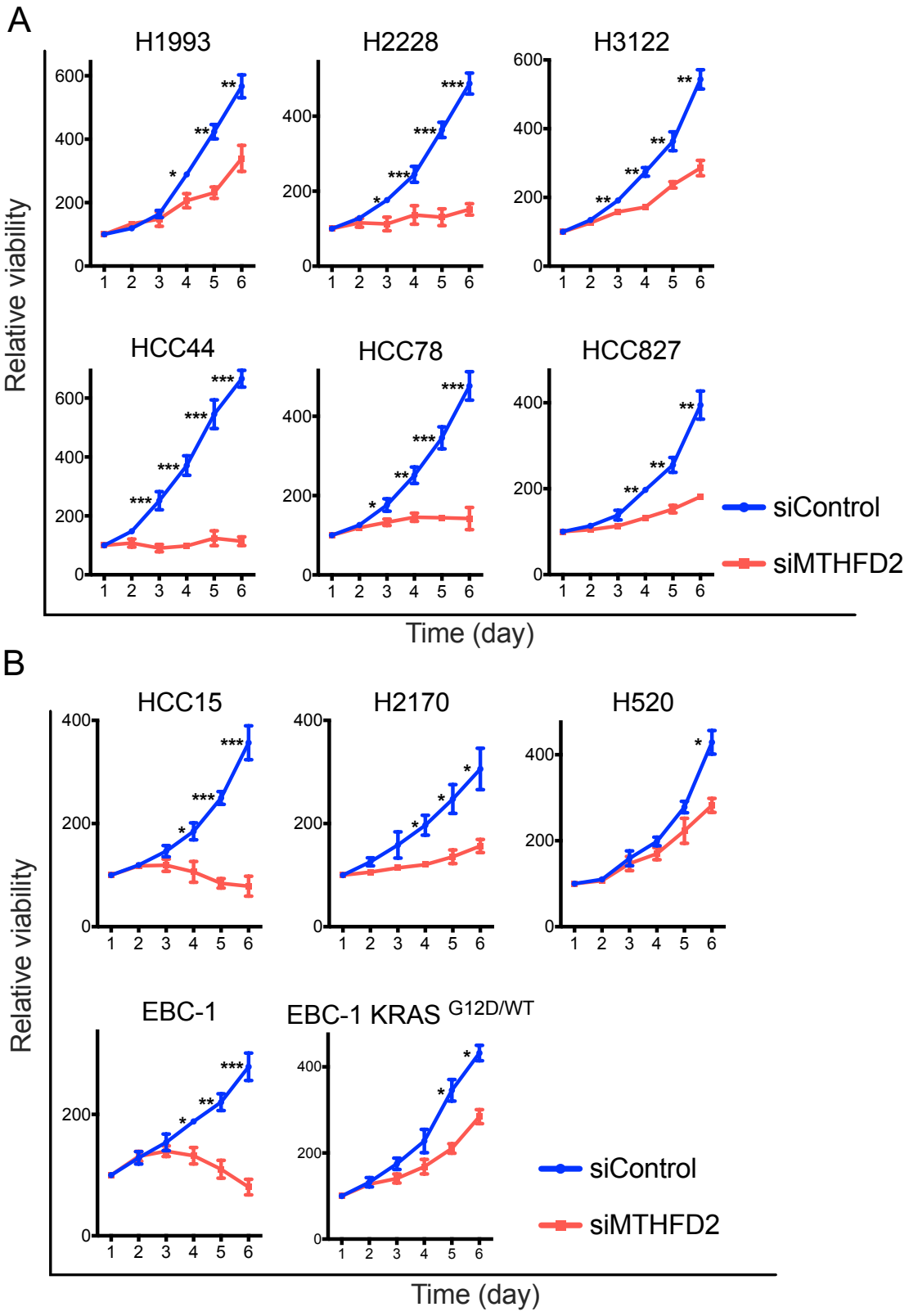
A
H1993
H2228
H3122
HCC44
HCC78
HCC827
Relative viability
Time (day)
siControl
siMTHFD2
B
HCC15
H2170
H520
EBC-1
EBC-1 KRAS G12D/WT
Relative viability
Time (day)
siControl
siMTHFD2

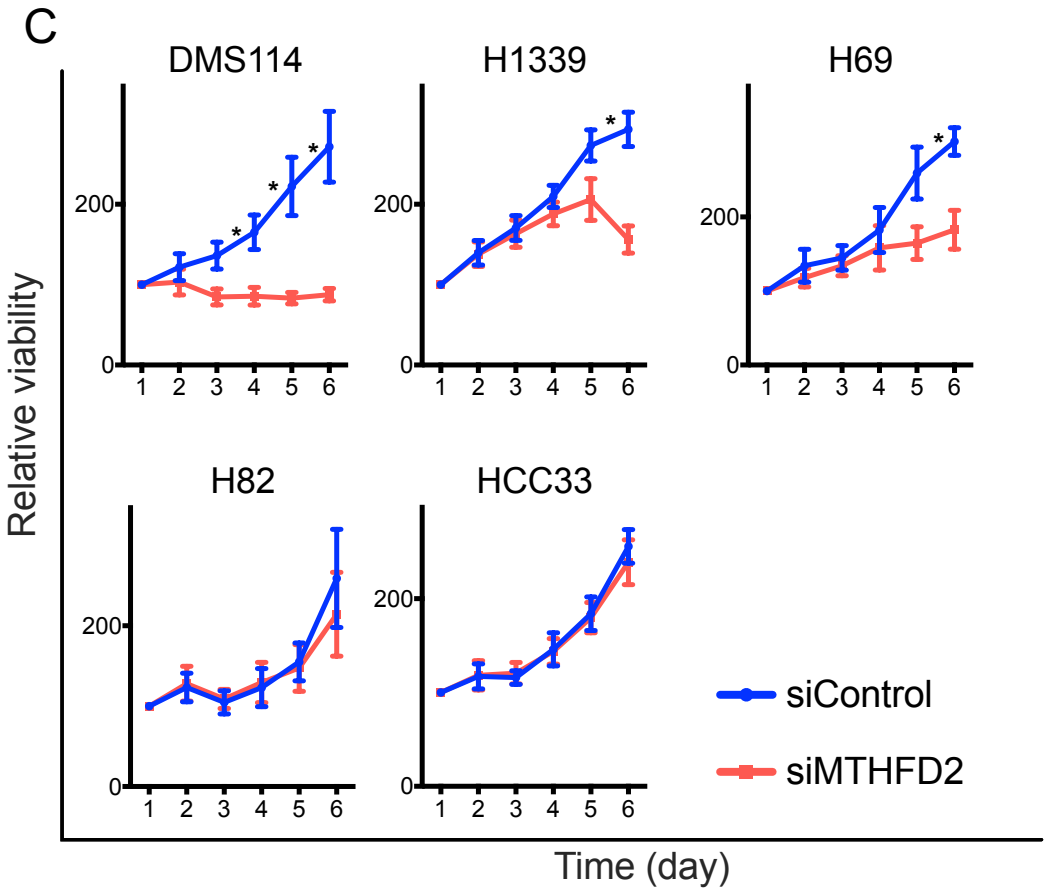

Figure 15: Knockdown of MTHFD2 significant reduced cell proliferation of lung cancer cell lines. Cell viability assays showing the cell proliferation of the AC (A), SQCLC (B) ,SCLC cell lines (C) after transfecting of siRNA against MTHFD2 or control siRNA (the data are represented as mean ± *SEM* of at least three independent experiments with three technical replicates each, two-tailed Student's t-test: * $P < 0.05$,** $P < 0.01$,*** $P < 0.001$).

4.2.4 MTHFD1 enzyme in human lung cancer cell lines.

In figure 16 A, western blot analysis revealed that MTHFD1 protein was abundantly expressed in AC, SQCLC and SCLC cell lines. Western blot bands displayed the highest expression of MTHFD1 protein in the SQCLC cell line H2170. The other SQCLC, AC, and SCLC cell lines showed similar MTHFD1 protein levels (Figure 16 B). Next, cells were transfected with MTHFD1 siRNA or control siRNA for 96 h. As shown in figure 16 C, MTHFD1 siRNA clearly inhibited the expression of MTHFD1 protein in both AC and SQCLC cell lines but not in all SCLC cell lines compared to control siRNA.

Furthermore, cell viability assays were performed to detect cell proliferation after treatment with MTHFD1 siRNA or control siRNA. AC cell lines treated with MTHFD1 siRNA, showed dramatic growth arrest (Figure 17 A). Particularly the proliferation of HCC44 cells was significantly inhibited from day 2. SQCLC cell lines showed similar changes and cell proliferation was significantly decreased after transfection with MTHFD1 siRNA (Figure 17 B). Among SQCLC cell lines, HCC15 was outstanding, since the proliferation was strongly decreased from day 2 after treatment with MTHFD1 siRNA. Consistent with western blot analysis results, not all SCLC cell lines showed response to MTHFD1 siRNA (Figure 17 C). Cell proliferation of DMS114, H1339 and H69 cell line was significantly reduced from day 4 or day 5.

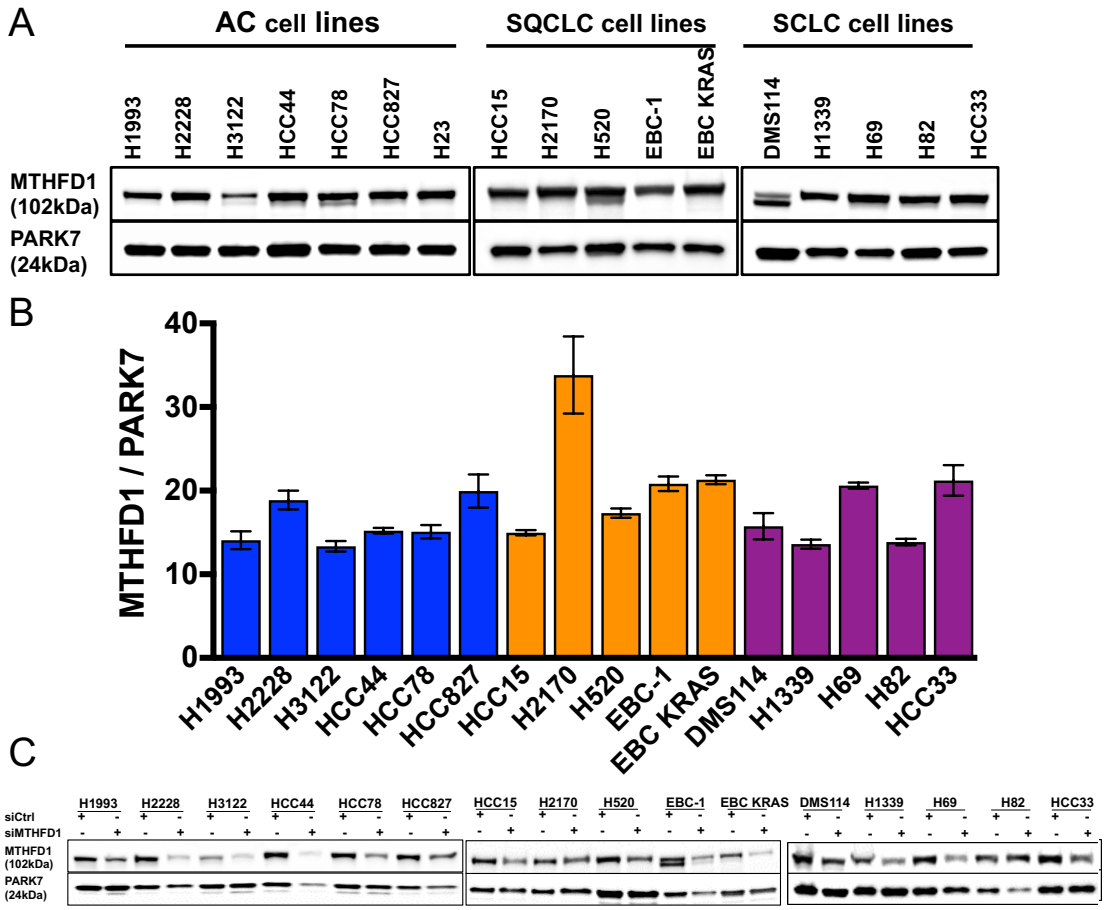

Figure 16: Expression of MTHFD1 in human lung cancer cell lines. (A). Western blot analysis showing the expression of MTHFD1 protein in AC, SQCLC and SCLC cell lines. PARK7 used as loading control. Relative molecular mass in kDa is shown on the left. The pictures are representative of three independent experiments. (B). Signal intensities of MTHFD1 from AC, SQCLC and SCLC cell lines were normalized to PARK7 using ImageJ (the data are represented as mean ± *SEM* of three independent experiments). (C). Western blot analysis showing the effect of control siRNA and MTHFD1 siRNA on expression of MTHFD1 at protein lever in AC, SQCLC and SCLC cell lines after transfecting for 96 h.

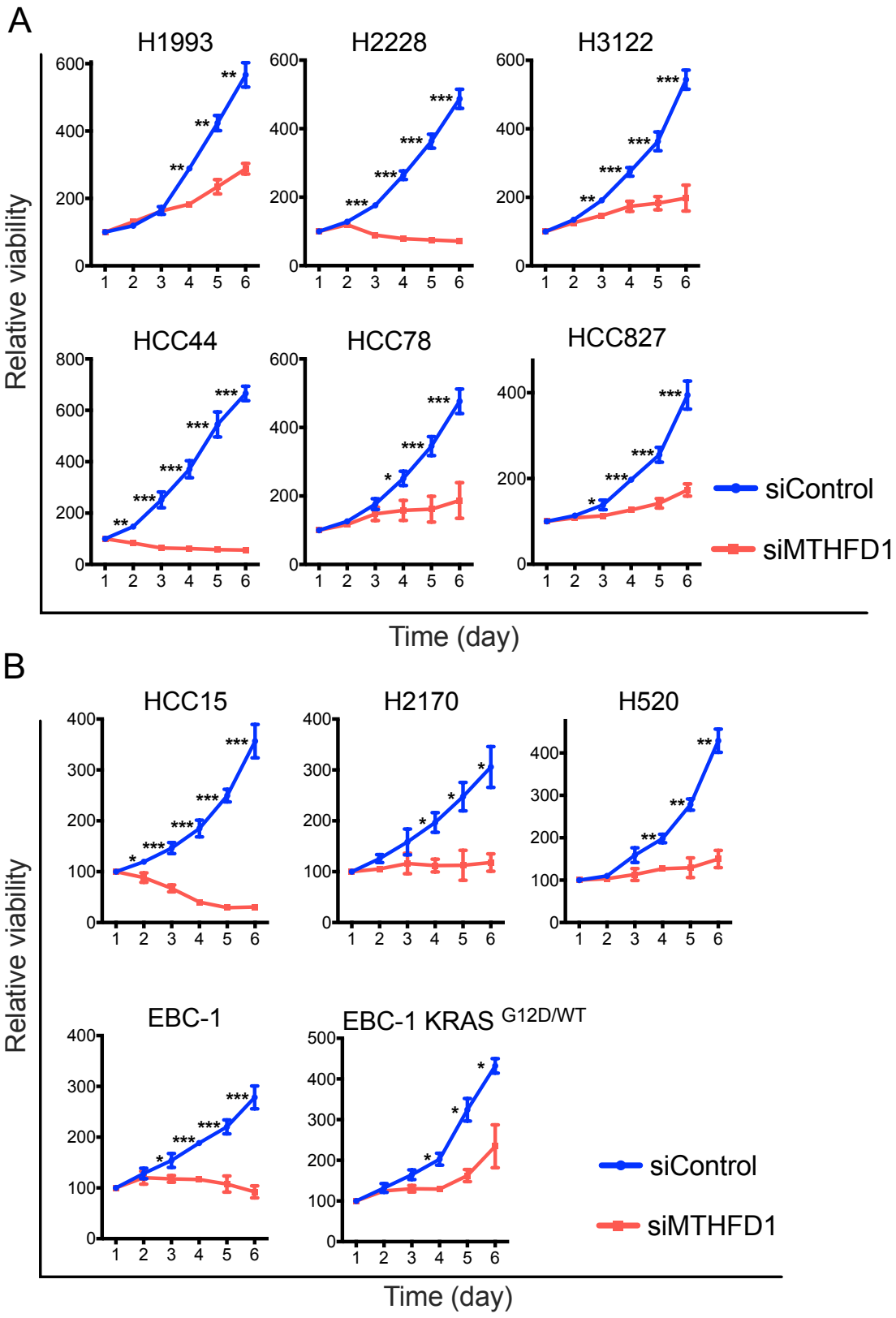
A
H1993
H2228
H3122
HCC44
HCC78
HCC827
Relative viability
Time (day)
siControl
siMTHFD1
B
HCC15
H2170
H520
EBC-1
EBC-1 KRAS G12D/WT
Relative viability
Time (day)
siControl
siMTHFD1

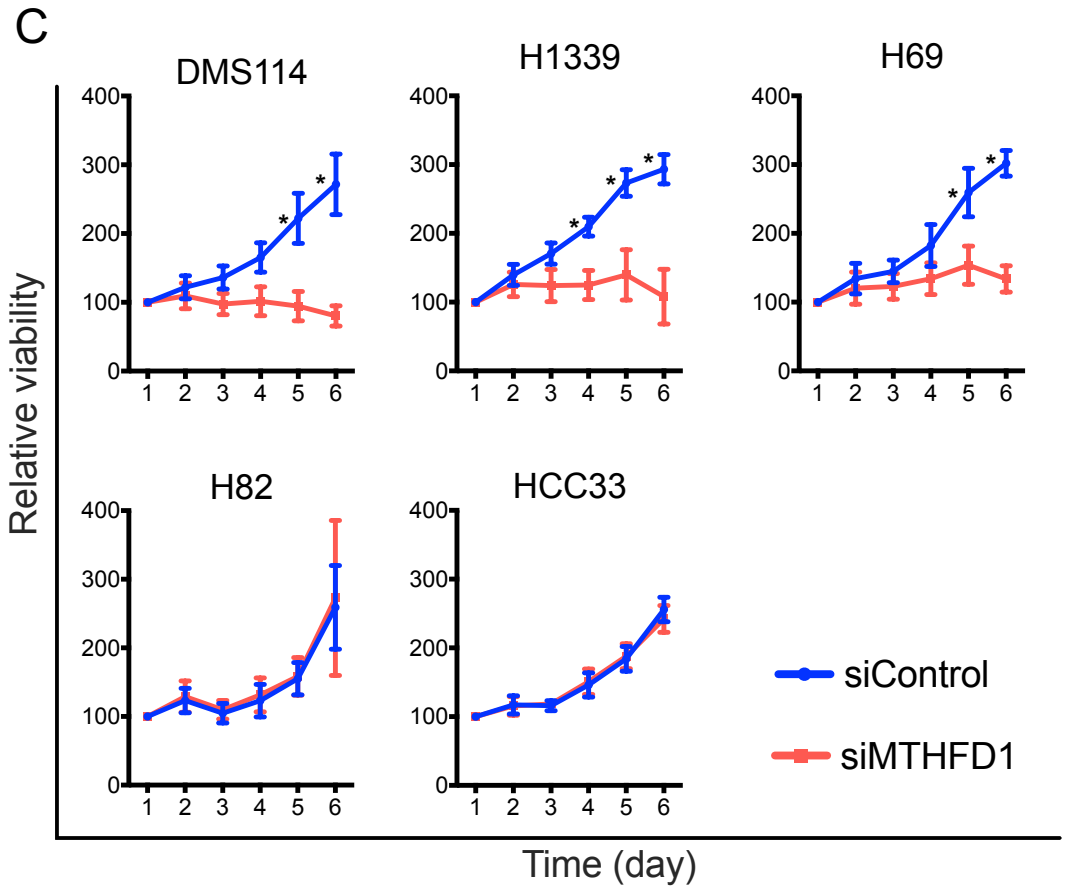

Figure 17: Knockdown of MTHFD1 significant reduced cell proliferation of lung cancer cell lines. Cell viability assays showing the cell proliferation of the AC (A), SQCLC (B) ,SCLC cell lines (C) after transfecting of siRNA against MTHFD1 or control siRNA (the data are represented as mean ± *SEM* of at least three independent experiments with three technical replicates each, two-tailed Student's t-test: * $P < 0.05$,** $P < 0.01$,*** $P < 0.001$).

4.2.5 TYMS enzyme in human lung cancer cell lines.

Western blot analysis indicated that TYMS protein was widely expressed in AC, SQCLC and SCLC cell lines (Figure 18 A). ImageJ software was used to normalize the western blot bands and results were presented in figure 18 B. TYMS protein was expressed in all human lung cancer cell lines but in various degree. Among AC cell lines, HCC44 and H2228 were the two with the highest expression. Among SCLC cell lines, H82 and HCC33 were the two with the highest expression. TYMS protein expression in the SQCLC cell line H520 was higher than all other human lung cancer cell lines. Next, all cell lines were

transfected with TYMS siRNA or control siRNA for 96 h, western blot analysis were performed to verify TYMS protein expression was remarkably decreased by TYMS siRNA in comparison to control siRNA (Figure 18 C).

Furthermore, cell proliferation was accessed using cell viability assay. Cells were seeded in 96 well plates and treated with TYMS siRNA or control siRNA. Cell proliferation of all AC cell lines was severely inhibited by TYMS siRNA starting from day 3 or day 4 in comparison to control siRNA and decreased to 50.0 % at day 6 (Figure 19 A). Cell proliferation of SQCLC cell lines HCC15 and EBC-1 was significantly decreased from day 3 to less than 50.0 % at day 6. Cell proliferation of the EBC-1 KRAS $^{G12D/WT}$ cell line was significantly inhibited from day 5 and by 50.0 % at day 6. TYMS siRNA showed no impact on the remaining SQCLC cell lines (Figure 19 B). In SCLC cell lines, only cell proliferation of the DMS114 and H1339 cell line was significantly inhibited to 50.0 % at day 6 (Figure 19 C).

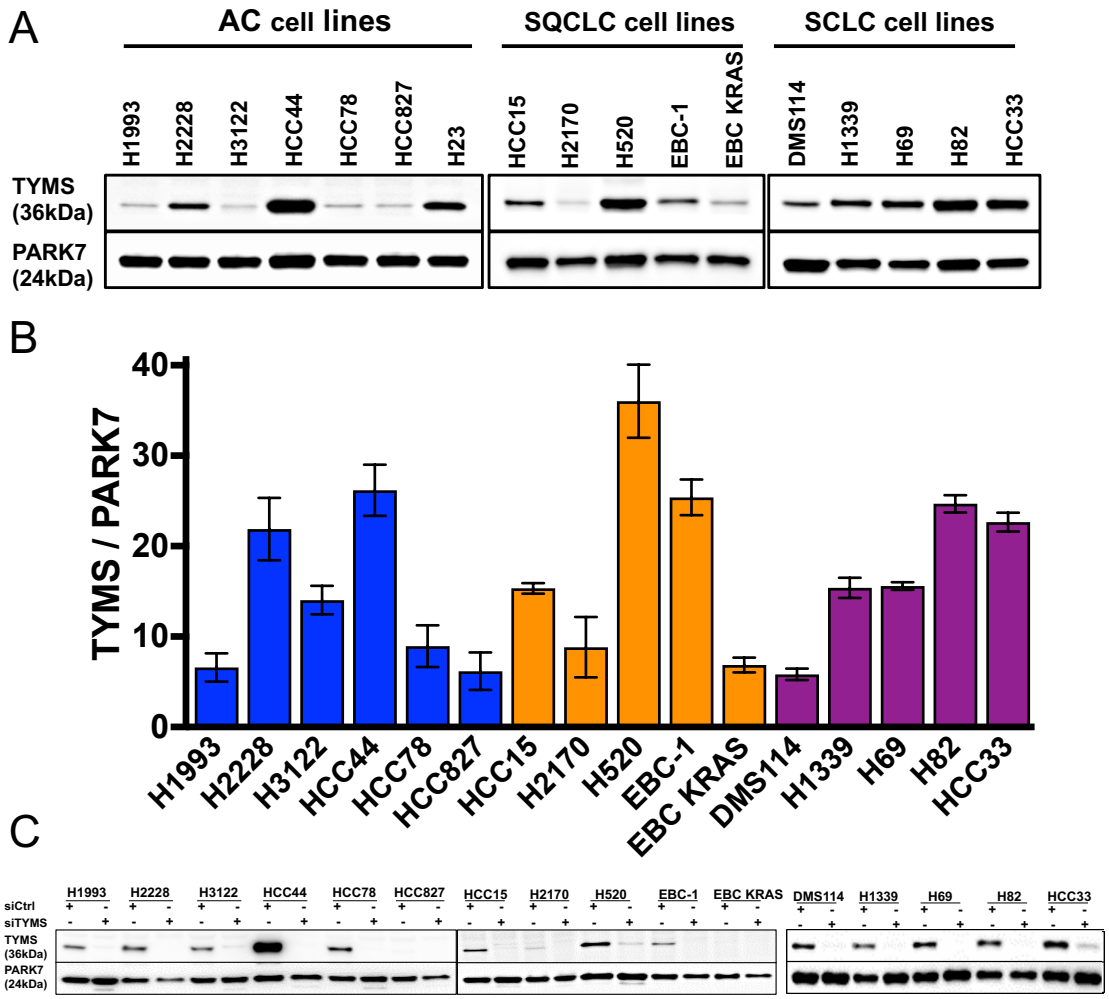

Figure 18: Expression of TYMS in human lung cancer cell lines. (A). Western blot analysis showing the expression of TYMS protein in AC, SQCLC and SCLC cell lines. PARK7 used as loading control. Relative molecular mass in kDa is shown on the left. The pictures are representative of three independent experiments. (B). Signal intensities of TYMS from AC, SQCLC and SCLC cell lines were normalized to PARK7 using ImageJ (the data are represented as mean ± *SEM* of three independent experiments). (C). Western blot analysis showing the effect of control siRNA and TYMS siRNA on expression of TYMS at protein lever in AC, SQCLC and SCLC cell lines after transfecting for 96 h.

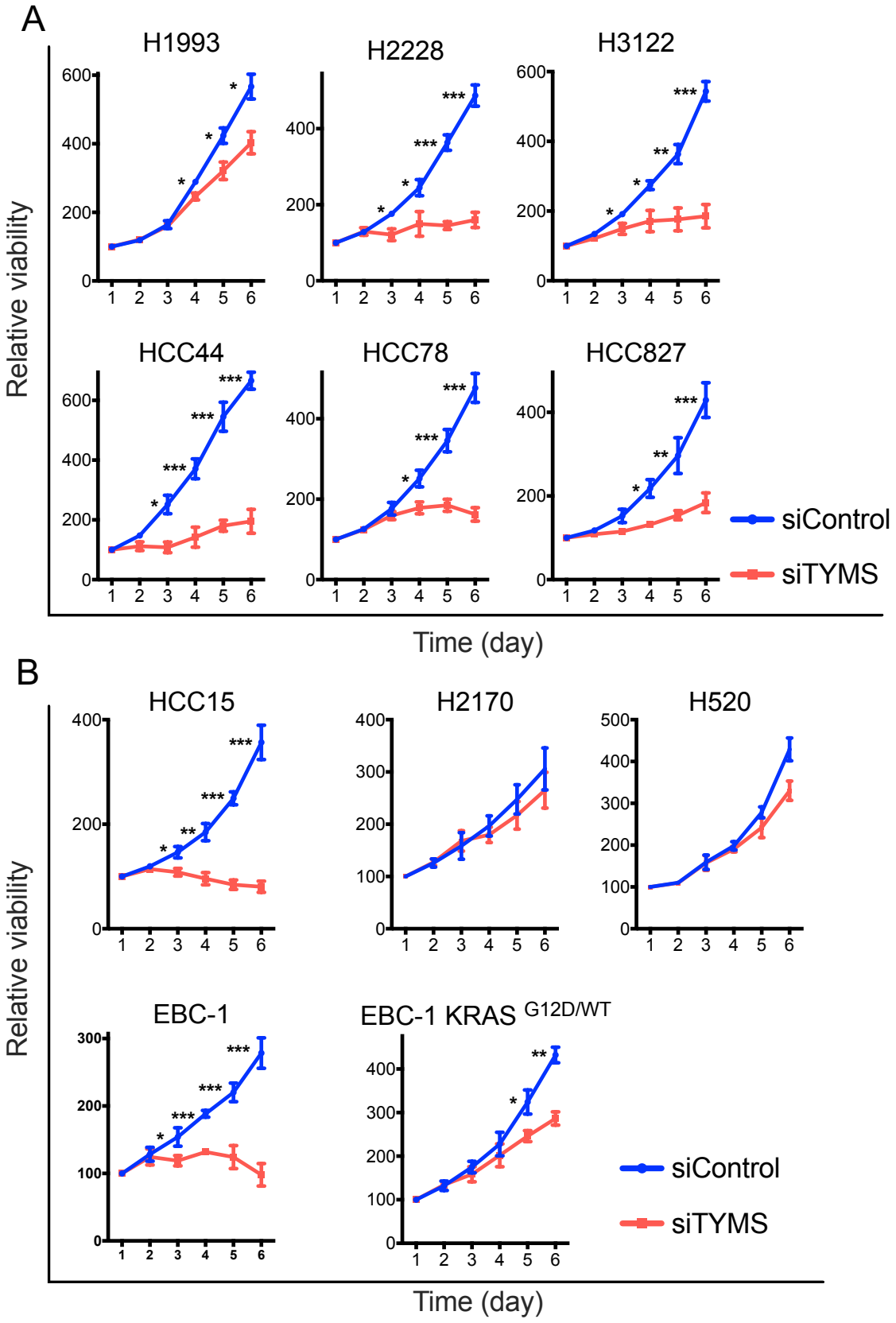
A
H1993
H2228
H3122
HCC44
HCC78
HCC827
Relative viability
Time (day)
siControl
siTYMS
B
HCC15
H2170
H520
EBC-1
EBC-1 KRAS G12D/WT
Relative viability
Time (day)
siControl
siTYMS

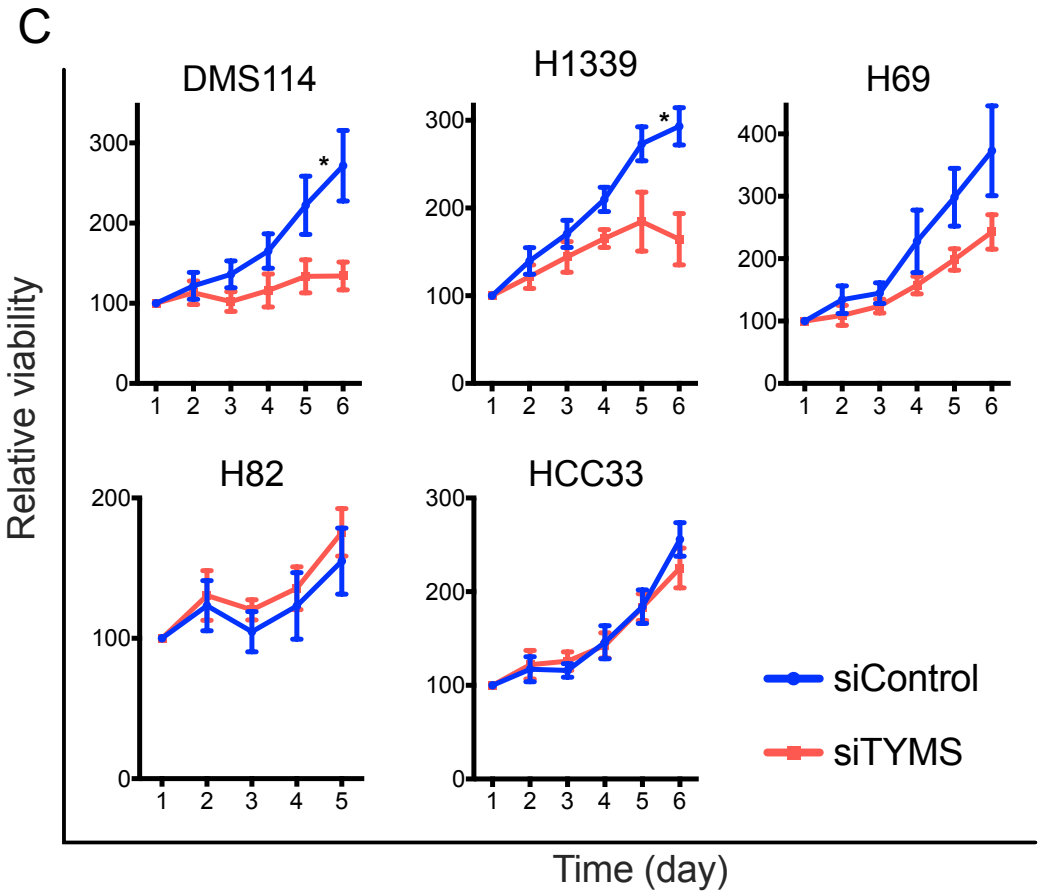

Figure 19: Knockdown of TYMS significant reduced cell proliferation of lung cancer cell lines. Cell viability assays showing the cell proliferation of the AC (A), SQCLC (B), SCLC cell lines (C) after transfecting of siRNA against TYMS or control siRNA (the data are represented as mean ± *SEM* of at least three independent experiments with three technical replicates each, two-tailed Student's t-test: * $P < 0.05$,** $P < 0.01$,*** $P < 0.001$).

4.3 Association between one-carbon metabolism enzymes and cytotoxic responsiveness to cisplatin and pemetrexed in human lung cancer cell lines

Chemotherapy is the basic treatment for patients with lung cancer. Cisplatin and pemetrexed are the first-line medications. As we found that expression of one-carbon metabolism enzymes correlated with overall survival for patients with lung cancer, we further investigated the correlation between one-carbon metabolism enzymes and cytotoxic responsiveness to cisplatin and pemetrexed in human lung cancer cell lines. Cell viability assays were

performed to evaluate the effects of cisplatin and pemetrexed on the viability of AC, SQCLC and SCLC cell lines. The IC50 for cisplatin and pemetrexed were calculated on the basis of dose-response curves. Afterwards, correlation analysis was used to investigate the relationship between the expression of one-carbon metabolism proteins and IC50 values of cisplatin and pemetrexed in AC, SQCLC and SCLC cell lines.

4.3.1 Correlation of one-carbon metabolism proteins expression with cisplatin or pemetrexed sensitivity in human AC cell lines.

To evaluate the sensitivity of AC cell lines to cisplatin or pemetrexed treatment, the IC50 of cisplatin or pemetrexed was calculated from dose-response curves in all of the six described AC cell lines. As shown in figure 20 A and B, both agents reduced the cell viability in AC cell lines. The IC50 values for cisplatin ranged from 3.01 µM to 12.84 µM and for pemetrexed from 0.03 µM to 184.20 µM (Table 8). HCC44 and HCC827 showed the strongest resistance to pemetrexed (Figure 20 B). Even at the highest concentration (50 µM), pemetrexed only inhibited HCC44 and HCC827 cell viability by less than 5.0 % whereas cisplatin decreased cell viability by 80.0 % at 5 µM. HCC78 and H1993 showed the best response to pemetrexed (Figure 20 B). Cell viability decreased to less than 50.0 % at 0.05 µM.

Afterwards, we performed a Pearson's correlation analysis of one-carbon metabolism proteins expression with drug sensitivity in these lines and revealed that expression of MTHFD2 significantly and reciprocally correlated with pemetrexed resistance, with a Pearson coefficient of r = 0.871 (P = 0.024, Figure 20 D), indicating that the expression of MTHFD2 protein was associated with pemetrexed resistance in lung AC cell lines. However, correlation between the expression of MTHFD2 and IC50 of cisplatin was not significant (Figure 20 C). Moreover, there were no correlation between expression of PGDH3, SHMT2, MTHFD1, TYMS the and IC50 of cisplatin and pemetrexed (Figure 20 C, D)

Table 8: IC50 values of cisplatin and pemetrexed in AC cell lines

	Drugs			
	Cisplatin (μM)		Pemetrexed (μM)	
	IC50	95% CI *	IC50	95% CI
H1993	12.84	(11.03-14.96)	0.10	(0.03-0.38)
H2228	3.28	(2.27-4.68)	0.42	(0.08-6.90)
H3122	10.70	(9.37-12.22)	0.28	(0.09-1.01)
HCC44	1.88	(1.56-2.26)	184.20	(116.20-354.60)
HCC78	3.01	(2.12-4.25)	0.03	(0.01-0.06)
HCC827	10.76	(7.50-15.62)	158.5	(95.65-326.70)

*: 95% confidence intervals

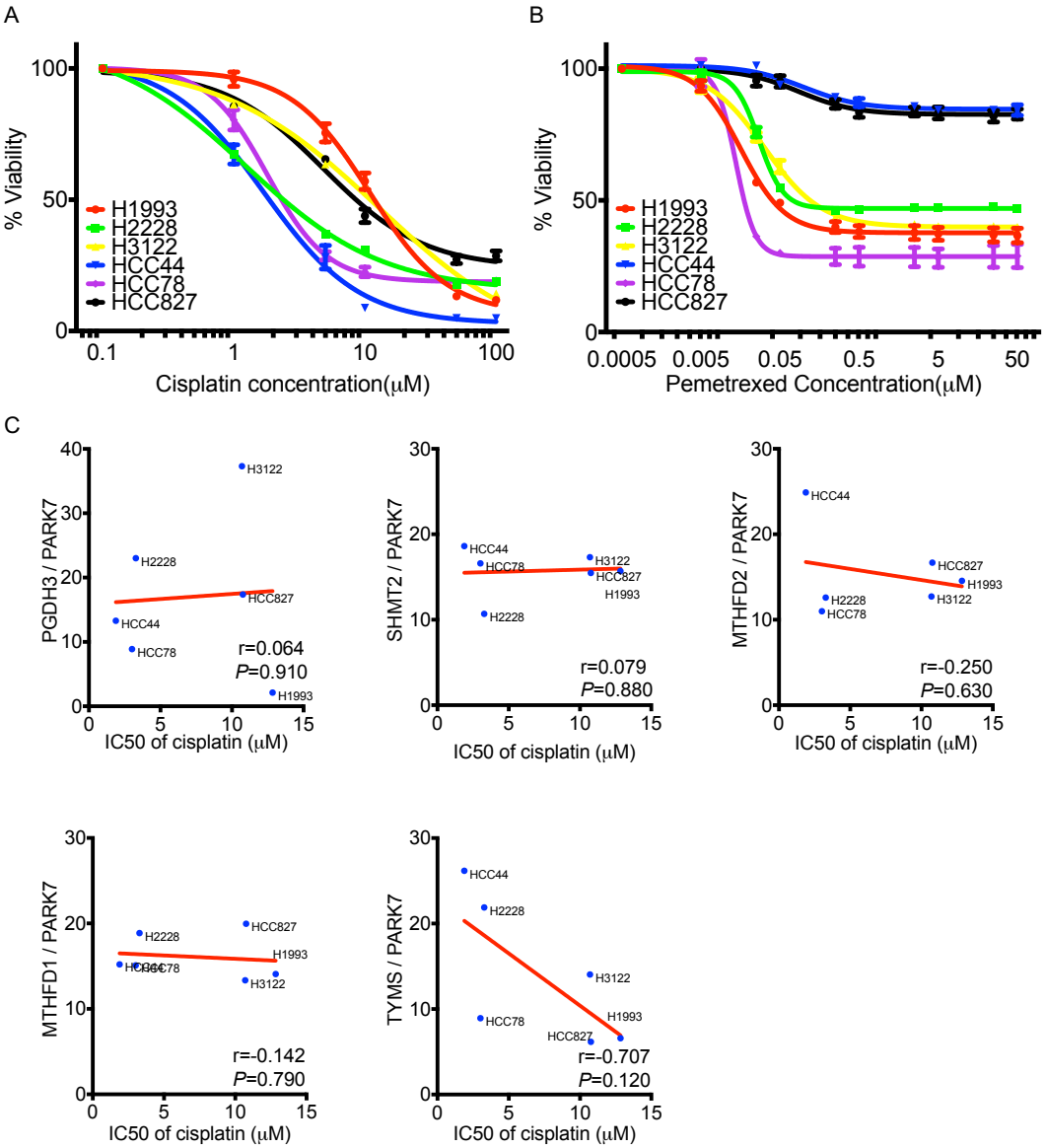
A
100
50
0
% Viability
H1993
H2228
H3122
HCC44
HCC78
HCC827
0.1
1
10
100
Cisplatin concentration(μM)
B
100
50
0
% Viability
H1993
H2228
H3122
HCC44
HCC78
HCC827
0.0005
0.005
0.05
0.5
5
50
Pemetrexed Concentration(μM)
C
PGDH3 / PARK7
H3122
H2228
HCC827
HCC44
HCC78
H1993
r=0.064
P=0.910
IC50 of cisplatin (μM)
SHMT2 / PARK7
HCC44
HCC78
H3122
HCC827
H1993
H2228
r=0.079
P=0.880
IC50 of cisplatin (μM)
MTHFD2 / PARK7
HCC44
HCC827
H1993
H2228
HCC78
H3122
r=-0.250
P=0.630
IC50 of cisplatin (μM)
MTHFD1 / PARK7
H2228
HCC827
H1993
H3122
r=-0.142
P=0.790
IC50 of cisplatin (μM)
TYMS / PARK7
HCC44
H2228
H3122
HCC78
H1993
HCC827
r=-0.707
P=0.120
IC50 of cisplatin (μM)

D

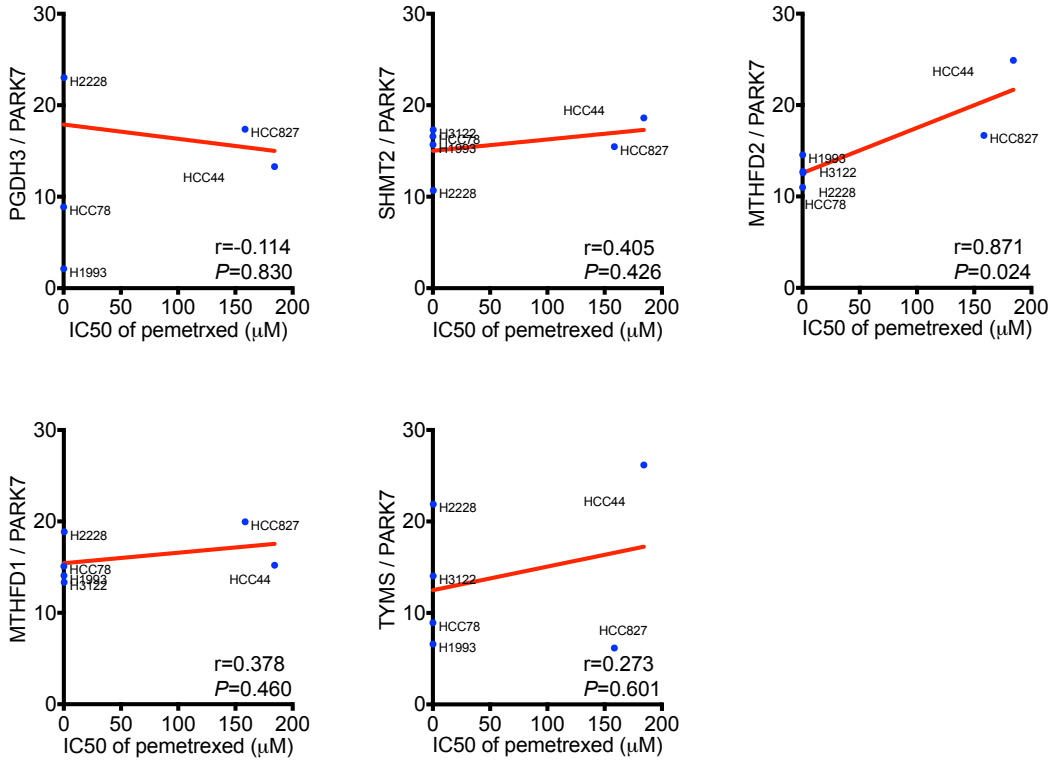

Figure 20: Correlation of one-carbon metabolism proteins expression with cisplatin or pemetrexed sensitivity in AC cell lines. Inhibitory dose-response curves for AC cell lines treated with cisplatin (A) for 72 h and pemetrexed (B) for 96 h are shown. The dots and bars represent as mean ± *SEM* of at least three independent experiments with three technical replicates each. (C and D). Pearson's correlation analyses of one-carbon metabolism protein expression with drug sensitivity are shown. Correlation curves show the correlation between the IC50 values of cisplatin (C) and pemetrexed (D) and the expression of one-carbon metabolism proteins in relation to loading control as obtained by western blot analysis.

4.3.2 Correlation of one-carbon metabolism proteins expression with cisplatin or pemetrexed sensitivity in human SQCLC cell lines.

To evaluate the sensitivity of SQCLC cell lines to cisplatin or pemetrexed treatment, the IC50 of cisplatin or pemetrexed was calculated from dose-response curves in all of the five described SQCLC cell lines. All SQCLC cell lines showed good response to cisplatin (Figure 21 A) but were resistant against pemetrexed (Figure 21 B). Cisplatin significantly inhibited cell viability of all SQCLC cell lines by 80.0 %, pemetrexed only inhibited cell viability by

less than 50.0 % except for H520. The IC50 values of cisplatin and pemetrexed in SQCLC cell lines were calculated and represented in table 9 on the basis of dose-response curves: the IC50 values of cisplatin ranged from 4.41 μM to 23.98 μM and from 1.62 μM to 70.79 μM for pemetrexed. There was no correlation between one-carbon metabolism protein expression and drug sensitivity by Pearson's correlation analysis in SQCLC cells (Figure 21 C, D).

Table 9: IC50 values of cisplatin and pemetrexed in SQCLC cell lines

	Drugs			
	Cisplatin (μM)		**Pemetrexed (μM)**	
	IC50	**95% CI ***	**IC50**	**95% CI**
HCC15	**23.98**	**(18.33-31.40)**	**70.79**	**(35.07-170.40)**
H2170	**4.41**	**(3.87-5.02)**	**59.98**	**(24.76-179.10)**
H520	**11.21**	**(9.08-13.87)**	**1.624**	**(0.82-3.23)**
EBC-1	**27.26**	**(24.17-30.73)**	**30.66**	**(8.51-89.73)**
EBC-1*KRAS*$^{G12D/WT}$	**16.53**	**(11.33-24.37)**	**28.35**	**(8.59-77.65)**

***: 95% confidence intervals**

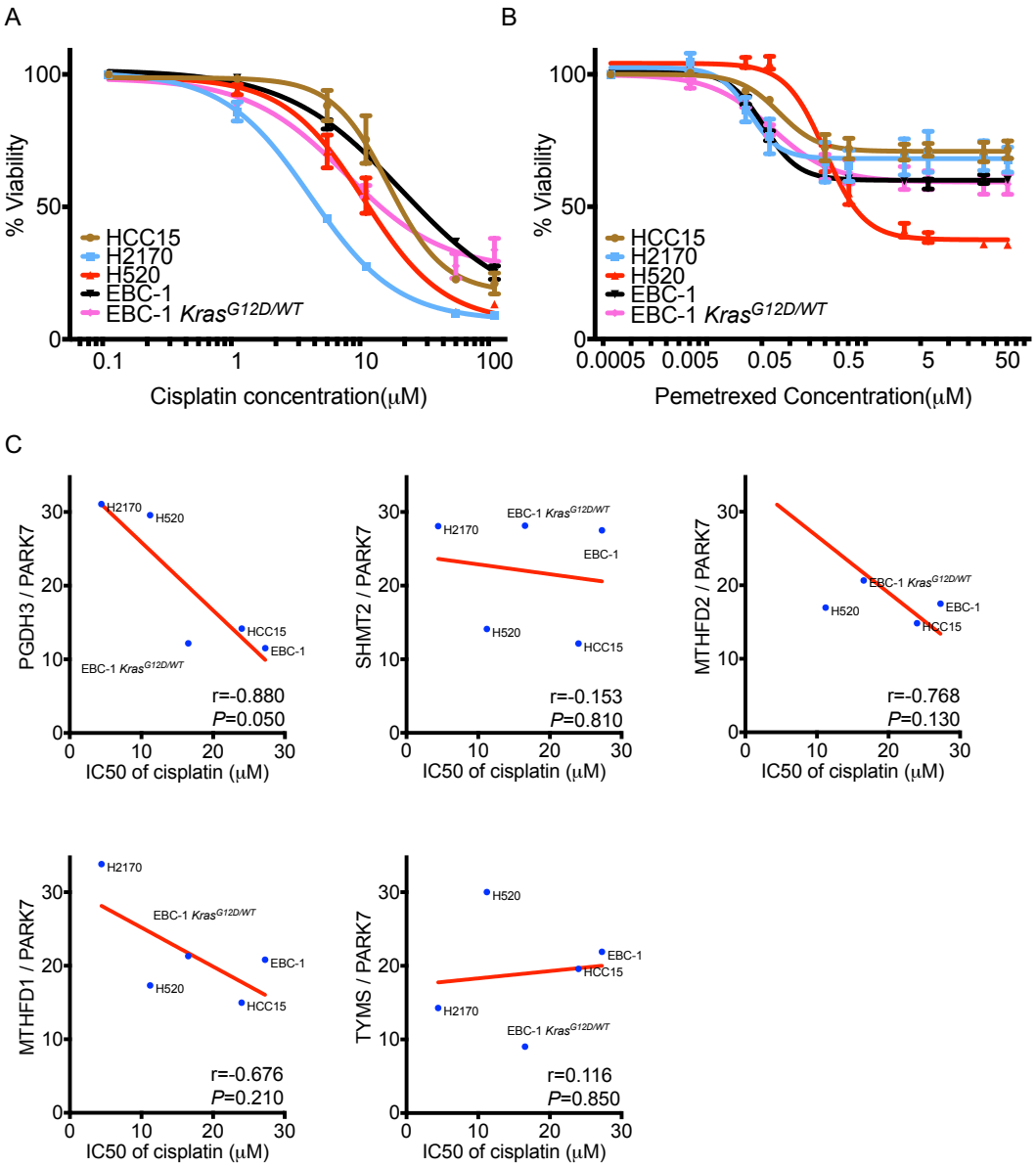
A
B
C
% Viability
HCC15
H2170
H520
EBC-1
EBC-1 KrasG12D/WT
Cisplatin concentration(μM)
Pemetrexed Concentration(μM)
PGDH3 / PARK7
SHMT2 / PARK7
MTHFD2 / PARK7
MTHFD1 / PARK7
TYMS / PARK7
IC50 of cisplatin (μM)
r=-0.880
P=0.050
r=-0.153
P=0.810
r=-0.768
P=0.130
r=-0.676
P=0.210
r=0.116
P=0.850

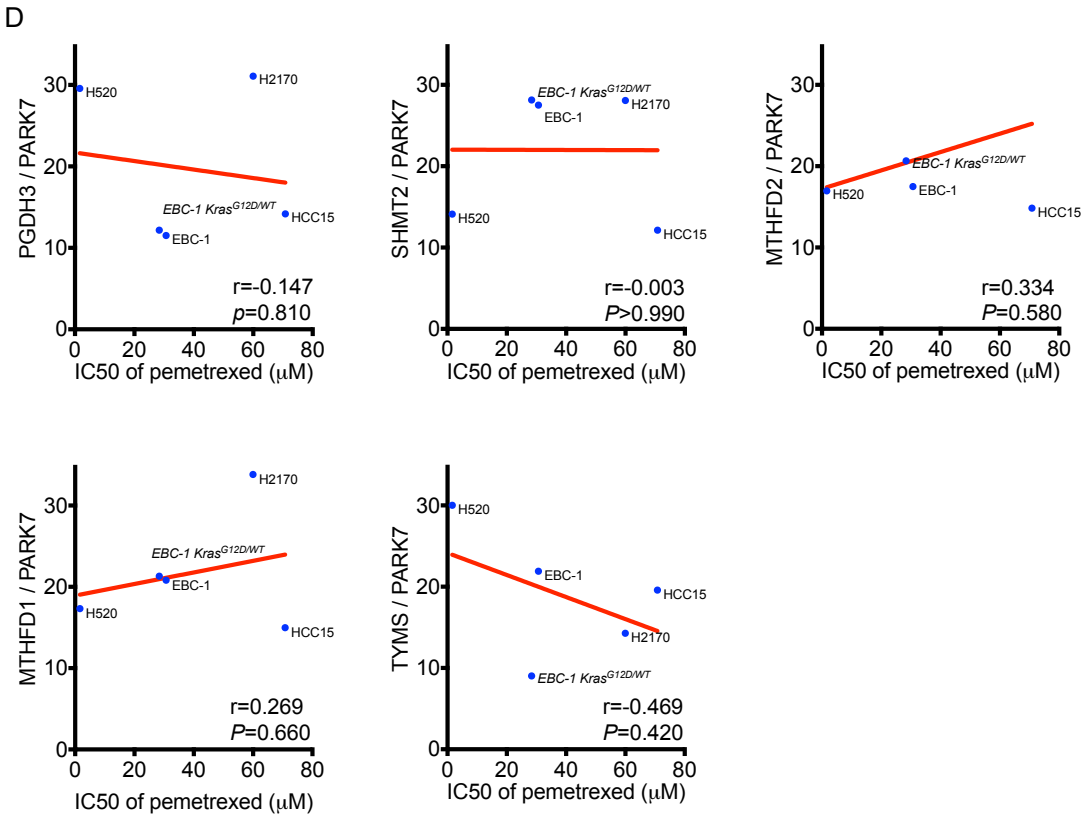

Figure 21: The expression of one-carbon metabolism protein is not associated with chemoresistance in SQCLC cell lines. Inhibitory dose-repose curves show the SQCLC cell lines treated with cisplatin (A) for 72 h and pemetrexed (B) for 96 h. The dots and bars represent the mean ± *SEM* of at least three independent experiments, each with three technical replicates. Correlation curves show the correlation between the IC50 values of cisplatin (C) and pemetrexed (D) and the expression of one-carbon metabolism proteins in SQCLC cell lines.

4.3.3 Correlation of one-carbon metabolism proteins expression with cisplatin or pemetrexed sensitivity in human SCLC cell lines.

To evaluate the sensitivity of SCLC cell lines to cisplatin or pemetrexed treatment, the IC50 of cisplatin or pemetrexed was calculated from dose-response curves in all of the five described SQCLC cell lines. Cell viability of SCLC cell lines was strongly inhibited by treatment of cisplatin except H69 (Figure 22 A). Cisplatin inhibited cell viability of H69 by only 40.0 % even at the highest concentration (100 μM). SCLC cell lines showed resistance to pemetrexed (Figure 22 B), although DMS114 could be inhibited by 60.0 % at the highest concentration of pemetrexed (50 μM). The IC50 values of cisplatin and pemetrexed were

calculated and shown in table 10 according to dose-response curves: the IC50 of cisplatin ranged from 2.96 μM to 15.58 μM and from 0.22 μM to 65.66 μM for pemetrexed. Subsequently, we used a Pearson's correlation analysis and found that expression of SHMT2 significantly and reciprocally correlated with cisplatin resistance (r = 0.926, *P* = 0.024) (Figure 22 C). However, we did not observe a significant correlation between one-carbon metabolism proteins expression and the response to pemetrexed in SCLC cell lines (Figure 22 D).

Table 10: IC50 values of cisplatin and pemetrexed in SCLC cell lines

	Drugs			
	Cisplatin (μM)		**Pemetrexed (μM)**	
	IC50	**95% CI ***	**IC50**	**95% CI**
DMS114	**6.79**	**(5.64-8.17)**	**0.22**	**(0.10-0.50)**
H1339	**2.96**	**(2.44-3.57)**	**4.02**	**(0.82-21.46)**
H69	**53.73**	**(20.00-132.20)**	**47.31**	**(16.84-147.80)**
H82	**3.70**	**(2.24-5.91)**	**58.39**	**(23.33-188.50)**
HCC33	**15.58**	**(12.10-20.17)**	**65.66**	**(32.04-157.40)**

***: 95% confidence intervals**

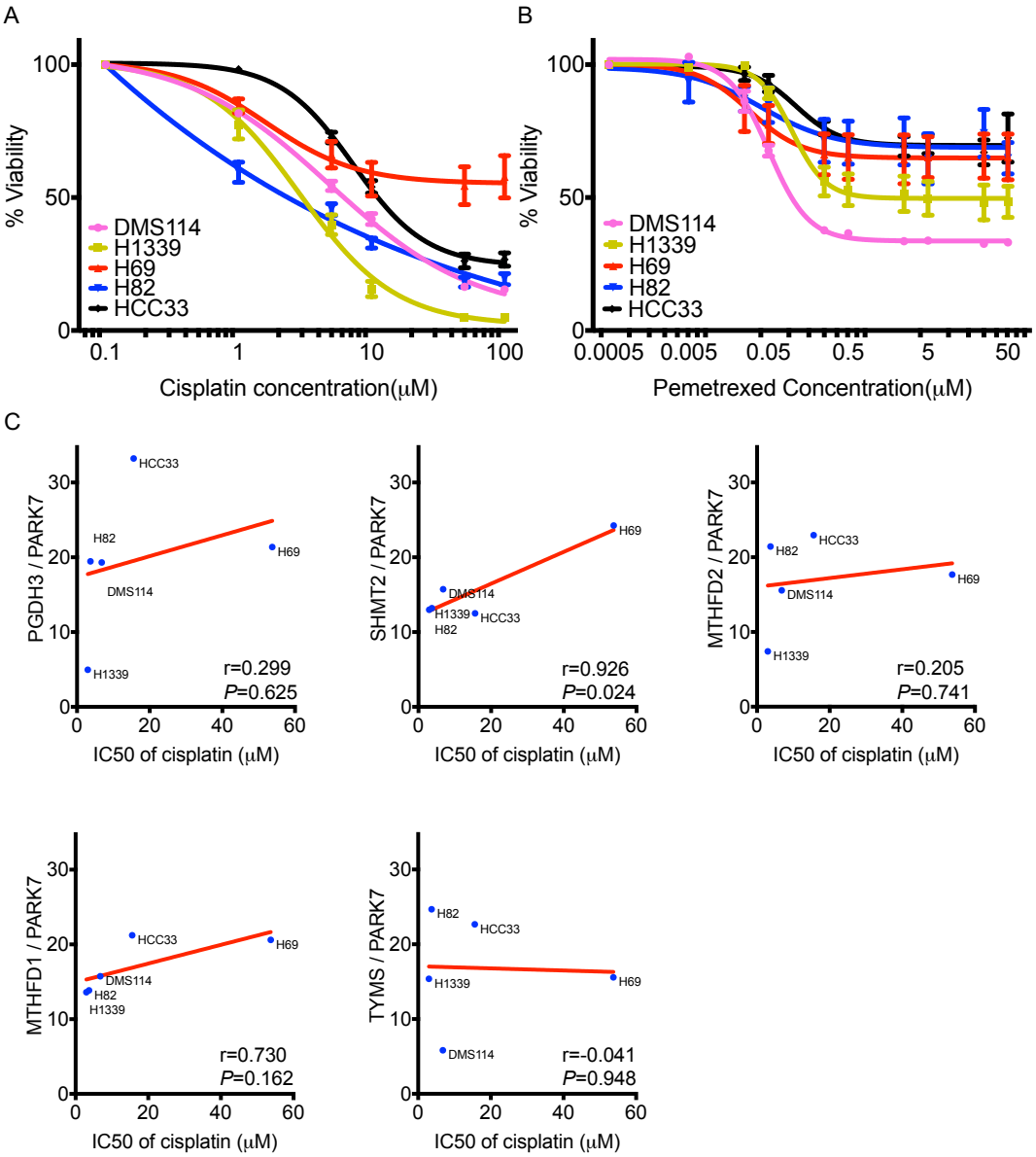
A
100
50
0
% Viability
DMS114
H1339
H69
H82
HCC33
0.1
1
10
100
Cisplatin concentration(μM)
B
100
50
0
% Viability
DMS114
H1339
H69
H82
HCC33
0.0005
0.005
0.05
0.5
5
50
Pemetrexed Concentration(μM)
C
PGDH3 / PARK7
HCC33
H82
H69
DMS114
H1339
r=0.299
P=0.625
IC50 of cisplatin (μM)
SHMT2 / PARK7
H69
DMS114
H1339
HCC33
H82
r=0.926
P=0.024
IC50 of cisplatin (μM)
MTHFD2 / PARK7
H82
HCC33
H69
DMS114
H1339
r=0.205
P=0.741
IC50 of cisplatin (μM)
MTHFD1 / PARK7
HCC33
H69
DMS114
H82
H1339
r=0.730
P=0.162
IC50 of cisplatin (μM)
TYMS / PARK7
H82
HCC33
H1339
H69
DMS114
r=-0.041
P=0.948
IC50 of cisplatin (μM)

D

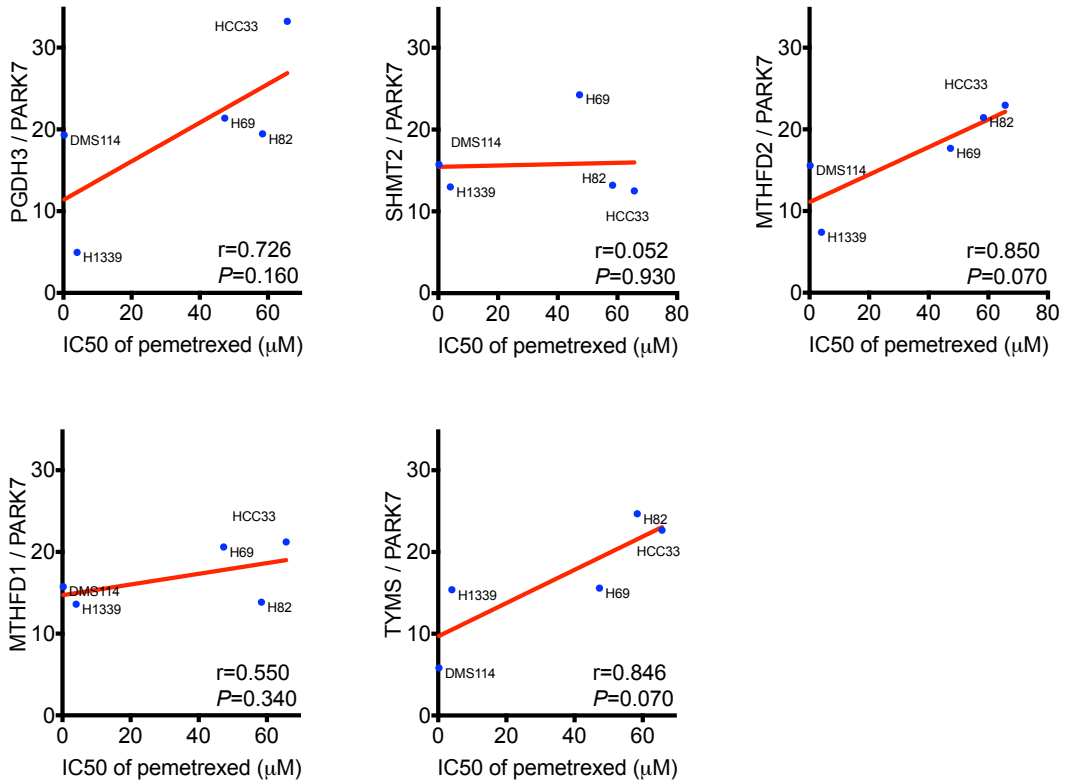

Figure 22: Correlation of one-carbon metabolism proteins expression with cisplatin or pemetrexed sensitivity in SCLC cell lines. Inhibitory dose-repose curves show the SCLC cell lines treated with cisplatin (A) for 72 h and pemetrexed (B) for 96 h. The dots and bars represent the mean ± SEM of at least three independent experiments, each with three technical replicates. Correlation curves show the correlation between the IC50 values of cisplatin (C) and pemetrexed (D) and the expression of one-carbon metabolism proteins in SCLC cell lines.

5 Discussion

The hyperproliferation of cancer cells commonly points to a high requirement on one-carbon metabolism, which could be developed as anticancer target. For example, the anti-folate drug aminopterin was already used successfully for acute lymphoblastic leukemia (ALL) in children in 1948 (Farber and Diamond 1948). Today, chemical variants of driven folate antagonists chemotherapeutic agents and are used to treat several cancer types by FDA approving (Locasale 2013) including lung cancer, ALL, breast cancer, bladder cancer and lymphomas (Chabner and Roberts 2005; Locasale 2013; Vander Heiden 2011).

A study pointed that the capacity of cell growth and proliferation is associated with cancer cells reprogram one-carbon metabolism (Boroughs and Deberardinis 2015). For example, PGDH3, the rate-limiting enzyme for serine synthesis, has been implicated in multiple cancers such as breast cancer, melanomas and NSCLC tumors (Denicola et al. 2015; Locasale et al. 2011; Maddocks et al. 2013; Possemato et al. 2011; Zhang et al. 2017). MTHFD2, a crucial enzyme in mitochondrial metabolism, indicated with a poor prognosis in breast cancer (Jain et al. 2012), hepatocellular carcinoma (Liu et al. 2016), pancreatic cancer (Noguchi et al. 2018) and a study showed that abolishment of MTHFD *in vitro* strongly inhibits remote metastasis of melanoma cells (Piskounova et al. 2015).

Hence, we first assessed the expression of one-carbon enzyme proteins by immunohistochemistry in human lung cancer specimens and showed that MTHFD2 and PGDH3 were strongly expressed in the three major lung cancer subtypes AC, SQCLC, and SCLC. Furthermore, MTHFD2 and PGDH3 expression were correlated with poor prognosis in patients with pulmonary adenocarcinoma, supporting previous studies in human pancreatic cancer, breast cancer, hepatocellular carcinoma (Liu et al. 2014; Liu et al. 2016; Song et al. 2018). Interestingly, although positive MTHFD2 staining was more frequent in SQCLC (81.2 %) and SCLC (81.6 %) than in AC cases (50.0 %), there was no correlation with prognosis in patients with SQCLC or SCLC. Surprisingly, residual one-carbon metabolic marks were not associated with overall survival in three subtypes of lung cancer.

Given that MTHFD2 within mitochondrial one-carbon metabolism can catalyze the NAD^+ dependent reactions (Tibbetts and Appling 2010). The folate cycle directly produces the nicotinamide adenine dinucleotide phosphate hydrogen and also it intersects with the methionine cycle to contribute product of glutathione (Maddocks et al. 2013).

In addition, several studies showed that enzymes level of the folate cycle correlate with oncogenes such as *KRAS*, *MYC*. For example, upregulation of the folate metabolism enzyme MTHFD2 in NSCLC cells with *KRAS*-mutant may be found a higher anti-folate activity (Moran et al. 2014). A report showed mTORC1, stimulating the mTHF cycle, provides one-carbon units to MTHFD2 to promote a production of purine nucleotides and contribute to affect cell growth (Ben-Sahra et al. 2016).

To study the expression and function of one-carbon metabolism enzymes *in vitro*, we used sixteen human lung cancer cell lines (six AC, five SQCLC and five SCLC) which recapitulate the histological classification. We analyzed the sensitivity of the three lung cancer subtypes to pemetrexed. Pemetrexed, is a novel anti-folate agent which inhibits THF cofactor-dependent enzymes, and is approved for the treatment of lung cancer and selected for some solid tumors like breast cancer (Chattopadhyay et al. 2007). As expected, our findings revealed that MTHFD2 expression in AC cell lines was correlated with sensitivity to pemetrexed. It is evident that the MTHFD2 result obtained here was in exceptionally good agreement with existing studies that gefitinib resistance depended on MTHFD2-mediated mitochondrial one carbon metabolism (Nishimura et al. 2019). Although MTHFD2 was markedly expressed in SQCLC and SCLC cell lines, there were no association between MTHFD2 protein levels and sensitivity to pemetrexed. This suggested that cell survival of AC cell lines may be particularly dependent on mitochondrial folate metabolism enzymes.

Additional, SHMT2, another mitochondrial one-carbon metabolism enzyme that is frequently overexpressed in lung cancer produces catalytically the glycine (Nilsson et al. 2014) which acts as substrate for MTHFD2 in one-carbon cycle. Accumulating evidence showed that SHMT2 expression is significantly increased in cancers such as ovarian cancer, breast cancer, colorectal cancer

and correlates with poor prognosis (Lee et al. 2014; Wang et al. 2017; Zhang et al. 2016). SHMT2 *in vitro* knockdown was associated with a reduction of cell proliferation and an inhibition of tumorigenicity in hepatocellular cancer cell lines (Woo et al. 2016). A synergistic effect of MTHFD2 (mitochondrial) and SHMT1 (cytosolic) in inhibiting colorectal carcinoma growth *in vivo* (Ducker et al. 2016) has been shown. However, we did not detect any correlation between SHMT2 expression and IC50 of pemetrexed in AC cell lines. Zhang et al. (2012) showed that glycine decarboxylases, such as PSAT1, PSPH, and SHMT1 and 2 do not significantly promote glycine uptake but promote glycolysis instead in NIH/3T3 cells with ectopic expression of SHMT, indicating a synergism between one-carbon metabolism and other metabolic pathways.

Cisplatin, an inhibitor of nucleotide metabolism and a well-known chemotherapeutic drug in various tumors, leads to death of cancer cells by interfering with the biosynthesis of cytidine, inhibition of ribonucleotide reductase (RNR) and preventing the formation of deoxynucleotides damaging DNA (Jamieson and Lippard 1999; Nilsson et al. 2014; Zamble and Lippard 1995). Hence, we also evaluated the relationship of one-carbon metabolism enzymes with the response to cisplatin but did not find any correlation in the tested cell lines.

Next, we used small interfering RNAs against *PGDH3, SHMT2, MTHFD2, MTHFD1* and *TYMS* to study the impact of these enzymes on cell proliferation. We demonstrated the *MTHFD2* gene strongly influenced cell proliferation in lung cancer. As described in the results section, cell proliferation decreased by 50.0 % in all AC and SQCLC cell lines and in 3 of 5 SCLC cell lines upon knockdown of *MTHFD2*. Moreover, it was observed in colon cancer and glioblastomas that cell proliferation and survival depend on *MTHFD2* (Gustafsson et al. 2015; Nilsson et al. 2014).

Recent research revealed that MTHFD2 enhanced malignancy and distant metastasis by regulation of redox homeostasis under various stress stimuli such as hypoxia and degradation of stroma in colorectal cancer (Ju et al. 2018). MTHFD2 expression is also elevated in colorectal cancer (CRC) and correlates with a poor prognosis (Gustafsson et al. 2017). Specifically, the first inhibitor of

MTHFD2 LY345899 significantly inhibits the colorectal cancer growth, promising a potential therapeutic agent for CRC treatment (Ju et al. 2018).

However, the regulatory mechanism of MTHFD2 in lung cancer cells is not yet clear. First, the MTHFD2 enzyme is necessary for the production of NADPH and it has been reported that disrupting of NADPH homeostasis enhances drug-induced apoptosis (Ju et al. 2017). For example, inhibition of serine-glycine biosynthesis by depletion of glutamine or PGDH3 induced apoptosis in EWS cells (Sen et al. 2018). It is well-known that SHMT2 is an important enzyme which regulates serine metabolism in mitochondria. SHMT2 knockdown produces auxotrophic effects for glycine (Zhang et al. 2012).

Ju et al. (2018) reported that MTHFD2 in CRC was transcriptionally upregulated by the oncogene cellular myelocytomatosis oncogen (*c-Myc)* rather than K-RAS downstream. *MYC* is a proto-typical oncogene which activates cell growth and proliferation, genes involved in the expression of metabolic enzymes from phosphoribosyl pyrophosphate (PRPP) to adenosine monophosphate and guanosine monophosphate in tumor-initiating cells (Wang et al. 2017) and purine and pyrimidine nucleotides biosynthesis along with inactivate apoptotic pathway (Liu et al. 2008; Pelengaris et al. 1999; Shchors et al. 2006). The RAS family encoding small enzymes that hydrolyze guanosine triphosphate belongs to the most frequently mutated group of genes in NSCLC (30.0 % of pulmonary adenocarcinomas (Ding et al. 2008) and 5.0 % of squamous cell carcinomas) (Downward 2003). These tumors carry an activating *RAS* mutation leading to constitutive activation of the RAS-ERK signaling pathway as an essential driver of proliferation, differentiation and cellular survival. Although direct inhibition of oncogenic *RAS* remains to be challenging in the future, MTHFD2 combining the first K-RAS inhibitor AMG 510 may be of interest as a potential therapeutic strategy.

One hypothesis is that silencing of MTHFD2 results in blockade of the cell cycle in adenocarcinoma cells. In support of this idea, MTHFD1 concentrated in the nucleus preferentially ensure to conserve thymidylate synthesis by consume other intermediate such as homocysteine in the cytoplasm lack of folate deficiency or during the cell arrest (Field et al. 2014). For example, Knockdown MTHFD1 with a specific RNA caused a strong decreased thymidylate

synthesis, on the other side, and increased uracil integration into DNA (Field et al. 2015). Moreover, aberrant MTHFD2 in colorectal cancer cells not only promoted cell proliferation, migratory and also affected cell death (Wei et al. 2019). Serine is partiality catabolized to pyrimidine and glutathione in a group of AC with high expression of PGDH3 (Piskounova et al. 2015). In order to produce RNA and DNA, proliferating cells by upregulating pyrimidine and purine metabolism supply a competent substrate (Field et al. 2014). Elevated generation of pyrimidines and purines is required for cell division.

Cells without p53 failed to the respond to serine depletion and cell cycle arrest preventing uncontrolled proliferation (Maddocks et al. 2013). The activated p53 regulated the serine biosynthesis through reducing PGDH3 protein and resulting serine deprivation (Maddocks et al. 2013). The *p53* mutations cause serine metabolism alteration that induced a strong decreased tumor growth in many tumors including lung cancer (Maddocks et al. 2013). Non-genotoxic stress activated the p53 suppress the PGDH3 protein expression, leading to enhancement of apoptosis in normal cells.(Kruiswijk et al. 2015). So, it is interesting that activation of p53 by serine starvation causes cell cycle arrest. Cell survival may be due to the serine cycle intersecting with glutathione synthesis cycle within cells (Kruiswijk et al. 2015; Maddocks et al. 2013).

In the present study, we also examined the expression of PGDH3, MTHFD1 and TYMS enzymes in human lung cancer cell lines, the correlation between expression of these enzymes and IC50 of pemetrexed or cisplatin, and cell proliferation after knockdown of these genes. The results did not reveal that expression of PGHD3, MTHFD1 or TYMS was associated with IC50 of pemetrexed and cisplatin.

6 Summary

In the present study, we investigated the role of one-carbon metabolism enzymes in human lung cancer.

First, we measured the expression and prognostic impact of the one-carbon metabolism enzymes PGDH3, SHMT2, MTHFD2, MTHFD1 and TYMS in human lung cancer samples using IHC and found that overexpression of PGDH3 and MTHFD2 is marker of poor prognosis in patients with AC. Next, we performed experiments to investigate the function of these enzymes in lung cancer cell lines including AC, SQCLC and SCLC cells. Our results showed that knockdown of these genes significantly reduced cellular proliferation in AC cell lines but not in most SQCLC and SCLC cell lines. Expression of MTHFD2 protein is positively correlated with IC50 of pemetrexed in AC cell lines. Altogether, the phenotypes we found supported that one-carbon metabolism enzymes promote proliferation of human lung cancer cells, especially in AC.

Overall, our study revealed the diversity of one-carbon metabolism in three different subtypes of lung cancer. Specifically, MTHFD2 was identified as an independent prognostic factor and the most promising anticancer target in pulmonary adenocarcinoma.

7 Reference

Adjei AA (2000): Pemetrexed: a multitargeted antifolate agent with promising activity in solid tumors. Ann Oncol 11, 1335-1341

Arriagada R, Dunant A, Pignon JP, Bergman B, Chabowski M, Grunenwald D, Kozlowski M, Le Pechoux C, Pirker R, Pinel MI, et al. (2010): Long-term results of the international adjuvant lung cancer trial evaluating adjuvant Cisplatin-based chemotherapy in resected lung cancer. J Clin Oncol 28, 35-42

Ben-Sahra I, Hoxhaj G, Ricoult SJH, Asara JM, Manning BD (2016): mTORC1 induces purine synthesis through control of the mitochondrial tetrahydrofolate cycle. Science 351, 728-733

Bolusani S, Young BA, Cole NA, Tibbetts AS, Momb J, Bryant JD, Solmonson A, Appling DR (2011): Mammalian MTHFD2L encodes a mitochondrial methylenetetrahydrofolate dehydrogenase isozyme expressed in adult tissues. J Biol Chem 286, 5166-5174

Borghaei H, Paz-Ares L, Horn L, Spigel DR, Steins M, Ready NE, Chow LQ, Vokes EE, Felip E, Holgado E, et al. (2015): Nivolumab versus Docetaxel in Advanced Nonsquamous Non-Small-Cell Lung Cancer. N Engl J Med 373, 1627-1639

Boroughs LK, Deberardinis RJ (2015): Metabolic pathways promoting cancer cell survival and growth. Nat Cell Biol 17, 351-359

Bray F, Ferlay J, Soerjomataram I, Siegel RL, Torre LA, Jemal A (2018): GLOBOCAN estimates of incidence and mortality worldwide for 36 cancers in 185 countries. CA Cancer J Clin 68, 394-424

Cancer Genome Atlas Research N (2014): Comprehensive molecular profiling of lung adenocarcinoma. Nature 511, 543-550

Chabner BA, Roberts TG (2005): Chemotherapy and the war on cancer. Nat Rev Cancer 5, 65-72

Chattopadhyay S, Moran RG, Goldman ID (2007): Pemetrexed: biochemical and cellular pharmacology, mechanisms, and clinical applications. Mol Cancer Ther 6, 404-417

Chen J, Chung F, Yang G, Pu M, Gao H, Jiang W, Yin H, Capka V, Kasibhatla S, Laffitte B, et al. (2013): Phosphoglycerate dehydrogenase is dispensable for breast tumor maintenance and growth. Oncotarget 4, 2502-2511

Christensen KE, MacKenzie RE (2006): Mitochondrial one-carbon metabolism is adapted to the specific needs of yeast, plants and mammals. Bioessays 28, 595-605

Christensen KE, Mackenzie RE (2008): Mitochondrial methylenetetrahydrofolate dehydrogenase, methenyltetrahydrofolate cyclohydrolase, and formyltetrahydrofolate synthetases. Vitam Horm 79, 393-410

Cunningham D, Zalcberg J, Smith I, Gore M, Pazdur R, Burris H, Meropol NJ, Kennealey G, Seymour L (1996): a novel thymidylate synthase inhibitor with clinical antitumour activity in a range of solid tumours. Ann Oncol 7, 179-182

Daidone F, Florio R, Rinaldo S, Contestabile R, Salvo ML, Cutruzzola F, Bossa F, Paiardini A (2011): In silico and in vitro validation of serine hydroxymethyltransferase as a chemotherapeutic target of the antifolate drug pemetrexed. Eur J Med Chem 46, 1616-1621

Dasari S, Tchounwou PB (2014): Cisplatin in cancer therapy: molecular mechanisms of action. Eur J Pharmacol 740, 364-378

DeNicola GM, Chen PH, Mullarky E, Sudderth JA, Hu Z, Wu D, Tang H, Xie Y, Asara JM, Huffman KE, et al. (2015): NRF2 regulates serine biosynthesis in non-small cell lung cancer. Nat Genet 47, 1475-1481

Ding L, Getz G, Wheeler DA, Mardis ER, McLellan MD, Cibulskis K, Sougnez C, Greulich H, Muzny DM, Morgan MB, et al. (2008): Somatic mutations affect key pathways in lung adenocarcinoma. Nature 455, 1069-1075

Djalalov S, Beca J, Hoch JS, Krahn M, Tsao MS, Cutz JC, Leighl NB (2014): Cost effectiveness of EML4-ALK fusion testing and first-line crizotinib treatment for patients with advanced ALK-positive non-small-cell lung cancer. J Clin Oncol 32, 1012-1019

Dominguez-Salas P, Cox SE, Prentice AM, Hennig BJ, Moore SE (2012): Maternal nutritional status, C(1) metabolism and offspring DNA methylation: a review of current evidence in human subjects. Proc Nutr Soc 71, 154-165

Downward J (2003): Targeting RAS signalling pathways in cancer therapy. Nat Rev Cancer 3, 11-22

Ducker GS, Rabinowitz JD (2017): One-Carbon Metabolism in Health and Disease. Cell Metab 25, 27-42

Ducker GS, Chen L, Morscher RJ, Ghergurovich JM, Esposito M, Teng X, Kang Y, Rabinowitz JD (2016): Reversal of Cytosolic One-Carbon Flux Compensates for Loss of the Mitochondrial Folate Pathway. Cell Metab 23, 1140-1153

Duruisseaux M, Esteller M (2018): Lung cancer epigenetics: From knowledge to applications. Semin Cancer Biol 51, 116-128

Farber S, Diamond LK (1948): Temporary remissions in acute leukemia in children produced by folic acid antagonist, 4-aminopteroyl-glutamic acid. N Engl J Med 238, 787-793

Fell DA, Snell K (1988): Control analysis of mammalian serine biosynthesis. Feedback inhibition on the final step. Biochem J 256, 97-101

Ferlay J, Colombet M, Soerjomataram I, Mathers C, Parkin DM, Pineros M, Znaor A, Bray F (2019): Estimating the global cancer incidence and mortality in 2018: GLOBOCAN sources and methods. Int J Cancer 144, 1941-1953

Field MS, Kamynina E, Watkins D, Rosenblatt DS, Stover PJ (2015): Human mutations in methylenetetrahydrofolate dehydrogenase 1 impair nuclear de novo thymidylate biosynthesis. Proc Natl Acad Sci USA 112, 400-405

Field MS, Kamynina E, Agunloye OC, Liebenthal RP, Lamarre SG, Brosnan ME, Brosnan JT, Stover PJ (2014): Nuclear enrichment of folate cofactors and methylenetetrahydrofolate dehydrogenase 1 (MTHFD1) protect de novo thymidylate biosynthesis during folate deficiency. J Biol Chem 289, 29642-29650

Gadgeel SM, Ruckdeschel JC, Patel BB, Wozniak A, Konski A, Valdivieso M, Hackstock D, Chen W, Belzer K, Burger AM, et al. (2011): Phase II study of pemetrexed and cisplatin, with chest radiotherapy followed by docetaxel in patients with stage III non-small cell lung cancer. J Thorac Oncol 6, 927-933

Garon EB, Rizvi NA, Hui R, Leighl N, Balmanoukian AS, Eder JP, Patnaik A, Aggarwal C, Gubens M, Horn L, et al. (2015): Pembrolizumab for the treatment of non-small-cell lung cancer. N Engl J Med 372, 2018-2028

George J, Lim JS, Jang SJ, Cun Y, Ozretic L, Kong G, Leenders F, Lu X, Fernandez-Cuesta L, Bosco G, et al. (2015): Comprehensive genomic profiles of small cell lung cancer. Nature 524, 47-53

Gustafsson R, Jemth AS, Gustafsson NM, Farnegardh K, Loseva O, Wiita E, Bonagas N, Dahllund L, Llona-Minguez S, Haggblad M, et al. (2017): Crystal Structure of the Emerging Cancer Target MTHFD2 in Complex with a Substrate-Based Inhibitor. Cancer Res 77, 937-948

Gustafsson Sheppard N, Jarl L, Mahadessian D, Strittmatter L, Schmidt A, Madhusudan N, Tegner J, Lundberg EK, Asplund A, Jain M, et al. (2015): The folate-coupled enzyme MTHFD2 is a nuclear protein and promotes cell proliferation. Sci Rep 5, 15029

Hebbring SJ, Chai Y, Ji Y, Abo RP, Jenkins GD, Fridley B, Zhang J, Eckloff BW, Wieben ED, Weinshilboum RM (2012): Serine hydroxymethyltransferase 1 and 2: gene sequence variation and functional genomic characterization. J Neurochem 120, 881-890

Herbst RS, Baas P, Kim DW, Felip E, Perez-Gracia JL, Han JY, Molina J, Kim JH, Arvis CD, Ahn MJ, et al. (2016): Pembrolizumab versus docetaxel for previously treated, PD-L1-positive, advanced non-small-cell lung cancer: a randomised controlled trial. Lancet 387, 1540-1550

Jain M, Nilsson R, Sharma S, Madhusudhan N, Kitami T, Souza AL, Kafri R, Kirschner MW, Clish CB, Mootha VK (2012): Metabolite profiling identifies a key role for glycine in rapid cancer cell proliferation. Science 336, 1040-1044

Jamieson ER, Lippard SJ (1999): Structure, Recognition, and Processing of Cisplatin-DNA Adducts. Chem Rev 99, 2467-2498

Ju HQ, Lu YX, Wu QN, Liu J, Zeng ZL, Mo HY, Chen Y, Tian T, Wang Y, Kang TB, et al. (2017): Disrupting G6PD-mediated Redox homeostasis enhances chemosensitivity in colorectal cancer. Oncogene 36, 6282-6292

Ju HQ, Lu YX, Chen DL, Zuo ZX, Liu ZX, Wu QN, Mo HY, Wang ZX, Wang DS, Pu HY, et al. (2018): Modulation of Redox Homeostasis by Inhibition of MTHFD2 in Colorectal Cancer. J Natl Cancer Inst 6, 584-596

Kim D, Fiske BP, Birsoy K, Freinkman E, Kami K, Possemato RL, Chudnovsky Y, Pacold ME, Chen WW, Cantor JR, et al. (2015): SHMT2 drives glioma cell survival in ischaemia but imposes a dependence on glycine clearance. Nature 520, 363-367

Koseki J, Konno M, Asai A, Colvin H, Kawamoto K, Nishida N, Sakai D, Kudo T, Satoh T, Doki Y, et al. (2018): Enzymes of the one-carbon folate metabolism as anticancer targets predicted by survival rate analysis. Sci Rep 8, 303

Kris MG, Johnson BE, Berry LD, Kwiatkowski DJ, Iafrate AJ, Wistuba, II, Varella-Garcia M, Franklin WA, Aronson SL, Su PF, et al. (2014): Using multiplexed assays of oncogenic drivers in lung cancers to select targeted drugs. Jama 311, 1998-2006

Kruiswijk F, Labuschagne CF, Vousden KH (2015): p53 in survival, death and metabolic health: a lifeguard with a licence to kill. Nat Rev Mol Cell Biol 16, 393-405

Lee GY, Haverty PM, Li L, Kljavin NM, Bourgon R, Lee J, Stern H, Modrusan Z, Seshagiri S, Zhang Z, et al. (2014): Comparative oncogenomics identifies PSMB4 and SHMT2 as potential cancer driver genes. Cancer Res 74, 3114-3126

Lehtinen L, Ketola K, Makela R, Mpindi JP, Viitala M, Kallioniemi O, Iljin K (2013): High-throughput RNAi screening for novel modulators of vimentin expression identifies MTHFD2 as a regulator of breast cancer cell migration and invasion. Oncotarget 4, 48-63

Liu F, Liu Y, He C, Tao L, He X, Song H, Zhang G (2014): Increased MTHFD2 expression is associated with poor prognosis in breast cancer. Tumour Biol 35, 8685-8690

Liu X, Huang Y, Jiang C, Ou H, Guo B, Liao H, Li X, Yang D (2016): Methylenetetrahydrofolate dehydrogenase 2 overexpression is associated with tumor aggressiveness and poor prognosis in hepatocellular carcinoma. Dig Liver Dis 48, 953-960

Liu YC, Li F, Handler J, Huang CR, Xiang Y, Neretti N, Sedivy JM, Zeller KI, Dang CV (2008): Global regulation of nucleotide biosynthetic genes by c-Myc. PLoS One 3, 2722

Locasale JW (2013): Serine, glycine and one-carbon units: cancer metabolism in full circle. Nat Rev Cancer 13, 572-583

Locasale JW, Grassian AR, Melman T, Lyssiotis CA, Mattaini KR, Bass AJ, Heffron G, Metallo CM, Muranen T, Sharfi H, et al. (2011): Phosphoglycerate dehydrogenase diverts glycolytic flux and contributes to oncogenesis. Nat Genet 43, 869-874

Longley DB, Harkin DP, Johnston PG (2003): 5-fluorouracil: mechanisms of action and clinical strategies. Nat Rev Cancer 3, 330-338

Maddocks OD, Berkers CR, Mason SM, Zheng L, Blyth K, Gottlieb E, Vousden KH (2013): Serine starvation induces stress and p53-dependent metabolic remodelling in cancer cells. Nature 493, 542-546

Marx A, Chan JK, Coindre JM, Detterbeck F, Girard N, Harris NL, Jaffe ES, Kurrer MO, Marom EM, Moreira AL, et al. (2015): The 2015 World Health Organization Classification of Tumors of the Thymus: Continuity and Changes. J Thorac Oncol 10, 1383-1395

Mehrmohamadi M, Liu X, Shestov AA, Locasale JW (2014): Characterization of the usage of the serine metabolic network in human cancer. Cell Rep 9, 1507-1519

Minton DR, Nam M, McLaughlin DJ, Shin J, Bayraktar EC, Alvarez SW, Sviderskiy VO, Papagiannakopoulos T, Sabatini DM, Birsoy K, et al. (2018): Serine Catabolism by SHMT2 Is Required for Proper Mitochondrial Translation Initiation and Maintenance of Formylmethionyl-tRNAs. Mol Cell 69, 610-621

Miyo M, Konno M, Colvin H, Nishida N, Koseki J, Kawamoto K, Tsunekuni K, Nishimura J, Hata T, Takemasa I, et al. (2017): The importance of mitochondrial folate enzymes in human colorectal cancer. Oncol Rep 37, 417-425

Mok TS, Wu YL, Thongprasert S, Yang CH, Chu DT, Saijo N, Sunpaweravong P, Han B, Margono B, Ichinose Y, et al. (2009): Gefitinib or carboplatin-paclitaxel in pulmonary adenocarcinoma. N Engl J Med 361, 947-957

Moran DM, Trusk PB, Pry K, Paz K, Sidransky D, Bacus SS (2014): KRAS mutation status is associated with enhanced dependency on folate metabolism pathways in non-small cell lung cancer cells. Mol Cancer Ther 13, 1611-1624

Morgensztern D, Du L, Waqar SN, Patel A, Samson P, Devarakonda S, Gao F, Robinson CG, Bradley J, Baggstrom M, et al. (2016): Adjuvant Chemotherapy for Patients with T2N0M0 NSCLC. J Thorac Oncol 11, 1729-1735

Mullarky E, Mattaini KR, Vander Heiden MG, Cantley LC, Locasale JW (2011): PHGDH amplification and altered glucose metabolism in human melanoma. Pigment Cell Melanoma Res 24, 1112-1115

Mullarky E, Lucki NC, Beheshti Zavareh R, Anglin JL, Gomes AP, Nicolay BN, Wong JC, Christen S, Takahashi H, Singh PK, et al. (2016): Identification of a small molecule inhibitor of 3-phosphoglycerate dehydrogenase to target serine biosynthesis in cancers. Proc Natl Acad Sci USA 113, 1778-1783

Nakaoku T, Tsuta K, Ichikawa H, Shiraishi K, Sakamoto H, Enari M, Furuta K, Shimada Y, Ogiwara H, Watanabe S, et al. (2014): Druggable oncogene fusions in invasive mucinous lung adenocarcinoma. Clin Cancer Res 20, 3087-3093

Newman AC, Maddocks ODK (2017): One-carbon metabolism in cancer. Br J Cancer 116, 1499-1504

Nilsson R, Jain M, Madhusudhan N, Sheppard NG, Strittmatter L, Kampf C, Huang J, Asplund A, Mootha VK (2014): Metabolic enzyme expression highlights a key role for MTHFD2 and the mitochondrial folate pathway in cancer. Nat Commun 5, 3128

Nishimura T, Nakata A, Chen X, Nishi K, Meguro-Horike M, Sasaki S, Kita K, Horike SI, Saitoh K, Kato K, et al. (2019): Cancer stem-like properties and gefitinib resistance are dependent on purine synthetic metabolism mediated by the mitochondrial enzyme MTHFD2. Oncogene 38, 2464-2481

Nizzoli R, Tiseo M, Gelsomino F, Bartolotti M, Majori M, Ferrari L, De Filippo M, Rindi G, Silini EM, Guazzi A, et al. (2011): Accuracy of fine needle aspiration cytology in the pathological typing of non-small cell lung cancer. J Thorac Oncol 6, 489-493

Noguchi K, Konno M, Koseki J, Nishida N, Kawamoto K, Yamada D, Asaoka T, Noda T, Wada H, Gotoh K, et al. (2018): The mitochondrial one-carbon metabolic pathway is associated with patient survival in pancreatic cancer. Oncol Lett 16, 1827-1834

Okamoto H, Watanabe K, Kunikane H, Yokoyama A, Kudoh S, Asakawa T, Shibata T, Kunitoh H, Tamura T, Saijo N (2007): Randomised phase III trial of carboplatin plus etoposide vs split doses of cisplatin plus etoposide in elderly or poor-risk patients with extensive disease small-cell lung cancer: JCOG 9702. Br J Cancer 97, 162-169

Pacold ME, Brimacombe KR, Chan SH, Rohde JM, Lewis CA, Swier LJ, Possemato R, Chen WW, Sullivan LB, Fiske BP, et al. (2016): A PHGDH inhibitor reveals coordination of serine synthesis and one-carbon unit fate. Nat Chem Biol 12, 452-458

Paez JG, Janne PA, Lee JC, Tracy S, Greulich H, Gabriel S, Herman P, Kaye FJ, Lindeman N, Boggon TJ, et al. (2004): EGFR mutations in lung cancer: correlation with clinical response to gefitinib therapy. Science 304, 1497-1500

Paz-Ares L, de Marinis F, Dediu M, Thomas M, Pujol JL, Bidoli P, Molinier O, Sahoo TP, Laack E, Reck M, et al. (2012): Maintenance therapy with pemetrexed plus best supportive care versus placebo plus best supportive care after induction therapy with pemetrexed plus cisplatin for advanced non-squamous non-small-cell lung cancer: a double-blind, phase 3, randomised controlled trial. Lancet Oncol 13, 247-255

Paz-Ares LG, de Marinis F, Dediu M, Thomas M, Pujol JL, Bidoli P, Molinier O, Sahoo TP, Laack E, Reck M, et al. (2013): Final overall survival results of the phase III study of maintenance pemetrexed versus placebo immediately after induction treatment with pemetrexed plus cisplatin for advanced nonsquamous non-small-cell lung cancer. J Clin Oncol 31, 2895-2902

Pelengaris S, Littlewood T, Khan M, Elia G, Evan G (1999): Reversible activation of c-Myc in skin: induction of a complex neoplastic phenotype by a single oncogenic lesion. Mol Cell 3, 565-577

Pikman Y, Puissant A, Alexe G, Furman A, Chen LM, Frumm SM, Ross L, Fenouille N, Bassil CF, Lewis CA, et al. (2016): Targeting MTHFD2 in acute myeloid leukemia. J Exp Med 213, 1285-1306

Piskounova E, Agathocleous M, Murphy MM, Hu Z, Huddlestun SE, Zhao Z, Leitch AM, Johnson TM, DeBerardinis RJ, Morrison SJ (2015): Oxidative stress inhibits distant metastasis by human melanoma cells. Nature 527, 186-191

Politi K, Herbst RS (2015): Lung cancer in the era of precision medicine. Clin Cancer Res 21, 2213-2220

Possemato R, Marks KM, Shaul YD, Pacold ME, Kim D, Birsoy K, Sethumadhavan S, Woo HK, Jang HG, Jha AK, et al. (2011): Functional genomics reveal that the serine synthesis pathway is essential in breast cancer. Nature 476, 346-350

Reck M, Rodriguez-Abreu D, Robinson AG, Hui R, Csoszi T, Fulop A, Gottfried M, Peled N, Tafreshi A, Cuffe S, et al. (2016): Pembrolizumab versus Chemotherapy for PD-L1-Positive Non-Small-Cell Lung Cancer. N Engl J Med 375, 1823-1833

Rekhtman N, Brandt SM, Sigel CS, Friedlander MA, Riely GJ, Travis WD, Zakowski MF, Moreira AL (2011): Suitability of thoracic cytology for new therapeutic paradigms in non-small cell lung carcinoma: high accuracy of tumor subtyping and feasibility of EGFR and KRAS molecular testing. J Thorac Oncol 6, 451-458

Salazar MC, Rosen JE, Wang Z, Arnold BN, Thomas DC, Herbst RS, Kim AW, Detterbeck FC, Blasberg JD, Boffa DJ (2017): Association of Delayed Adjuvant Chemotherapy With Survival After Lung Cancer Surgery. JAMA Oncol 3, 610-619

Samanta D, Park Y, Andrabi SA, Shelton LM, Gilkes DM, Semenza GL (2016): PHGDH Expression Is Required for Mitochondrial Redox Homeostasis, Breast

Cancer Stem Cell Maintenance, and Lung Metastasis. Cancer Res 76, 4430-4442

Sandler A, Gray R, Perry MC, Brahmer J, Schiller JH, Dowlati A, Lilenbaum R, Johnson DH (2006): Paclitaxel-carboplatin alone or with bevacizumab for non-small-cell lung cancer. N Engl J Med 355, 2542-2550

Scagliotti GV, Gridelli C, de Marinis F, Thomas M, Dediu M, Pujol JL, Manegold C, San Antonio B, Peterson PM, John W, et al. (2014): Efficacy and safety of maintenance pemetrexed in patients with advanced nonsquamous non-small cell lung cancer following pemetrexed plus cisplatin induction treatment: A cross-trial comparison of two phase III trials. Lung Cancer 85, 408-414

Scagliotti GV, Parikh P, von Pawel J, Biesma B, Vansteenkiste J, Manegold C, Serwatowski P, Gatzemeier U, Digumarti R, Zukin M, et al. (2008): Phase III study comparing cisplatin plus gemcitabine with cisplatin plus pemetrexed in chemotherapy-naive patients with advanced-stage non-small-cell lung cancer. J Clin Oncol 26, 3543-3551

Schiller JH, Harrington D, Belani CP, Langer C, Sandler A, Krook J, Zhu J, Johnson DH (2002): Comparison of four chemotherapy regimens for advanced non-small-cell lung cancer. N Engl J Med 346, 92-98

Sen N, Cross AM, Lorenzi PL, Khan J, Gryder BE, Kim S, Caplen NJ (2018): EWS-FLI1 reprograms the metabolism of Ewing sarcoma cells via positive regulation of glutamine import and serine-glycine biosynthesis. Mol Carcinog 57, 1342-1357

Shane B, Stokstad EL (1985): Vitamin B12-folate interrelationships. Annu Rev Nutr 5, 115-141

Shchors K, Shchors E, Rostker F, Lawlor ER, Brown-Swigart L, Evan GI (2006): The Myc-dependent angiogenic switch in tumors is mediated by interleukin 1beta. Genes Dev 20, 2527-2538

Shih C, Chen VJ, Gossett LS, Gates SB, MacKellar WC, Habeck LL, Shackelford KA, Mendelsohn LG, Soose DJ, Patel VF, et al. (1997): LY231514, a pyrrolo[2,3-d]pyrimidine-based antifolate that inhibits multiple folate-requiring enzymes. Cancer Res 57, 1116-1123

Shim HS, Kenudson M, Zheng Z, Liebers M, Cha YJ, Hoang Ho Q, Onozato M, Phi Le L, Heist RS, Iafrate AJ (2015): Unique Genetic and Survival Characteristics of Invasive Mucinous Adenocarcinoma of the Lung. J Thorac Oncol 10, 1156-1162

Siegel RL, Miller KD, Jemal A (2018): Cancer statistics, 2018. CA Cancer J Clin 68, 7-30

Siegel RL, Miller KD, Jemal A (2019): Cancer statistics, 2019. CA Cancer J Clin 69, 7-34

Skoulidis F, Heymach JV (2019): Co-occurring genomic alterations in non-small-cell lung cancer biology and therapy. Nat Rev Cancer 19, 495-509

Smith PG, Marshman E, Newell DR, Curtin NJ (2000): Dipyridamole potentiates the in vitro activity of MTA (LY231514) by inhibition of thymidine transport. Br J Cancer 82, 924-930

Snell K (1984): Enzymes of serine metabolism in normal, developing and neoplastic rat tissues. Adv Enzyme Regul 22, 325-400

Snell K, Weber G (1986): Enzymic imbalance in serine metabolism in rat hepatomas. Biochem J 233, 617-620

Snell K, Natsumeda Y, Weber G (1987): The modulation of serine metabolism in hepatoma 3924A during different phases of cellular proliferation in culture. Biochem J 245, 609-612

Song Z, Feng C, Lu Y, Lin Y, Dong C (2018): PHGDH is an independent prognosis marker and contributes cell proliferation, migration and invasion in human pancreatic cancer. Gene 642, 43-50

Stipanuk MH (2004): Sulfur amino acid metabolism: pathways for production and removal of homocysteine and cysteine. Annu Rev Nutr 24, 539-577

Stover P, Schirch V (1990): Serine hydroxymethyltransferase catalyzes the hydrolysis of 5,10-methenyltetrahydrofolate to 5-formyltetrahydrofolate. J Biol Chem 265, 14227-14233

Stover PJ (2004): Physiology of folate and vitamin B12 in health and disease. Nutr Rev 62, 3-12

Takada M, Fukuoka M, Kawahara M, Sugiura T, Yokoyama A, Yokota S, Nishiwaki Y, Watanabe K, Noda K, Tamura T, et al. (2002): Phase III study of concurrent versus sequential thoracic radiotherapy in combination with cisplatin and etoposide for limited-stage small-cell lung cancer. J Clin Oncol 20, 3054-3060

Takeuchi K, Soda M, Togashi Y, Suzuki R, Sakata S, Hatano S, Asaka R, Hamanaka W, Ninomiya H, Uehara H, et al. (2012): RET, ROS1 and ALK fusions in lung cancer. Nat Med 18, 378-381

Tedeschi PM, Vazquez A, Kerrigan JE, Bertino JR (2015): Mitochondrial Methylenetetrahydrofolate Dehydrogenase (MTHFD2) Overexpression Is Associated with Tumor Cell Proliferation and Is a Novel Target for Drug Development. Mol Cancer Res 13, 1361-1366

Tibbetts AS, Appling DR (2010): Compartmentalization of Mammalian folate-mediated one-carbon metabolism. Annu Rev Nutr 30, 57-81

Travis WD, Brambilla E, Nicholson AG, Yatabe Y, Austin JHM, Beasley MB, Chirieac LR, Dacic S, Duhig E, Flieder DB, et al. (2015): Impact of Genetic,

Clinical and Radiologic Advances Since the 2004 Classification. J Thorac Oncol 10, 1243-1260

Vander Heiden MG (2011): Targeting cancer metabolism: a therapeutic window opens. Nat Rev Drug Discov 10, 671-684

Vansteenkiste J, Crino L, Dooms C, Douillard JY, Faivre-Finn C, Lim E, Rocco G, Senan S, Van Schil P, Veronesi G, et al. (2014): early-stage non-small-cell lung cancer consensus on diagnosis, treatment and follow-up. Ann Oncol 25, 1462-1474

Wang X, Yang K, Xie Q, Wu Q, Mack SC, Shi Y, Kim LJY, Prager BC, Flavahan WA, Liu X, et al. (2017): Purine synthesis promotes maintenance of brain tumor initiating cells in glioma. Nat Neurosci 20, 661-673

Wei Y, Liu P, Li Q, Du J, Chen Y, Wang Y, Shi H, Wang Y, Zhang H, Xue W, et al. (2019): The effect of MTHFD2 on the proliferation and migration of colorectal cancer cell lines. Onco Targets Ther 12, 6361-6370

Williams EA (2012): Folate, colorectal cancer and the involvement of DNA methylation. Proc Nutr Soc 71, 592-597

Wisniewski JR, Mann M (2016): A Proteomics Approach to the Protein Normalization Problem: Selection of Unvarying Proteins for MS-Based Proteomics and Western Blotting. J Proteome Res 15, 2321-2326

Woo CC, Chen WC, Teo XQ, Radda GK, Lee PT (2016): Downregulating serine hydroxymethyltransferase 2 (SHMT2) suppresses tumorigenesis in human hepatocellular carcinoma. Oncotarget 7, 53005-53017

Yang M, Vousden KH (2016): Serine and one-carbon metabolism in cancer. Nat Rev Cancer 16, 650-662

Yoshino H, Nohata N, Miyamoto K, Yonemori M, Sakaguchi T, Sugita S, Itesako T, Kofuji S, Nakagawa M, Dahiya R, et al. (2017): PHGDH as a Key Enzyme for Serine Biosynthesis in HIF2alpha-Targeting Therapy for Renal Cell Carcinoma. Cancer Res 77, 6321-6329

Zamble DB, Lippard SJ (1995): Cisplatin and DNA repair in cancer chemotherapy. Trends Biochem Sci 20, 435-439

Zhang B, Zheng A, Hydbring P, Ambroise G, Ouchida AT, Goiny M, Vakifahmetoglu-Norberg H, Norberg E (2017): PHGDH Defines a Metabolic Subtype in Lung Adenocarcinomas with Poor Prognosis. Cell Rep 19, 2289-2303

Zhang L, Chen Z, Xue D, Zhang Q, Liu X, Luh F, Hong L, Zhang H, Pan F, Liu Y, et al. (2016): Prognostic and therapeutic value of mitochondrial serine hydroxyl-methyltransferase 2 as a breast cancer biomarker. Oncol Rep 36, 2489-2500

Zhang WC, Shyh-Chang N, Yang H, Rai A, Umashankar S, Ma S, Soh BS, Sun LL, Tai BC, Nga ME, et al. (2012): Glycine decarboxylase activity drives non-small cell lung cancer tumor-initiating cells and tumorigenesis. Cell 148, 259-272

Publications

Saha S, **Yao S**, Elakad O, Lois AM, Petri HH, Buentzel J, Hinterthaner M, Danner BC, Ströbel P, Emmert A, et al. (2020): UDP-glucose 6-dehydrogenase expression as a predictor of survival in patients with pulmonary adenocarcinoma. IJS Oncol 5, 85 (shared first authorship)

Buentzel J, **Yao S**, Elakad O, Lois AM, Brunies J, Konig J, Hinterthaner M, Danner BC, Ströbel P, Emmert A, et al. (2019): Expression and prognostic impact of alpha thalassemia/mental retardation X-linked and death domain-associated protein in human lung cancer. Medicine 98, 16712 (shared first authorship)

Bohnenberger H, Kaderali L, Ströbel P, Yepes D, Plessmann U, Dharia NV, **Yao S**, Heydt C, Merkelbach-Bruse S, Emmert A, et al. (2018): Comparative proteomics reveals a diagnostic signature for pulmonary head-and-neck cancer metastasis. EMBO Mol Med 10, 8428

Elakad O, Lois AM, Schmitz K, **Yao S**, Hugo S, Lukat L, Hinterthaner M, Danner BC, Emmert A, Jessen KR, et al. (2020): Fibroblast growth factor receptor 1 gene amplification and protein expression in human lung cancer. Cancer Med 10, 3574-3583

Acknowledgements

First of all, I would like to express my heartfelt thanks to Prof. Dr. med. Philipp Ströbel and Prof. Dr. med. Volker Ellenrieder, for supervising my doctoral work.

Secondly, my profound gratitude should go to Dr. med Hanibal Bohnenberger, for provision of topic of the thesis and the thorough and educational guidance through my doctoral work. He has given me not only great instructions and encouragements throughout the process of performing experiments and writing the thesis but also plenty of help in student registration and life. I could not have finished my doctoral work and thesis without his patient guidance and help.

I also want to thank Dr. sc. hum. Stefan Küffer, Ms. Pamela Nissen and Ms. Jenny Appelhans, for fruitful discussions and technical assistance.

Thanks Chinese Scholarship Council for supporting me to pursue my doctoral diploma and providing funding.